Dissipaton Equation of Motion Theory

YiJing Yan (严以京)
University of Science and Technology of China

Intended Learning Outcomes

Get familiar with the DEOM theory, an exact and universal method in quantum mechanics of open systems

➢ **DEOM : Quasi-particle generalization to the widely used hierarchical equations of motion (HEOM) formalism**

DEOM = HEOM + dissipaton algebra

➢ **DEOM construction = Schrödinger eq. + dissipaton algebra**

➢ **DEOM evaluations of measurable quantities & illustrations**

➢ **Prospects of further developments and applications**

Outline

- ➤ **Quantum mechanics of open systems: Background**

- ➤ **The HEOM formalism: Machineries & applications**

- ➤ **HEOM-QUICK package**

- ➤ **The DEOM theory and applications**

- ➤ **Prospects**

Open Quantum Systems
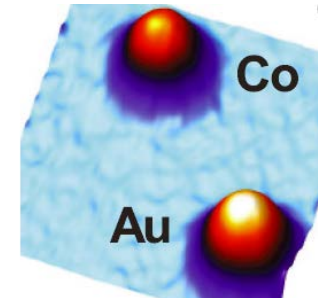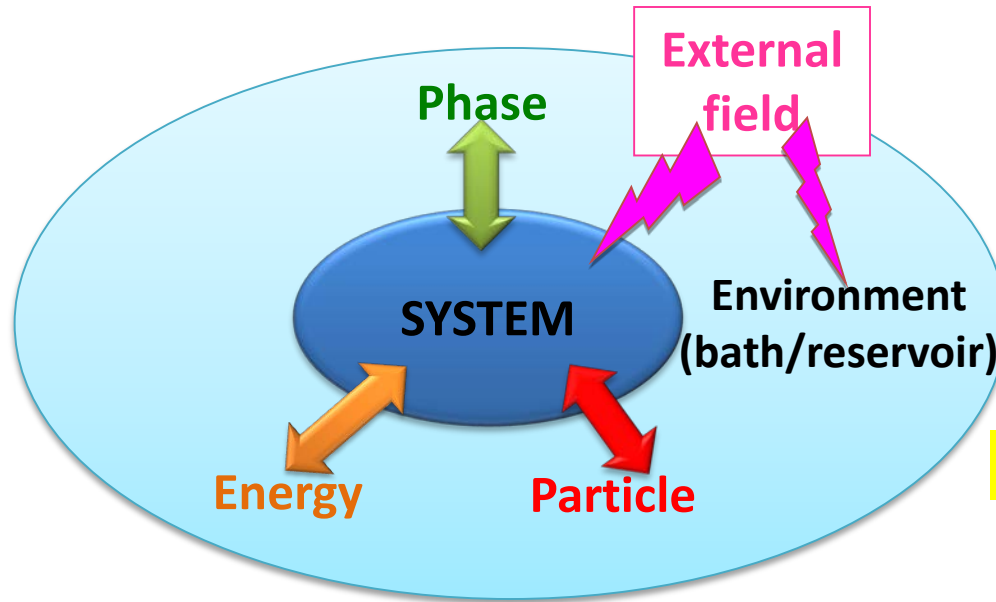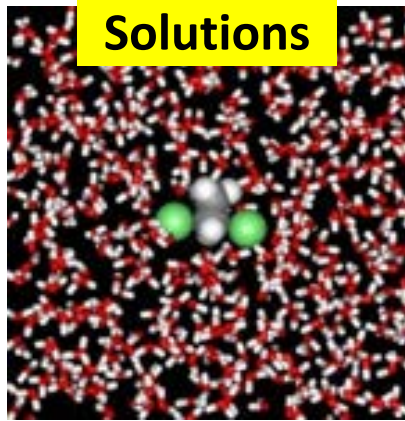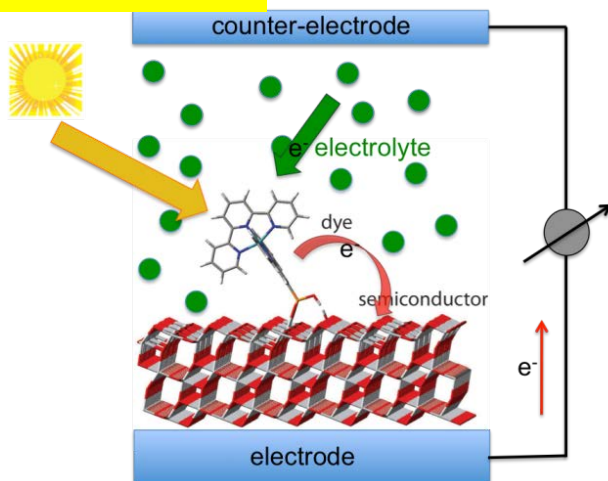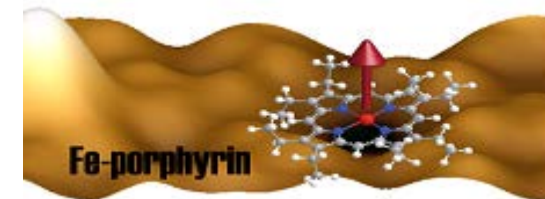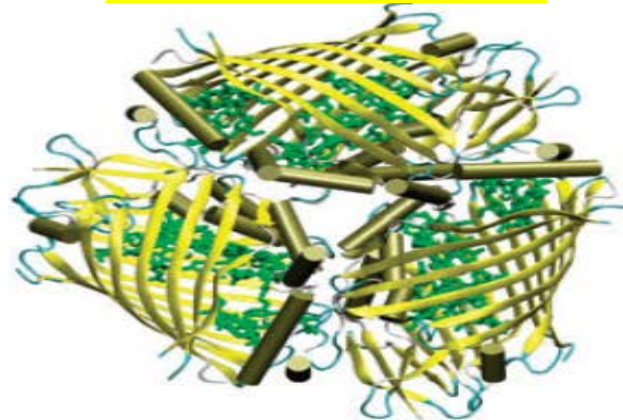
Control of local quantum states

Zhao, Yang, and Hou et al. *Science* 309, 1542 (2005)

dehydrogenated-CoPc/Au(111)

local S= 1/2 state

Parks et al. *Science* 328, 1370 (2010)

Co(tpy-SH)$_2$

local S=1 state

embedded in break junction

dehydrogenated-CoPc/Au(111)

local S= 1/2 state

Kondo peak

Kondo physics: Requirements

- **Local magnetic moment (spin-unpaired *d*-electron)**

- **Strong e-e Coulomb interaction**

- **Screening of local spin by surrounding free electrons**

- **Low temperature (suppressing thermal fluctuations)**
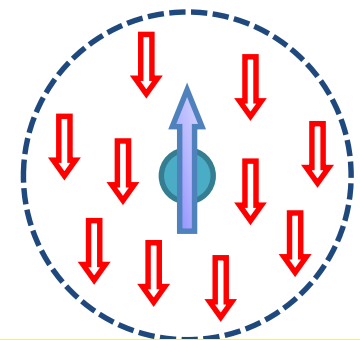
Kondo Singlet

Control of local quantum states

T< T_K : **Local magnetic moment screened by free electrons, forming a Kondo singlet**
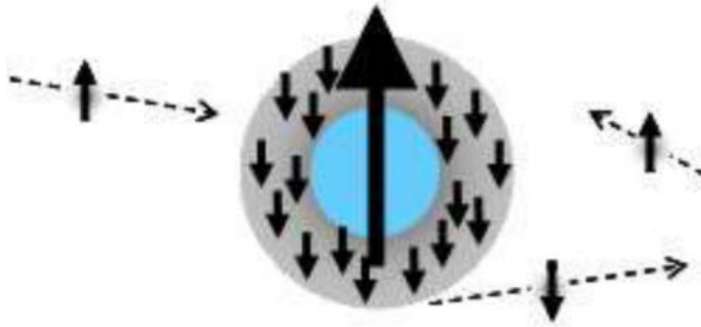
T > T_K : No Kondo

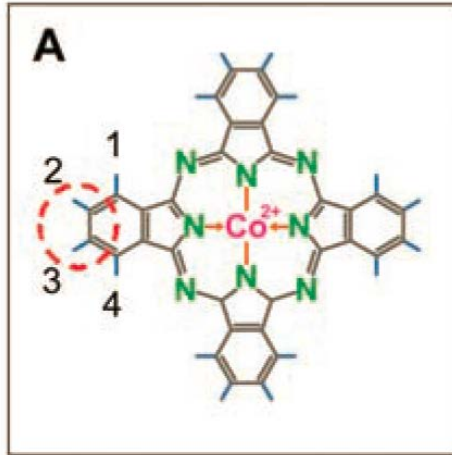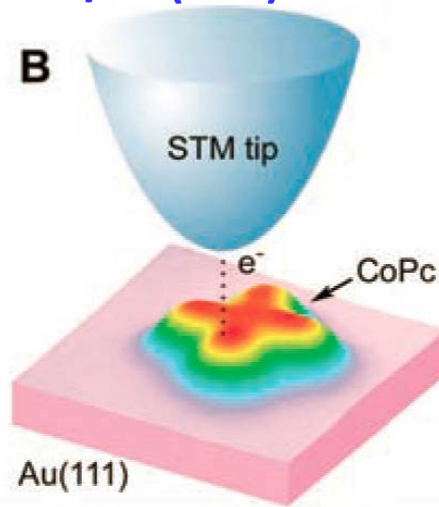# Control of local quantum states

Zhao, Yang, and Hou et al. *Science* 309, 1542 (2005)

dehydrogenated-CoPc/Au(111)

local S= 1/2 state

Parks et al. *Science* 328, 1370 (2010)

Co(tpy-SH)$_2$

local S=1 state

embedded in break junction
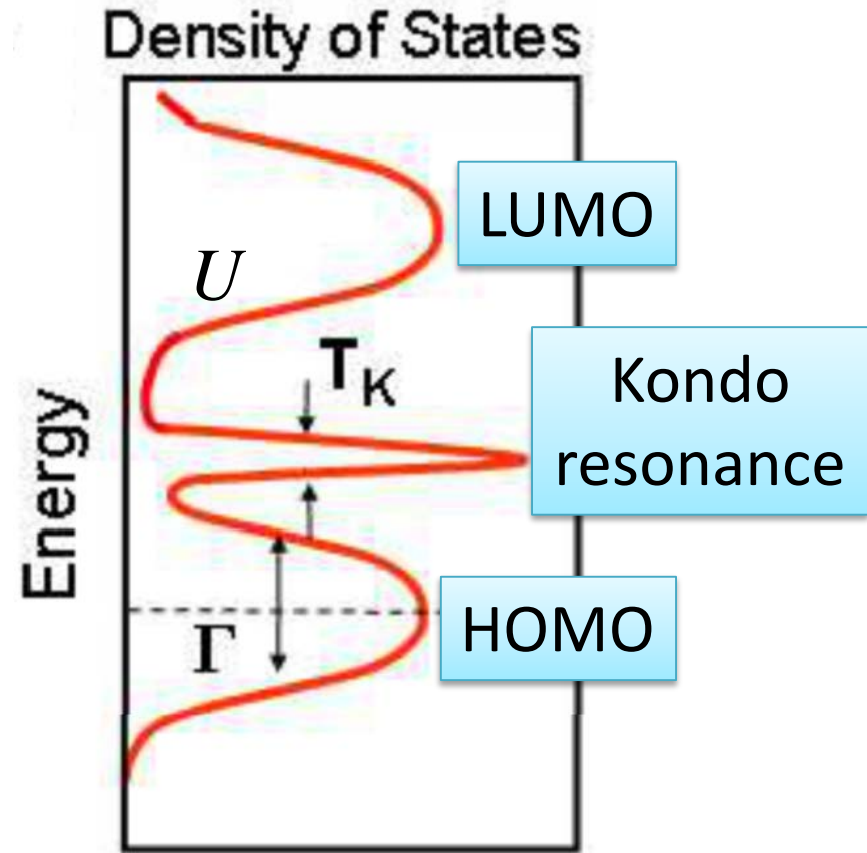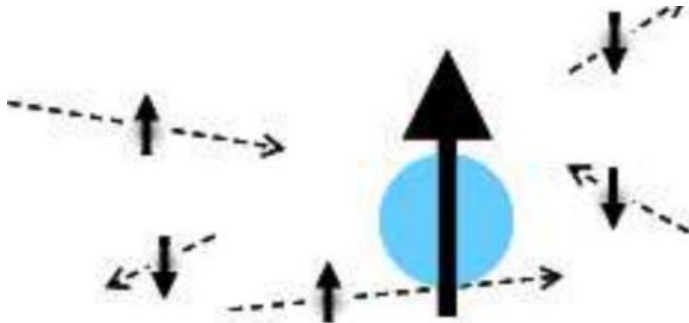
Control of local quantum states

Competition between Kondo resonance and spin-orbit coupling

octahedral field — axial distortion + spin-orbit coupling

$S_z = -1, +1$

D

$S_z = -1, 0, +1$

$S_z = 0$

Parks et al. *Science* 328, 1370 (2010)

Co(tpy-SH)$_2$

local S=1 state

Device A

V (mV)

Δ Electrode spacing (Å)

0.7 0.9 1.1 1.3
dI/dV (e^2/h)

Device A

increasing stretching

dI/dV (e^2/h)

V (mV)

SiO$_2$ Δx Au

Δz Si

Pushing screw
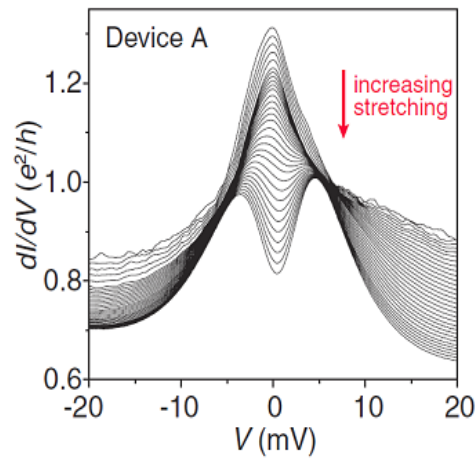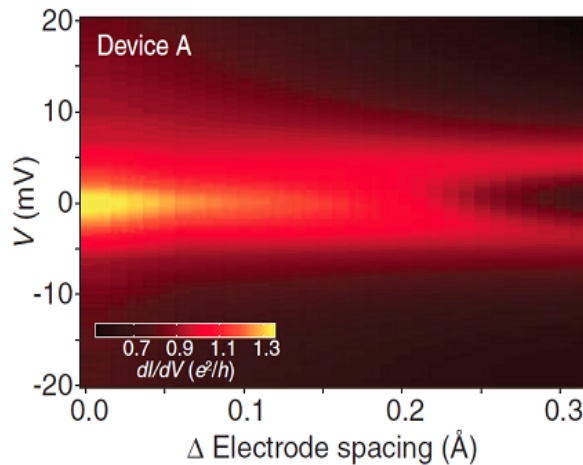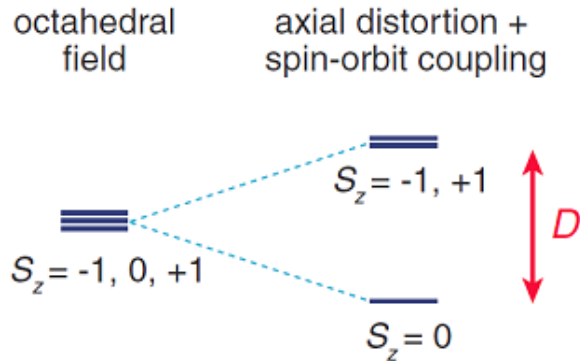
Split of Kondo peak by magnetic anisotropy energy D
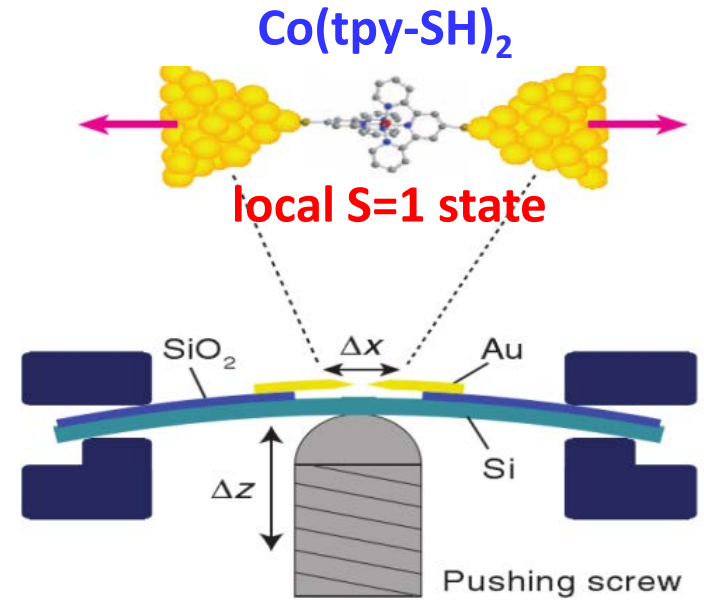
embedded in break junction

Challenges for theoretical study

Strong correlation:
- **Large DoF ($\sim 10^{23}$)**
- **High degeneracy**
- **Nonperturbative**

Related properties:
- **Mott metal-insulator transition**
- **Superconductivity; …**

Local quantum system: Highly accurate quantum mechanical methods

Environment (DoF $\sim 10^{23}$): Thermodynamics limit
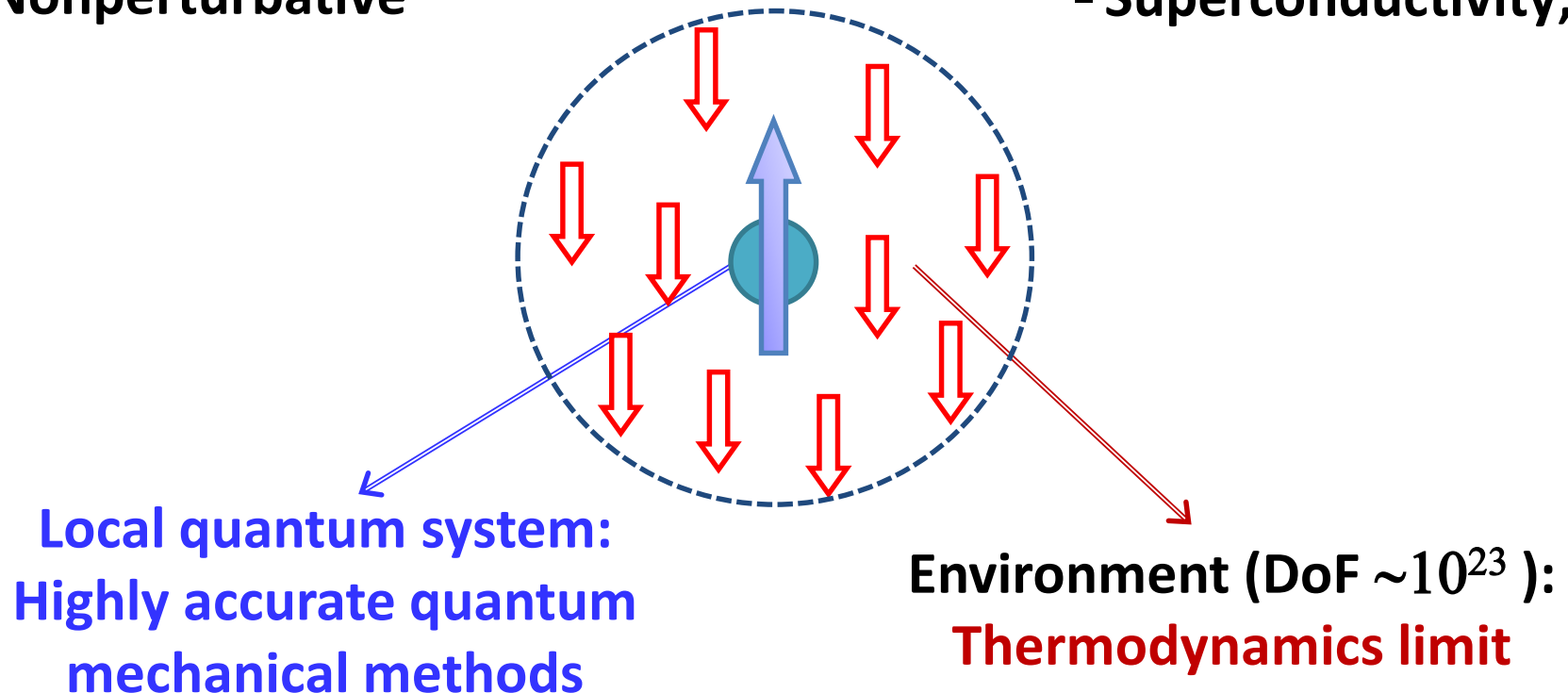
Challenges for theoretical study

- **Large composite systems with surface/interface**

- **Crucial roles of material environment**

- **Strong electron correlation (multi-reference nature)**

- **Computation of nonequilibrium response properties**

A first-principles based approach

- **DFT/post-DFT methods for geometric/electronic structure**

- **Quantum impurity model involving explicit e-e interaction and impurity-environment couplings**

- **On demand of accurate, universal & efficient solver/methods for strongly correlated impurity systems**

Quantum impurity model

$$H_{\text{total}} = \underbrace{H_{\text{impurity}}}_{} + \underbrace{h_{\text{env}}}_{} + H_{\text{sys-env}}$$

Arbitrary **Noninteracting** **Linear**

Multi-level Anderson impurity model

$$H_{\text{impurity}} = \sum_{us} E_{us}\hat{n}_{us} + \sum_{u} U_u \hat{n}_{u\uparrow}\hat{n}_{u\downarrow} + \sum_{u>v}\sum_{ss'} U_{uv}\hat{n}_{us}\hat{n}_{vs'}$$

$$h_{\text{env}} = \sum_{\alpha=\text{L,R}}\sum_{ks} \epsilon_{\alpha ks}\hat{d}^\dagger_{\alpha ks}\hat{d}_{\alpha ks}$$

$$H_{\text{sys-env}} = \sum_{\alpha uks} t_{\alpha uks}\hat{d}^\dagger_{\alpha ks}\hat{a}_{us} + \text{H.c.}$$

What else needed?

- **Temperature(s):** via Fermi func.
- Applied voltage/external field
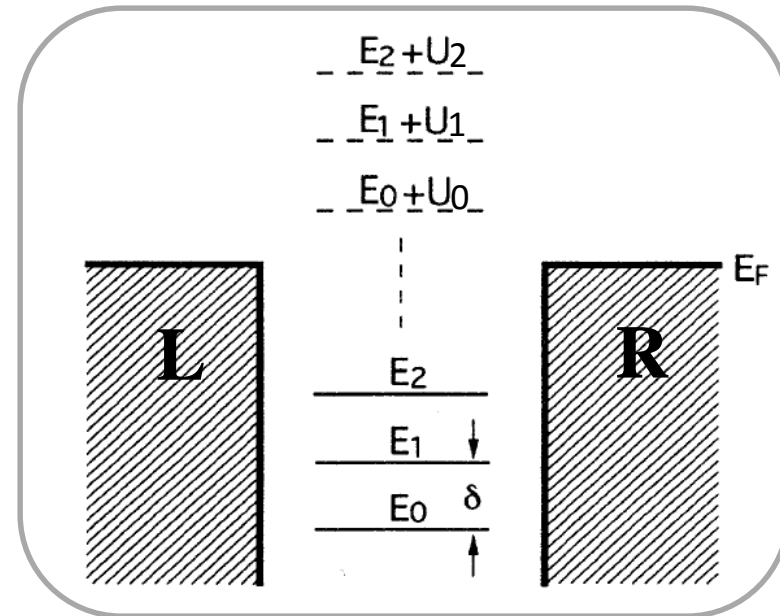
Quantum impurity model

$$H_{\text{total}} = H_{\text{impurity}} + h_{\text{env}} + H_{\text{sys-env}}$$

Arbitrary **Noninteracting** **Linear**

Gaussian-Wick's bath, completely characterized by

$$\langle \hat{F}^{\sigma}_{\alpha us}(t) \hat{F}^{\bar{\sigma}}_{\alpha vs}(0) \rangle^{\text{eq}}_{\text{B}} = \frac{1}{\pi} \int_{-\infty}^{\infty} d\omega \frac{e^{\sigma i \omega t} J^{\sigma}_{\alpha uvs}(\omega)}{1 + e^{\sigma \beta_\alpha \omega}}$$

where $\sigma = +, -$
and $\bar{\sigma} \equiv -\sigma$

Fluctuation-dissipation theorem

$$H_{\text{sys-env}} = \sum_{\alpha uks} t_{\alpha uks} \hat{d}^{\dagger}_{\alpha ks} \hat{a}_{us} + \text{H.c.} = \sum_{\alpha us} (\hat{F}^{+}_{\alpha us} \hat{a}^{-}_{us} + \hat{a}^{+}_{us} \hat{F}^{-}_{\alpha us})$$

where $\hat{a}^{+}_{us} \equiv \hat{a}^{\dagger}_{us} \equiv (\hat{a}^{-}_{us})^{\dagger}$ and $\hat{F}^{+}_{\alpha us} \equiv \sum_{k} t_{\alpha uks} \hat{d}^{\dagger}_{\alpha ks} \equiv (\hat{F}^{-}_{\alpha us})^{\dagger}$

hybridizing bath
environment modes

Existing Methods

- **Numerical renormalization group (NRG) :** Wilson (1975); Costi (1997); Weichselbaum and von Delft (2007)

- **Single- and many-body Green functions:** Kadanoff & Baym (1962); Myohanen et al. (2008); Thygesen & Rubio (2008)

- **Quantum Monte Carlo**: Hirsch & Fye (1986); Gull et al. (2011)

- **Real-time path-integral:** Muhlbacher & Rabani (2008); Weiss & Egger (2008); Segal, Millis & Reichman (2010)

- **Multi-layer-multi-configuration time-dependent Hartree:** Meyer (1990); Wang & Thoss 20(03)

- **Time-dependent density functional theory:** Kurth & Gross et al. (2010); Stefanucci & Kurth (2011)

- **Exact diagonalization:** Dagotto (1994); Caffarel & Krauth (1994); Si et al. (1994)

Quantum dissipation theories

> Let $\boxed{\rho(t) \equiv \mathrm{tr}_{\mathrm{B}}[\rho_{\mathrm{T}}(t)]}$ (reduced system density operator)

Total composite one satisfies **Schrödinger equation**:

$$\dot{\rho}_{\mathrm{T}}(t) = -i[H_{\mathrm{S}} + h_{\mathrm{B}} + H_{\mathrm{SB}}, \rho_{\mathrm{T}}(t)] \quad \text{(Liouville-von Neumann eq.)}$$

- **Quantum master equations to open system: Problems**

$$\dot{\rho}(t) = -(i\mathcal{L}_{\mathrm{S}} + \mathcal{R}_t)\rho(t)$$

(Nonperturb. & time-dep $\mathcal{R}$???)
dissipation superoperator

- **Feynman-Vernon path integral functional formalism (1963)** for the reduced system propagator:

$$\rho(t) = \mathcal{U}(t, t_0)\rho(t_0)$$

(Numerically very expensive!!!)

- **Hierarchical equations of motion method**: **Exact & tractable**

Outline

➤ Quantum mechanics of open systems: Background

➤ **The HEOM formalism: Machineries & applications**

➤ HEOM-QUICK package

➤ The DEOM theory and applications

➤ Prospects

Hierarchical equations of motion (HEOM)

$$\dot{\rho}_{\mathbf{j}}^{(n)} = -\left(i\mathcal{L}_{\mathrm{S}} + \sum_{r=1}^{n} \gamma_{jr}\right)\rho_{\mathbf{j}}^{(n)} - i\sum_{j} \mathcal{A}_{\bar{j}}\rho_{\mathbf{j}j}^{(n+1)} - i\sum_{r=1}^{n} \mathcal{C}_{jr}\rho_{\mathbf{j}_r^-}^{(n-1)}$$

Tier n

0

Reduced **system** density operator

1

2
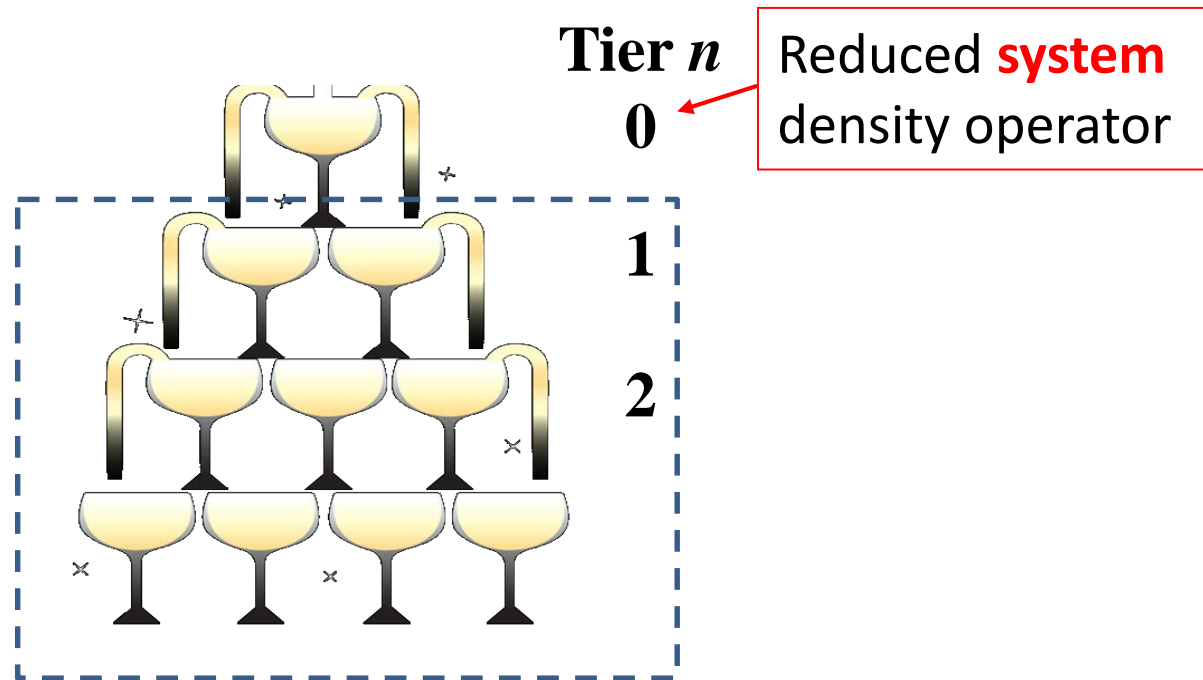
What do we obtain from HEOM?

$$\dot{\rho}_{\mathbf{j}}^{(n)} = -\left(i\mathcal{L}_{\mathrm{S}} + \sum_{r=1}^{n} \gamma_{jr}\right)\rho_{\mathbf{j}}^{(n)} - i\sum_{j}\mathcal{A}_{\bar{j}}\rho_{\mathbf{j}j}^{(n+1)} - i\sum_{r=1}^{n}\mathcal{C}_{jr}\rho_{\mathbf{j}_r^-}^{(n-1)}$$

➢ **Electronic structure:**

$$\boldsymbol{\rho}^{\mathrm{st}} \equiv \left\{\rho^{(0)}; \rho_{\mathbf{j}}^{(n>0)}\right\}^{\mathrm{st}} \qquad \textbf{(steady-state solutions)}$$

➢ **Expectation values:**

$$A(t) = \mathrm{tr}[\hat{A}\rho(t)] = \mathrm{tr}\left[\hat{A}\,\rho^{(0)}(t)\right] \qquad \textbf{(system properties)}$$

Electric current (hybrid system-reservoir property):

$$I_\alpha(t) = -2\,\mathrm{Im}\sum_{j\in\alpha}\mathrm{tr}\left[\hat{a}_\mu\,\rho_j^{(1)}(t)\right]$$

What do we obtain from HEOM?

$$\dot{\rho}_{\mathbf{j}}^{(n)} = -\left(i\mathcal{L}_{\mathrm{S}} + \sum_{r=1}^{n} \gamma_{jr}\right)\rho_{\mathbf{j}}^{(n)} - i\sum_{j} \mathcal{A}_{\bar{j}}\rho_{\mathbf{j}j}^{(n+1)} - i\sum_{r=1}^{n} \mathcal{C}_{jr}\rho_{\mathbf{j}_r^-}^{(n-1)}$$

➢ **Correlation functions:** $\quad \langle \hat{A}(t)\hat{B}(0)\rangle = \langle\!\langle A|\mathcal{G}(t)|B\rho^{\mathrm{st}}\rangle\!\rangle$

Note also the **time-reversal identity**: $\boxed{\langle \hat{B}^\dagger(0)\hat{A}(t)\rangle = \langle \hat{A}^\dagger(t)\hat{B}(0)\rangle^*}$

- **Nonequilibrium Green functions (nGFs) and spectrums**

$$G_{uv}^>(t) \equiv \langle \hat{a}_u^\dagger(t)\hat{a}_u(0)\rangle$$

$$G_{uv}^<(t) \equiv \langle \hat{a}_u(0)\hat{a}_u^\dagger(t)\rangle$$

and $\quad G_{uv}^r(t) \equiv -i\theta(t)\langle\{\hat{a}_v^\dagger(t), \hat{a}_u(0)\}\rangle$

- **Electric and heat currents versus nGFs**

$$I_\alpha = \frac{ie}{h}\int d\epsilon\, 2\Delta_\alpha(\epsilon)\Big\{G^<(\epsilon) + 2\,if_\alpha(\epsilon)\,\mathrm{Im}\,[G^r(\epsilon)]\Big\}$$

$$J_\alpha^{\mathrm{H}} = \frac{i}{h}\int d\epsilon\,(\epsilon - \mu_\alpha)\,2\Delta_\alpha(\epsilon)\Big\{G^<(\epsilon) + 2\,if_\alpha(\epsilon)\,\mathrm{Im}\,[G^r(\epsilon)]\Big\}$$

HEOM formalism (path integral based)

> **Bosonic: Tanimura & Kubo (1989); Shao & Yan (2004); YJY et al (2005)**

Reduced **system** density operator

Auxiliary Density Operators (*Physical* meanings?)

Tier 0
1
2
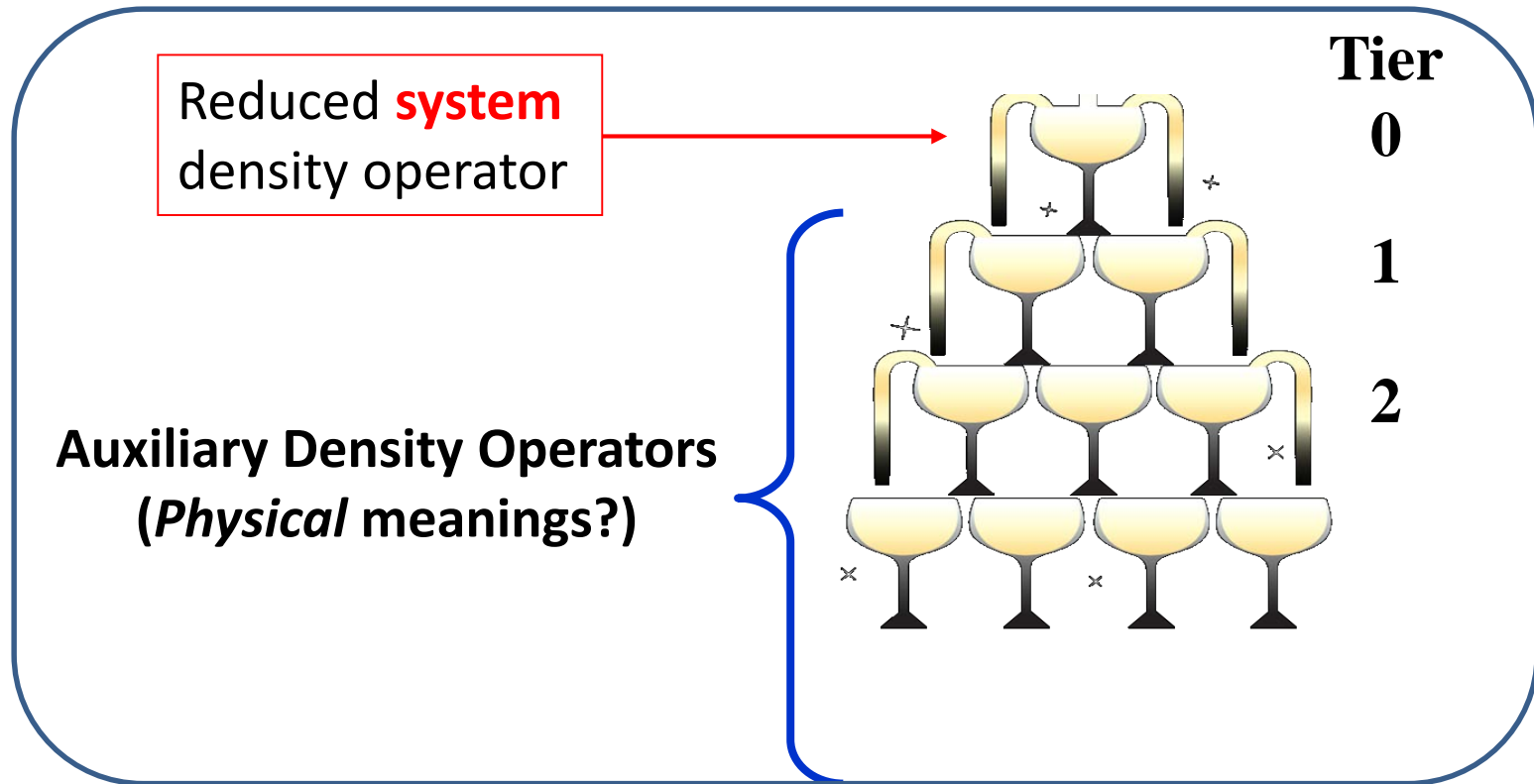
> **Fermionic: J. S. Jin, X. Zheng, YJY (2008), J. Chem. Phys., 128: 234703**

Grassmann numbers: $xy = -yx$ (rather than c-numbers)

HEOM formalism (path integral based)

size ∝ *K*

Reduced **system** density operator

Tier
0
1
2

Auxiliary Density Operators
(*Physical* meanings?)

Truncation at level *L*
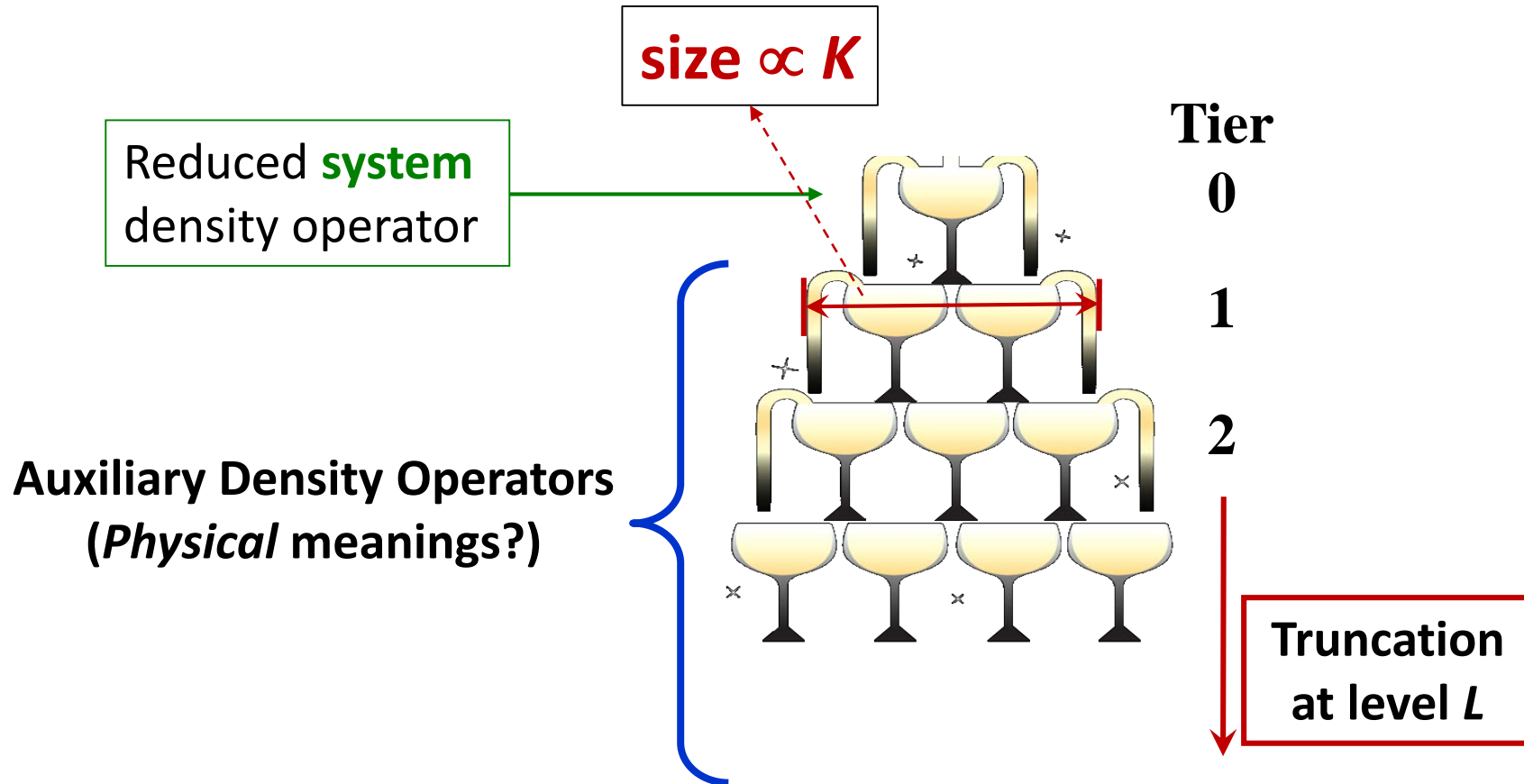
- *K* & *L* determine the size (computational cost) of HEOM
- *K*-**dissipatons** are used to unravel **reservoir memory**
- *K* increases **exponentially as *T* → 0**

HEOM formalism: Machineries (since 2009)

2009: Efficient propagator with on-the-fly numerical filter algorithm

2010: Padé spectrum decomposition of Bose/Fermi function

2011: Mixed Heisenberg-Schrödinger dynamics for multiple-dimensional spectroscopy evaluations

2015: Derivative hierarchy truncation scheme (**prescription-invariance**)

2015: Symmetry-determined pre-screening sparse-matrix method

2017: Efficient steady-state solver: Self-consistent iteration method

2019: Fano spectrum decomposition of Bose/Fermi function

- Q Shi (2017-): Matrix-product and clustered ADOs methods

- JS Shao/JS Cao & JL Wu/Y Zhao: Stochastic + HEOM

- JS Cao/A Aspuru-Guzik: Machine Learning + HEOM

- Kreisbeck et al (2011)/Strümpfer & Schulten (2012): Parallel/GPU codes

Unravel reservoir bath memory into K components

$$\langle \hat{F}^+_{\alpha u s}(t) \hat{F}^-_{\alpha v s}(0) \rangle^{\mathrm{eq}}_{\mathrm{B}} \propto \int_{-\infty}^{\infty} \mathrm{d}\omega \, e^{i\omega t} f^{\mathrm{Fermi}}(\omega; T) J_{\alpha u v s}(\omega)$$

$$\simeq \sum_{k=1}^{K} \eta_{\alpha k u v s} e^{-\gamma_k^\alpha t}$$

$K = \boldsymbol{N} + N'$

Sum-over-poles (SOP)

HEOM construction basis set

Tier

0

K

1

2

Reducing the horizontal K-dimension

e.g. Bose function: $\quad \dfrac{1}{1 - e^{-x}} = \dfrac{1}{2} + \dfrac{1}{2}\dfrac{\cosh(x/2)}{\sinh(x/2)}$
$(x = \beta\omega)$

➤ **MSD (Matsubara spectrum decomposition) -- Textbook**

$$\frac{1}{1 - e^{-x}} \approx \frac{1}{2} + \frac{1}{x} + \sum_{m=1}^{N}\left(\frac{1}{x + i2\pi m} + \frac{1}{x - i2\pi m}\right)$$

➤ **PSD (Pade spectrum decomposition) – Numerical standard now**

$$\frac{1}{1 - e^{-x}} \approx \frac{1}{2} + \frac{1}{x} + \sum_{j=1}^{N}\left(\frac{\eta_j}{x + i\xi_j} + \frac{\eta_j}{x - i\xi_j}\right)$$

$\{\xi_j\}>0$ & $\{\eta_j\}>0$:
Machine-precision !

- T. Ozaki, Phys. Rev. B **75**, 035123 2007
- J Hu, RX Xu, & YJY, *JCP* **133** (2010) 101106; **134**, 244106 (2011)

Superiority: PSD >> PFD > MSD

MSD (tradition method)

PFD (partial fraction decom.)
Croy & Saalmann, *Phys. Rev.* B 80, 073102 (2009) ; J Xu, RX Xu, YJY, *Chem. Phys.* 370, 109 (2010)

PSD (standard now)

Reducing the horizontal K-dimension

Search for the best SOP schemes for Fermi/Bose function

Padé
decomposition
scheme **(2010)**

Fano decomposition
scheme **(2019,
submitted)**

**Matsubara scheme
based HEOM (< 2010)**

**Non-SOP schemes
(2016,2017)**
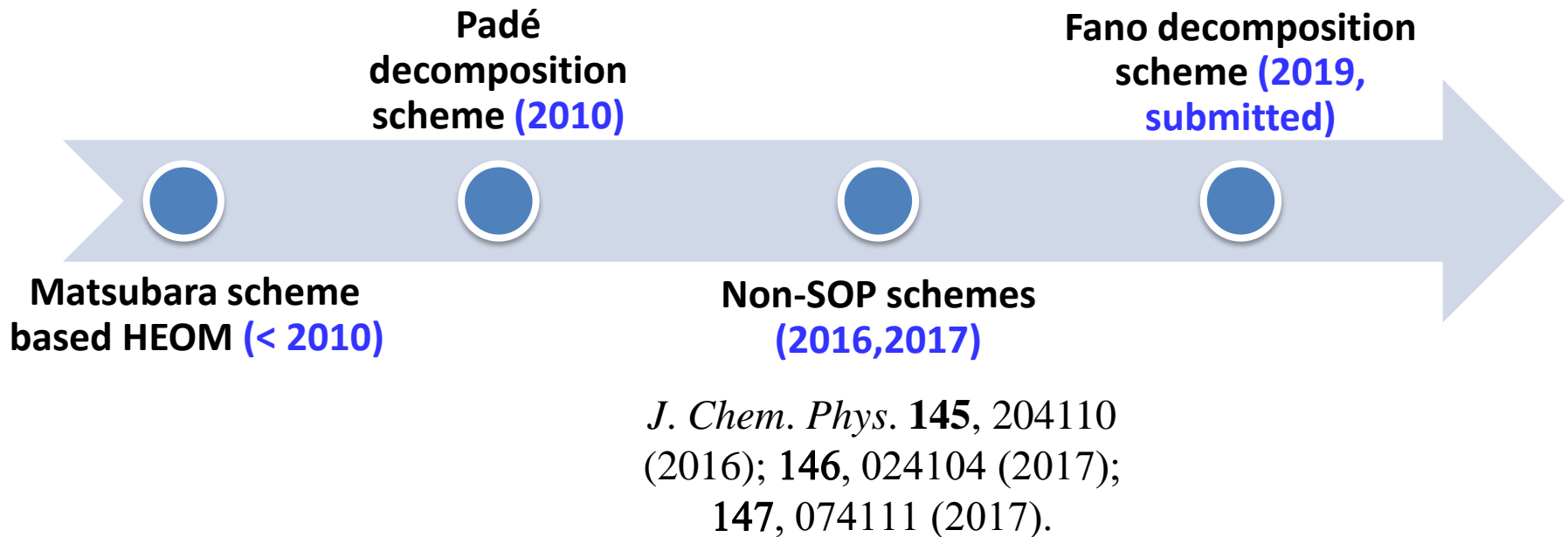
J. Chem. Phys. **145**, 204110
(2016); **146**, 024104 (2017);
147, 074111 (2017).

Search for the best SOP schemes for Fermi/Bose function

- **Focusing on the low-*T* domain w.r.t. a reference high T_0**

$$\Delta f(\omega, T; T_0) \equiv f^{\mathrm{Fermi}}(\omega, T) - f^{\mathrm{Fermi}}(\omega, T_0)$$
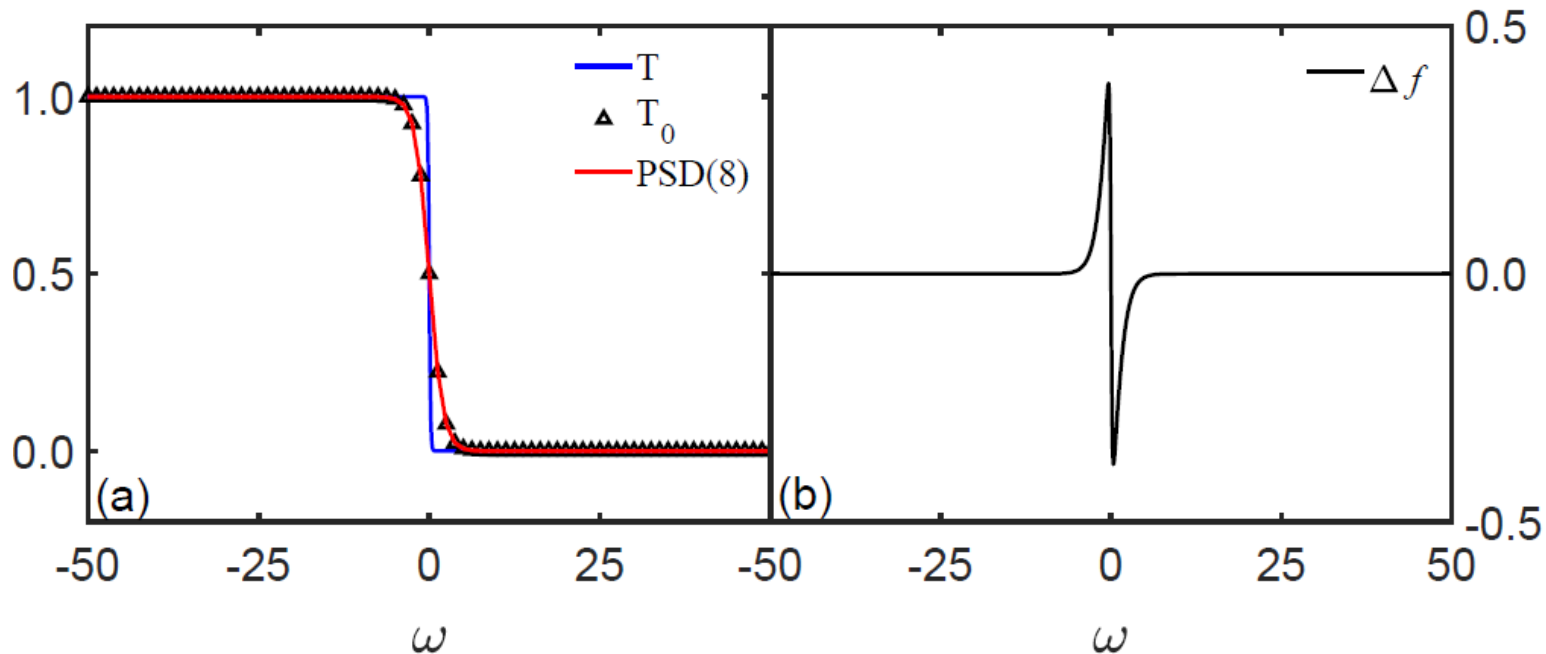
Search for the best SOP schemes for Fermi/Bose function

• **Focusing on the low-T domain w.r.t. a reference high T_0**

$$\Delta f(\omega, T; T_0) \approx \sum_{d=1}^{D} \frac{b_d \omega}{[1 + (a_d \omega)^2]^{j_d}}$$

Fano spectrum decomposition
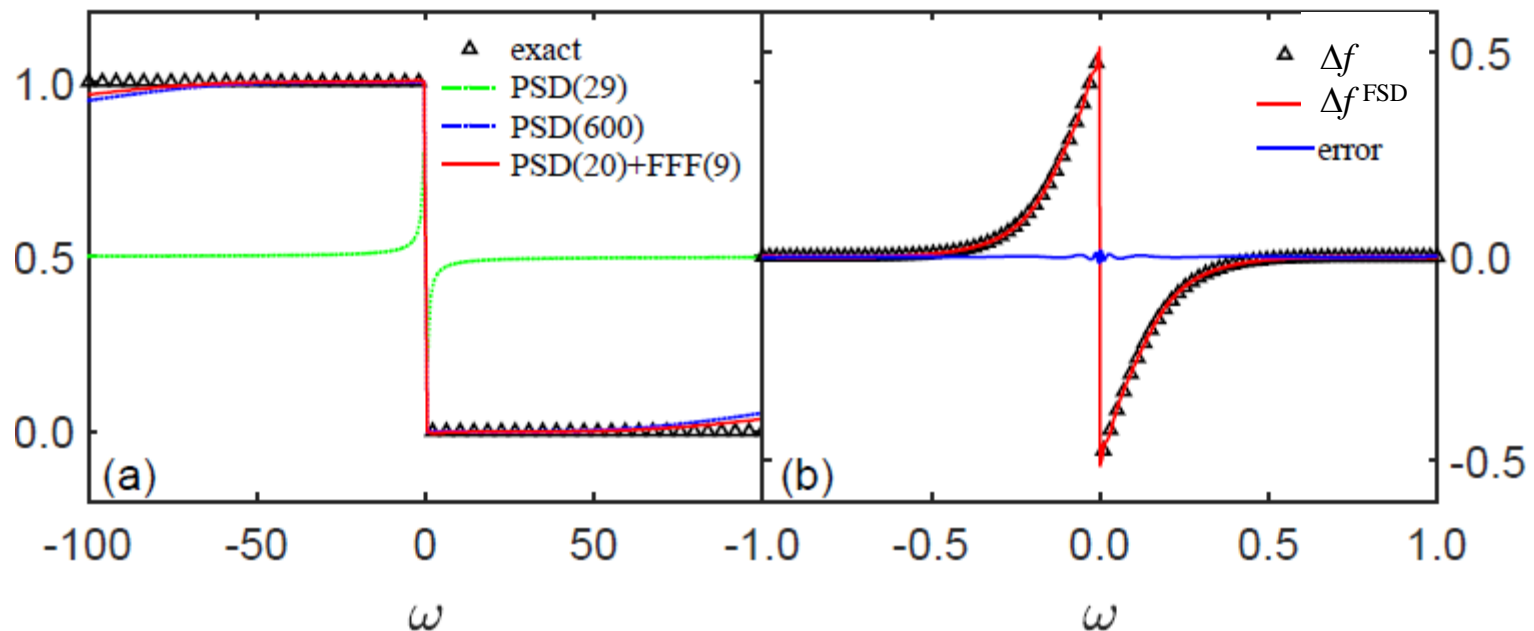
Superiority: FSD >> PSD for extremely low-T cases

Toward Experimental Low-T Regimes

Liquid N_2: 77 K;   Liquid He: 4 K

HEOM evaluation on SIAM:
Spectrum in Kondo regime

$T = 174$ K

$T = 23$ K
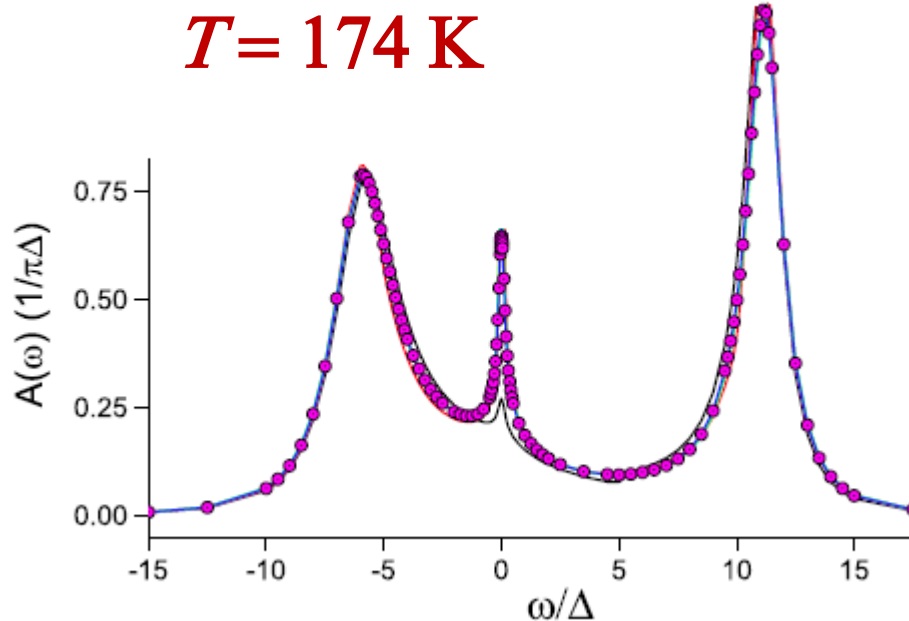
PSD scheme

Li, Zheng, YJY et al. *PRL* **109**, 266403 (2012)
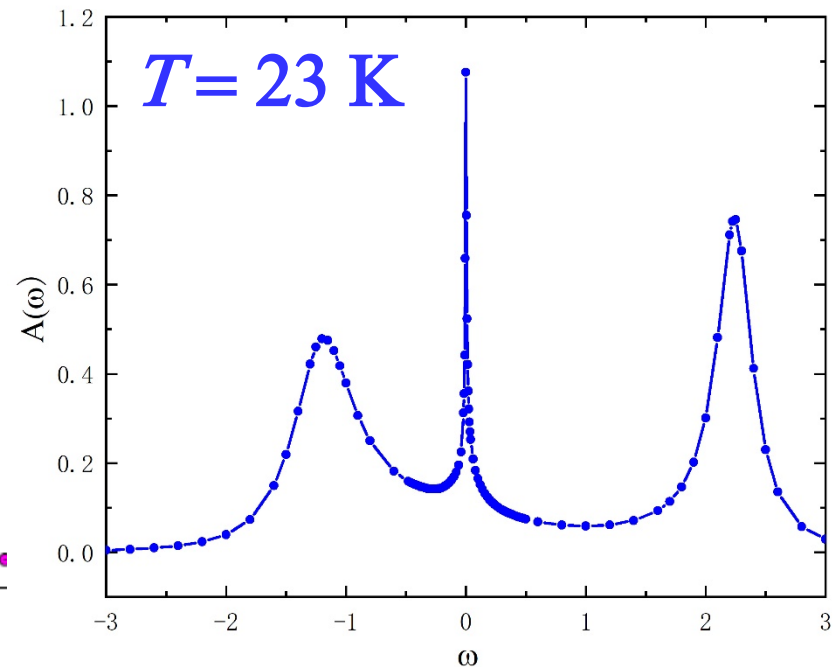
FSD scheme

Zhang, Zheng et al (unpublished)

HEOM: Nonperturbative in Nature

Existence of an exact and finite hierarchy level truncation

➢ **For fermion HEOM** $\rho_{j_1 \cdots j_n}^{(n > n_{\max})} = 0;$ $\qquad n_{\max} = N_\sigma N_u N_\alpha K$

$N_\sigma = 2$: **Parity of fermions**
N_v : **# of hybridization system modes**
N_α : # of baths (α = L,R)
K : Size of basis set (a large number)

➢ **For the exact $\rho^{(0)}$:** $\rho_{j_1 \cdots j_n}^{(n > n_{\max}^{(0)})} = 0;$ $\qquad n_{\max}^{(0)} = 2 N_\sigma N_u$

Han, Zheng, YJY et al, *J. Chem. Phys.* 148, 234108 (2018)

HEOM: Nonperturbative in Nature

Existence of an exact and finite hierarchy level truncation

TABLE I. $n_\uparrow$, $n_\downarrow$, and $\rho_{\uparrow\uparrow}$ of an SIAM calculated at different truncation tiers. The converged (unconverged) digits are marked by normal (italic) font. See the main text for the values of parameters.

L	$n_\uparrow$	$n_\downarrow$	$\rho_{\uparrow\uparrow}$
1	0.562 479 725 093	0.399 843 457 389	0.349 149 952 492
2	0.499 440 108 806	0.461 089 036 198	0.283 947 704 486
3	0.503 648 803 692	0.454 958 233 447	0.287 476 336 354
4	0.502 9*13 018 977*	0.456 3*07 175 157*	0.286 6*20 580 229*
5	0.502 9*53 417 487*	0.456 2*24 386 764*	0.286 6*84 865 267*
6	0.502 949 *750 959*	0.456 235 *095 328*	0.286 678 *062 145*
7	0.502 949 706 *728*	0.456 235 182 *013*	0.286 678 *050 832*
8	0.502 949 709 239	0.456 235 179 355	0.286 678 049 926
9	0.502 949 709 239	0.456 235 179 356	0.286 678 049 925
10	0.502 949 709 239	0.456 235 179 356	0.286 678 049 925

Accurate

Exact

Han, Zheng, YJY et al, *J. Chem. Phys.* 148, 234108 (2018)

HEOM: Numerical Accuracy

Local magnetic susceptibility

Electric current
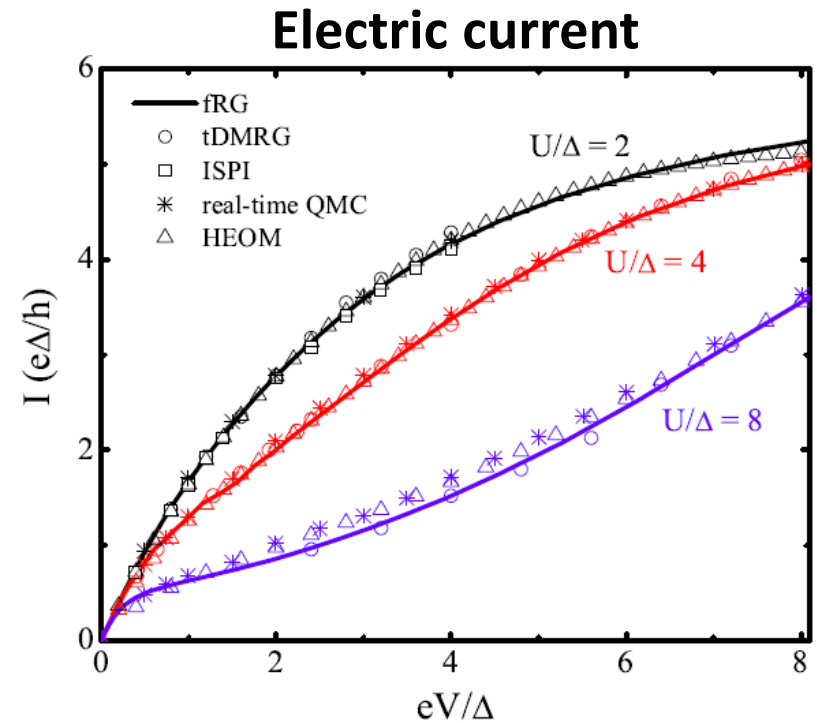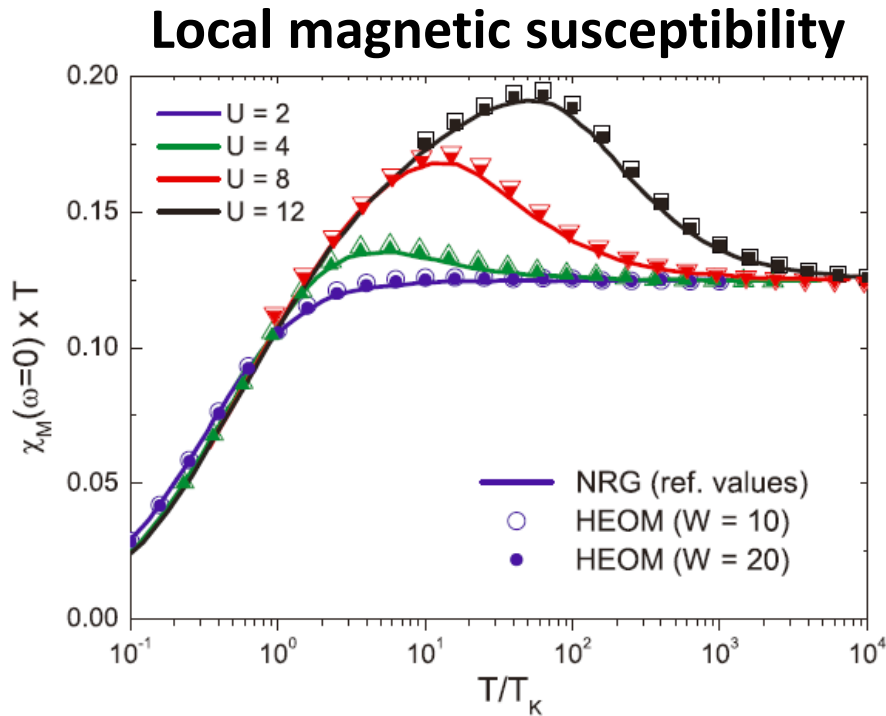
HEOM agree well with the standard methods such as NRG

J. Eckel et al., *New J. Phys.* **12**, 043042 (2010)
Wang and Zheng et al., *Phys. Rev. B* **88**, 035129 (2013)
Zheng, Yan, and Di Ventra, *Phys. Rev. Lett.* **111**, 086601 (2013)

HEOM: Numerical Accuracy

Single Impurity Anderson Model
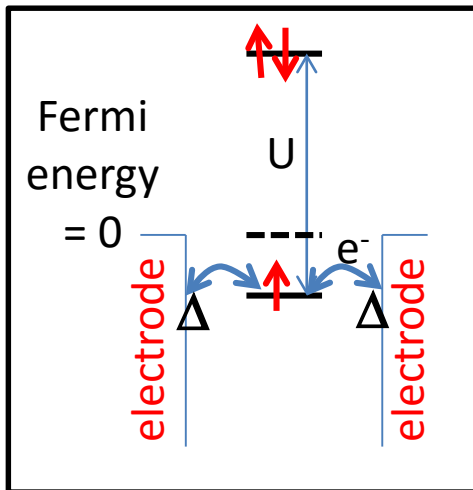
Δ: s-b coupling

U: Coulomb energy

Comparison to NRG evaluation on symmetric SIAM at a finite *T*
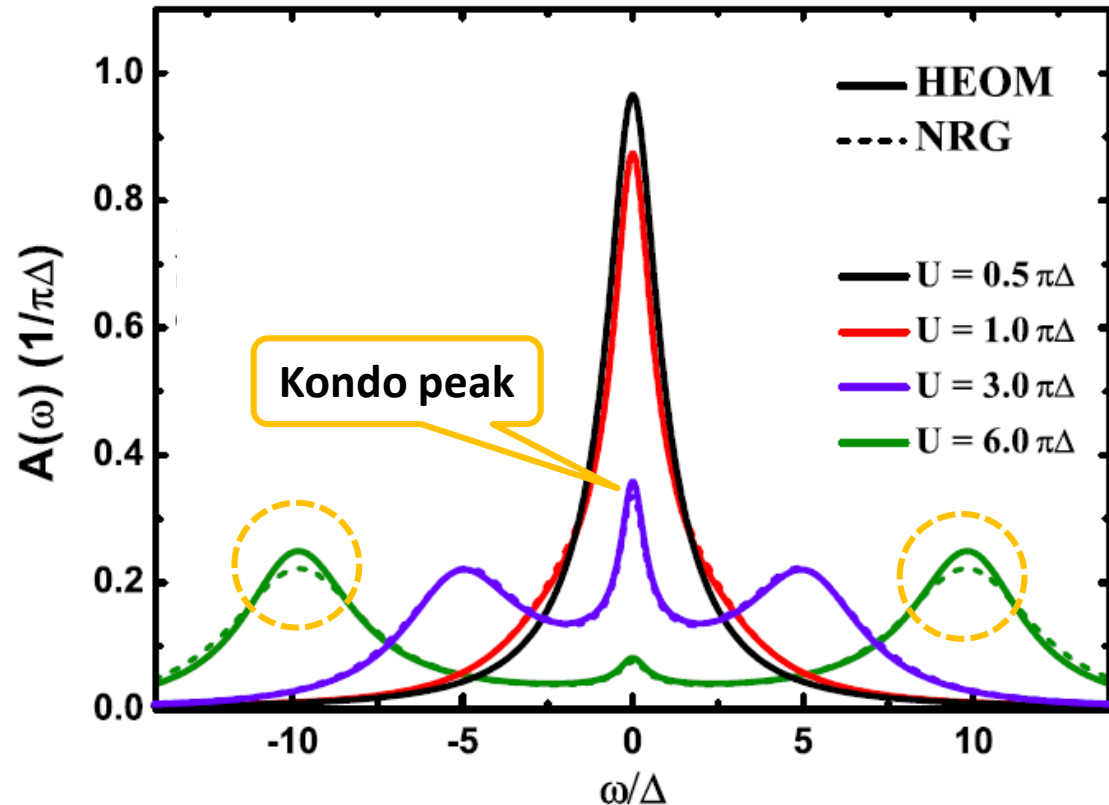
HEOM often more accurate & efficient than the "standard" methods

HEOM: Applications

Memristive system
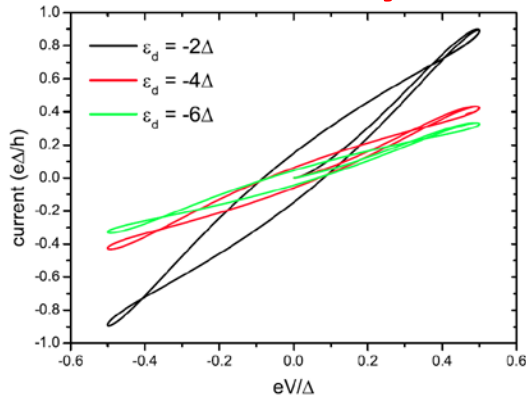
Phys. Rev. Lett. **111, 086601 (2013)**

Thermopower
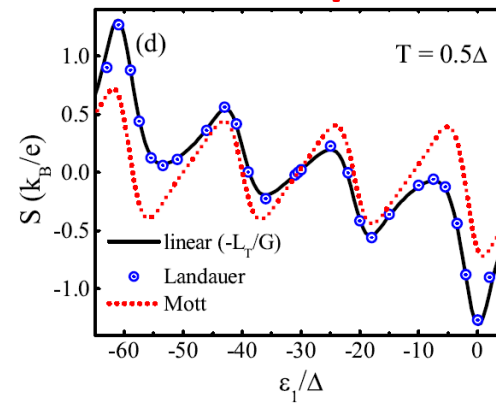
Phys. Rev. B **90, 165116 (2014)**

Impurity solver for DMFT
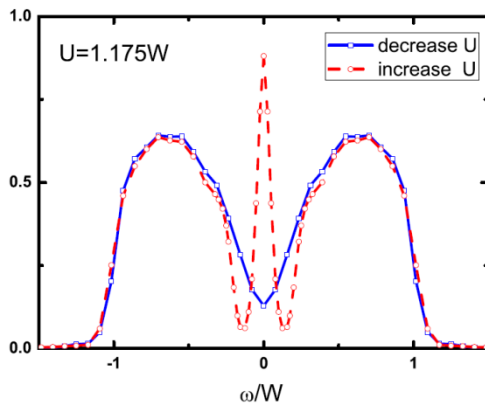
Phys. Rev. B **90, 045141 (2014)**

Measurement of local *T*
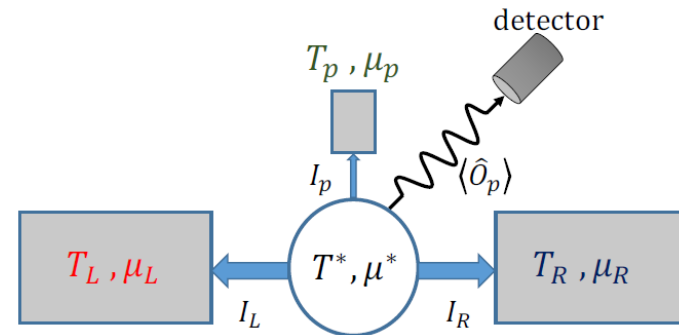
Phys. Rev. B **91, 205106 (2015)**

Outline

Outline

> **HEOM-QUICK package**

QUICK: QUantum **I**mpurity with a **C**orrelated **K**ernel

Combined DFT+HEOM approach for reality systems/processes

geometric and electronic structure (DFT)

parameters ⇨

strongly correlated quantum impurity model (HEOM)

Advanced Review

HEOM-QUICK: a program for accurate, efficient, and universal characterization of strongly correlated quantum impurity systems
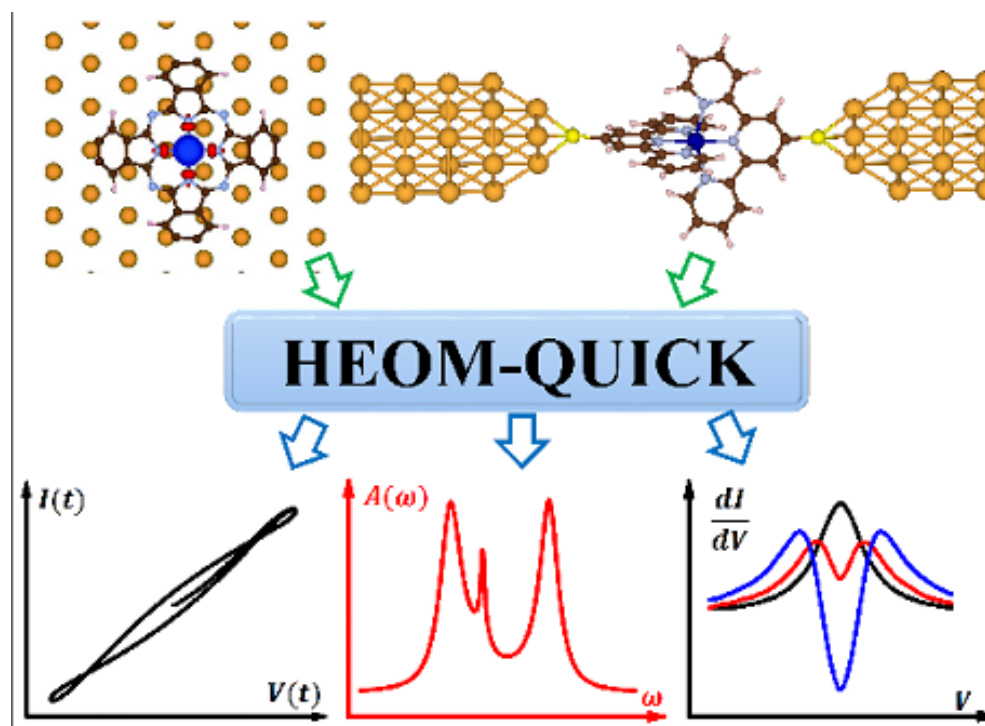
LvZhou Ye,[1] Xiaoli Wang,[1] Dong Hou,[1] Rui-Xue Xu,[1] Xiao Zheng[1]* and YiJing Yan[2]

HEOM-QUICK: a program for accurate, efficient, and universal characterization of strongly correlated quantum impurity systems

LvZhou Ye,[1] Xiaoli Wang,[1] Dong Hou,[1] Rui-Xue Xu,[1] Xiao Zheng[1]* and YiJing Yan[2]

d-CoPc/Au(111)

J. Chem. Phys. **141, 084713 (2014)**

few-layer CoPc/Pb(111)
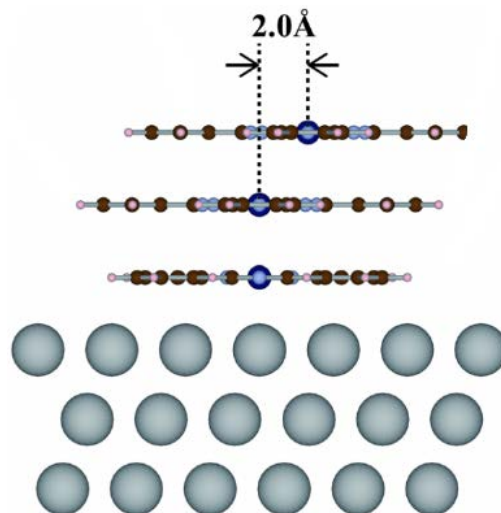
J. Chem. Phys. **145, 154301 (2016)**

FePc/Au(111)
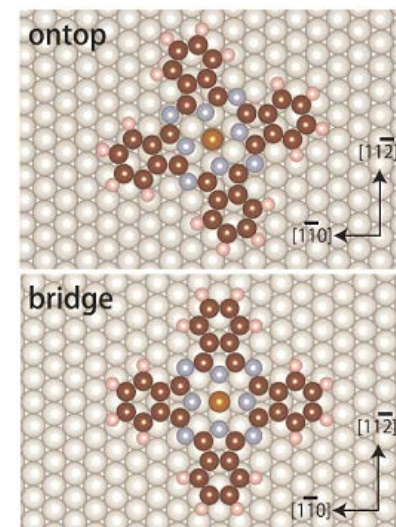
Phys. Rev. B **93, 125114 (2016)**

Au—Co(tpy-S)$_2$—Au

stretch   stretch
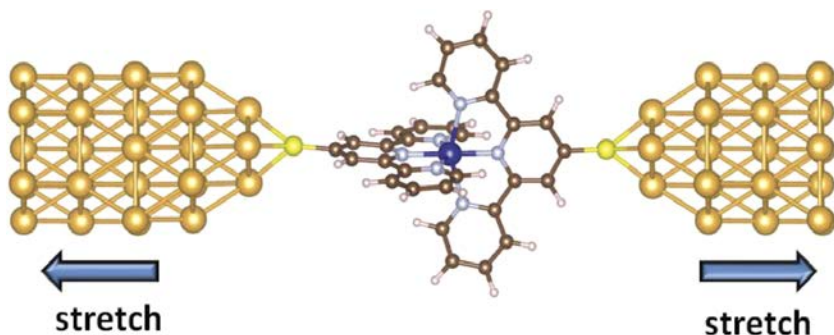
J. Chem. Phys. **144, 034101 (2016)**

FeOEP/Pb(111)

J. Phys. Chem. Lett. **9, 2418 (2018)**

Experiment

Kondo peak at low T

Zhao, Yang, and Hou et al. *Science* 309, 1542 (2005)

FIG. 2. (a) The molecular structure of the isolated CoPc. For the d-CoPc, the eight hydrogen atoms in the dashed squares are dissociated. (b) and (c) depict the top and side views of the optimized geometry of the composite d-CoPc/Au(111) adsorption system, respectively.

Yu, Zheng, and Yang et al. *J. Chem. Phys.* **141, 084713 (2014)**

Construct Anderson impurity model (AIM) from DFT+U result

Projected DOS of Co *d*-orbitals

Low *T*

Yu, Zheng, and Yang et al. *J. Chem. Phys.* 141, 084713 (2014)
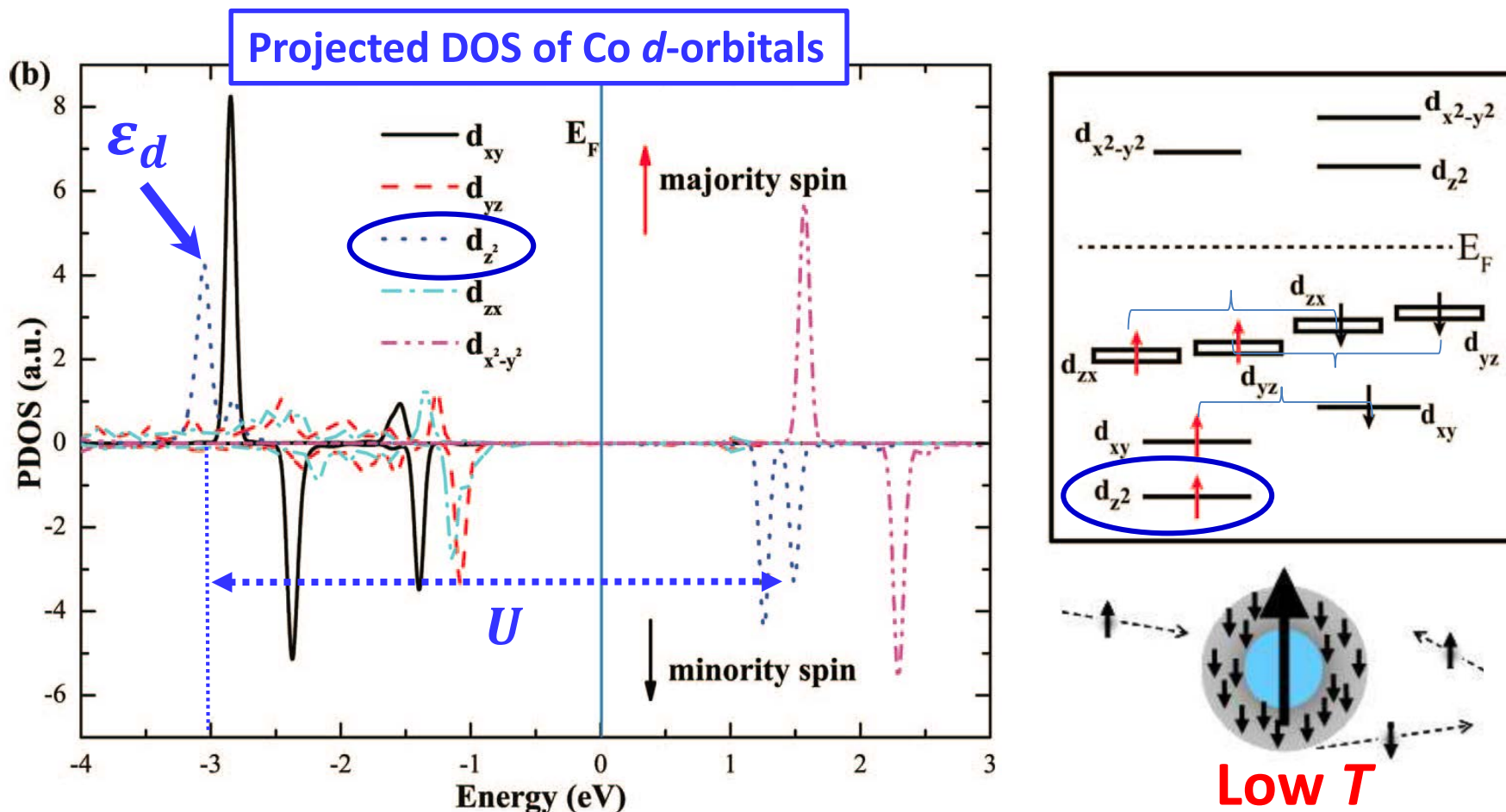
A. Kondo effect in d-CoPc/Au(111) composite

dI/dV spectra calculated by HEOM
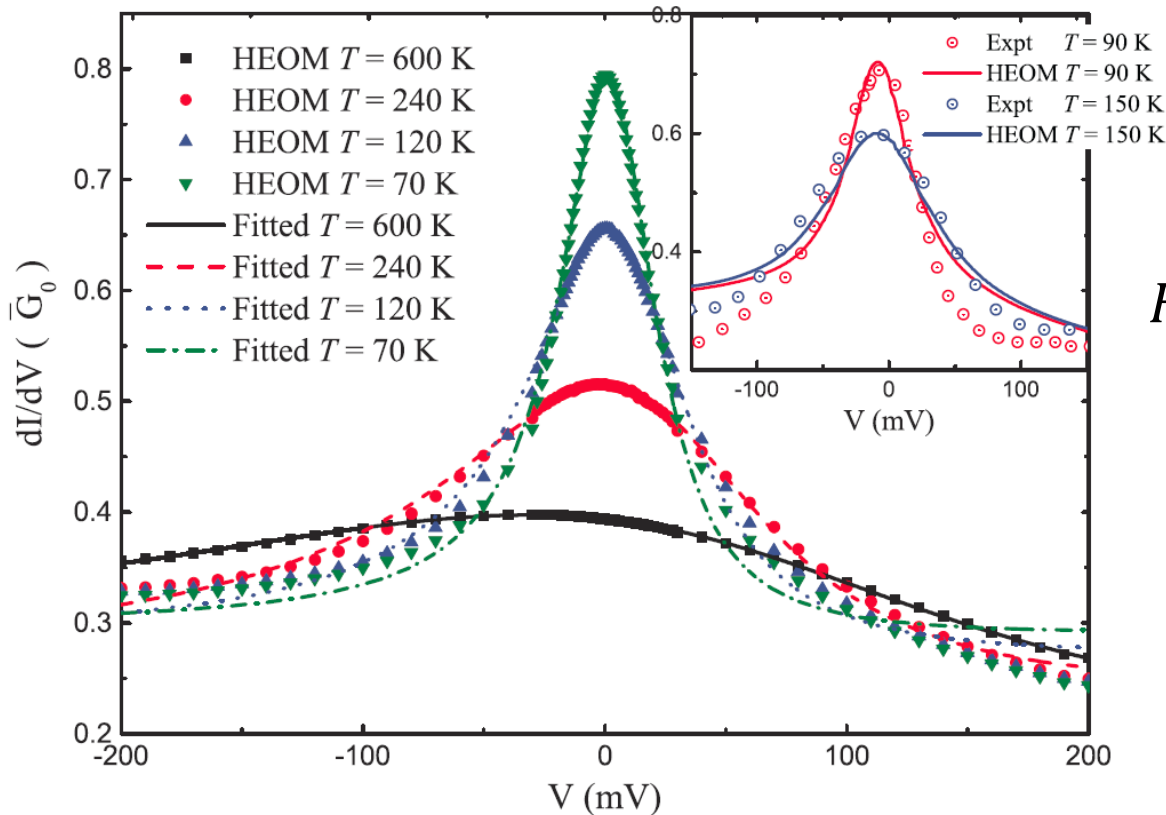
impurity Hamiltonian

$$H_{imp} = \varepsilon_d(\hat{n}_\uparrow + \hat{n}_\downarrow) + U\hat{n}_\uparrow\hat{n}_\downarrow$$

reservoir spectral func

$$\Delta(\omega) = \frac{\Delta W^2}{(\omega - \mu)^2 + W^2}$$

Kondo temperature $T_K = $ **200.2 ± 2.5 K** (*theo*) **vs 208 K** (*expt*)

High T_K ⇐ **strong coupling btw Co d_{z^2} orbital and Au states**

Yu, Zheng, and Yang et al. *J. Chem. Phys.* **141**, 084713 (2014)

Experiment

FeOEP/Pb(111)
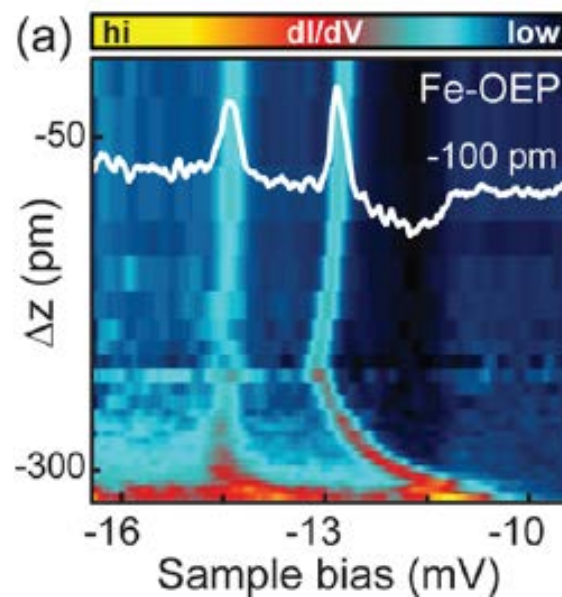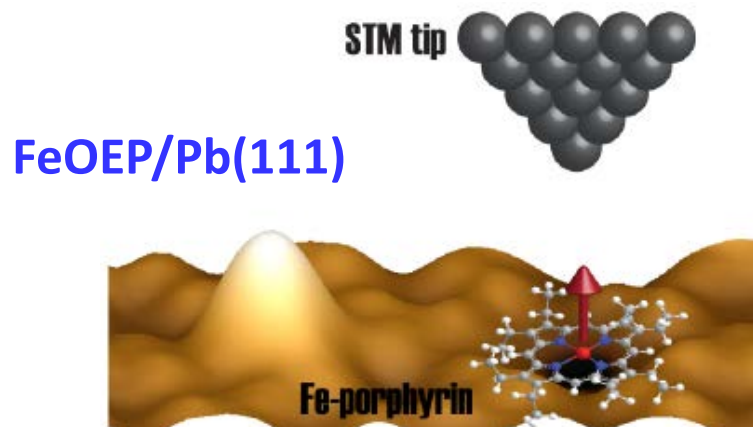
Magnetic anisotropy (D)
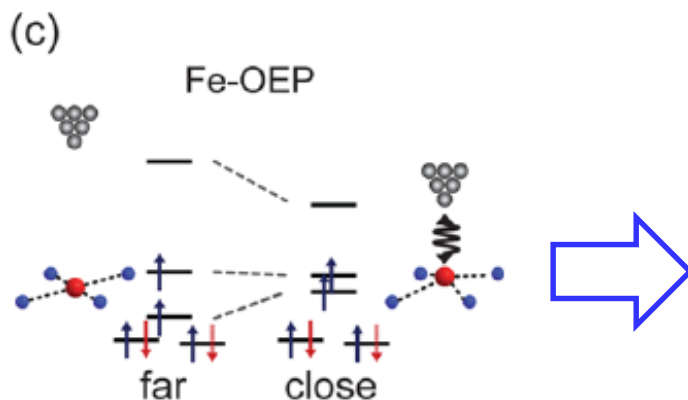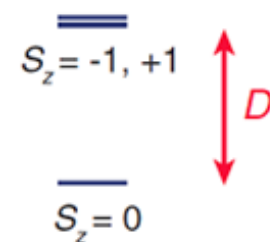
shifting of Fe 3d levels

Benjamin et al. *Nano Lett.* **15, 4024 (2015)**
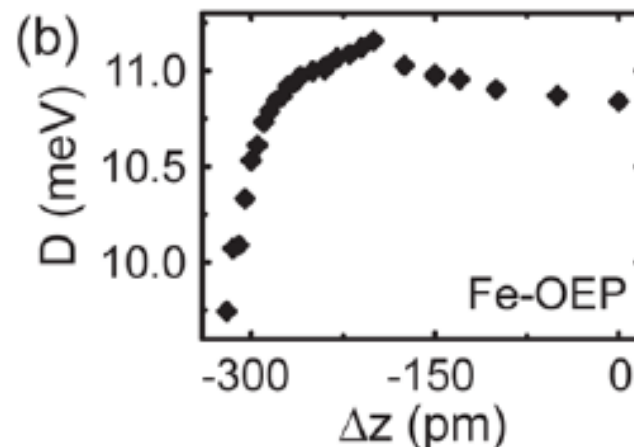
- **Evolution of geometric structure**

XL Wang, L. Yang, LZ Ye, X. Zheng, YJY. J. Phys. Chem. Lett. 9, 2418 (2018)
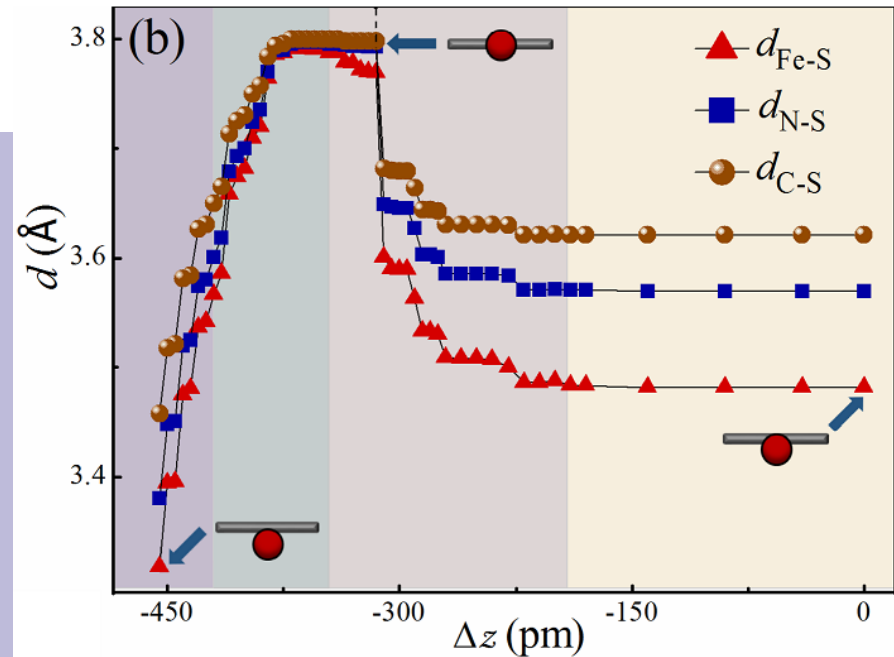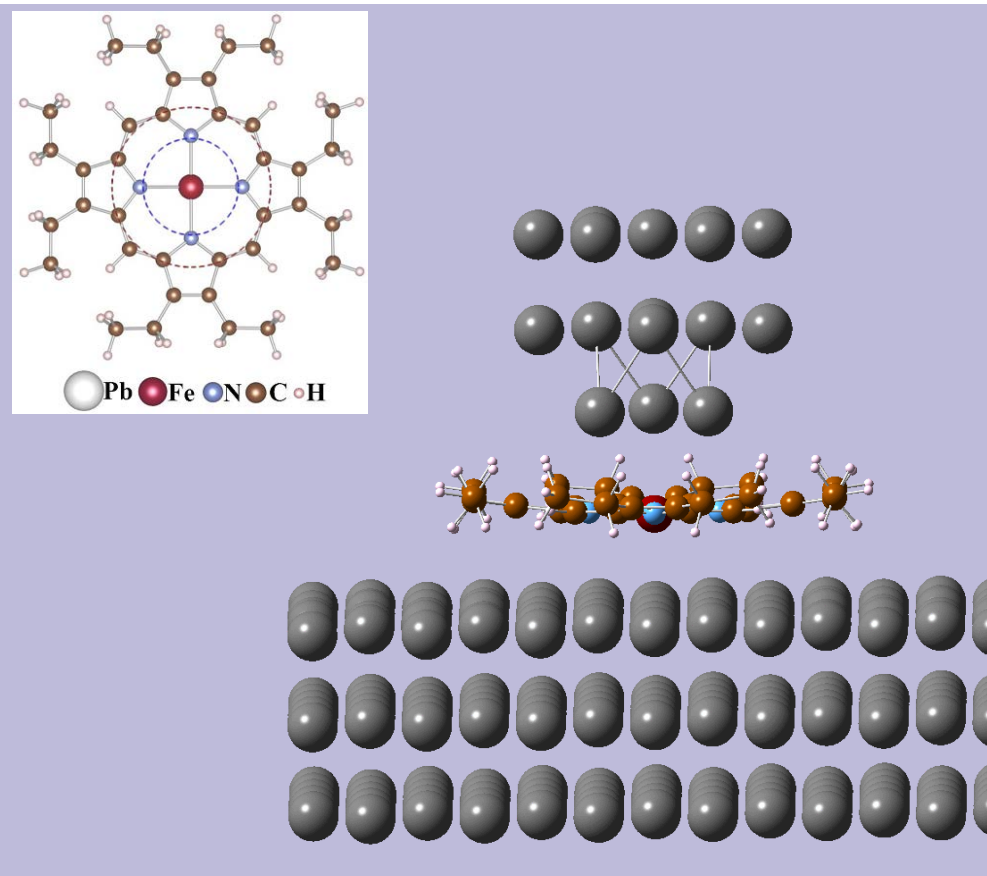
B. STM tip controlled magnetic anisotropy

Tuning of MA as tip approaches towards Pb(111) surface

$$D = D_{\text{FeOEP}}^{\text{CASSCF}} + \left(D_{\text{tip/FeOEP/Pb(111)}}^{\text{DFT}} - D_{\text{FeOEP}}^{\text{DFT}} \right)$$

XL Wang, L. Yang, LZ Ye, X. Zheng, YJY. J. Phys. Chem. Lett. 9, 2418 (2018)

B. STM tip controlled magnetic anisotropy

$d\pi$ d_{z^2}
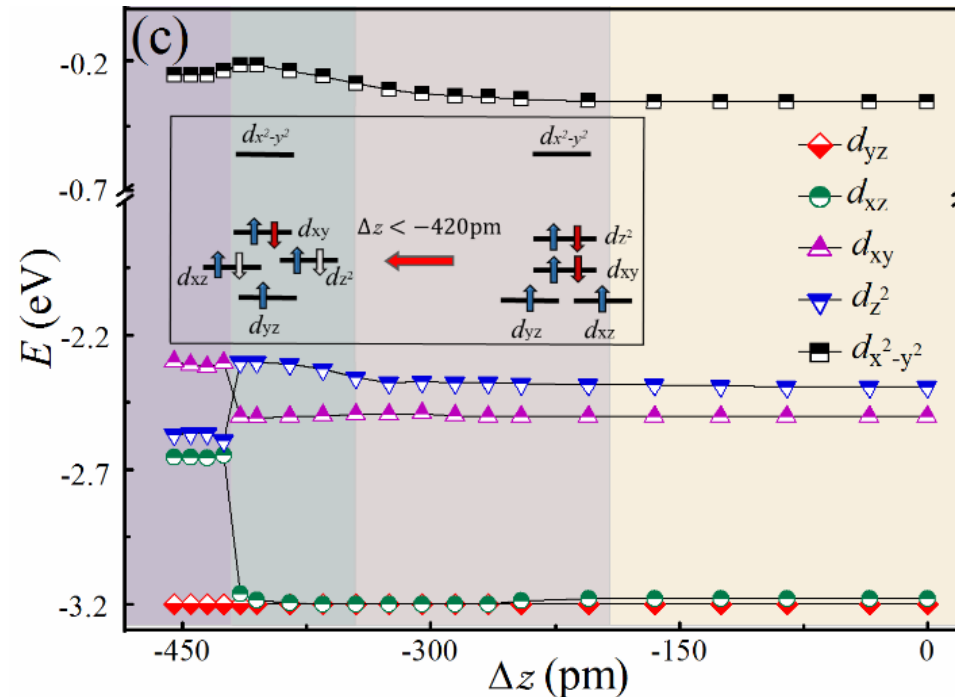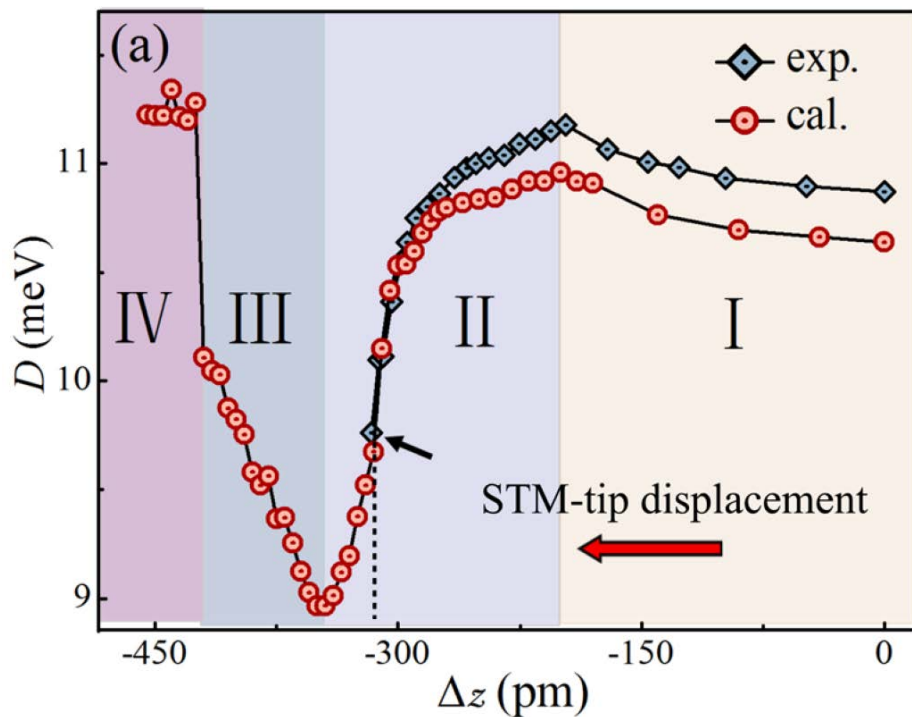
tip is far   **$(dxy)^2(dz^2)^2 (dxz)^1 (dyz)^1$**
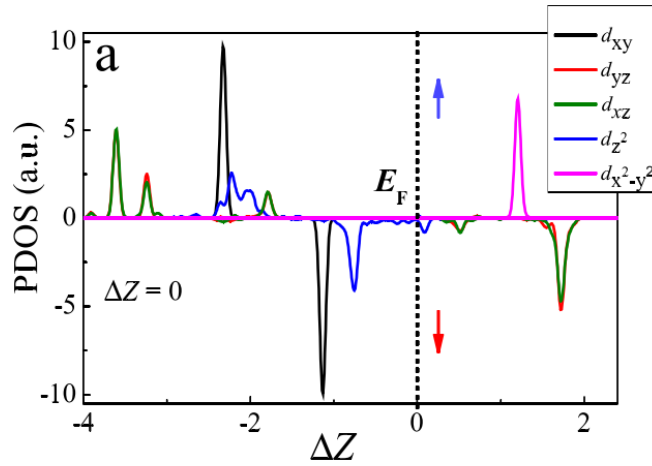
tip is near   **$(dxy)^2(dz^2)^{1.3} (dyz)^1 (dxz)^{1.4}$**
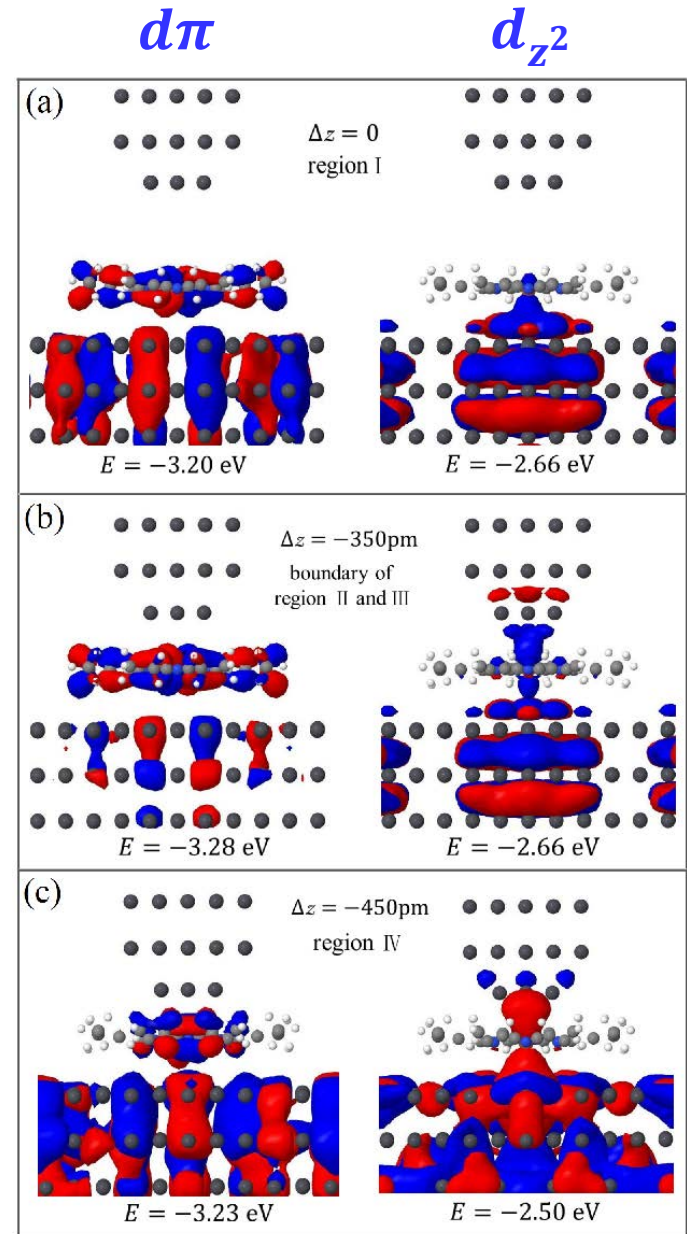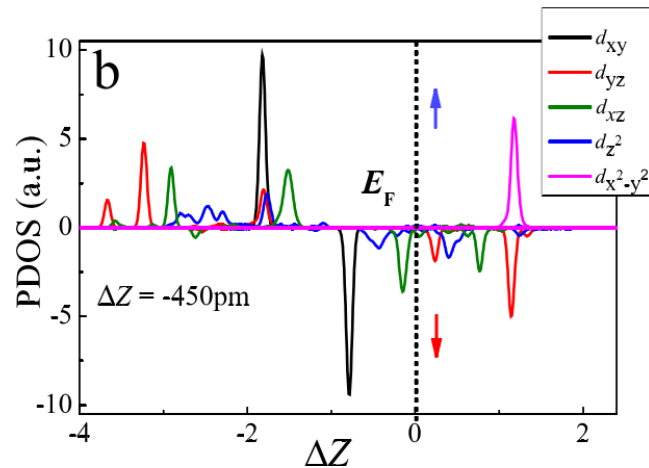
B. STM tip controlled magnetic anisotropy

Two-level Anderson impurity model

magnetic impurity

$$H_{\text{imp}} = \epsilon_a(\hat{n}_{a\uparrow} + \hat{n}_{a\downarrow}) + U_a \hat{n}_{a\uparrow}\hat{n}_{a\downarrow}$$
$$+ \epsilon_b(\hat{n}_{b\uparrow} + \hat{n}_{b\downarrow}) + U_b \hat{n}_{b\uparrow}\hat{n}_{b\downarrow} + DS_z^2.$$

maximal $d_{\text{Fe}-\text{S}}$

minimal $d_{\text{Fe}-\text{S}}$
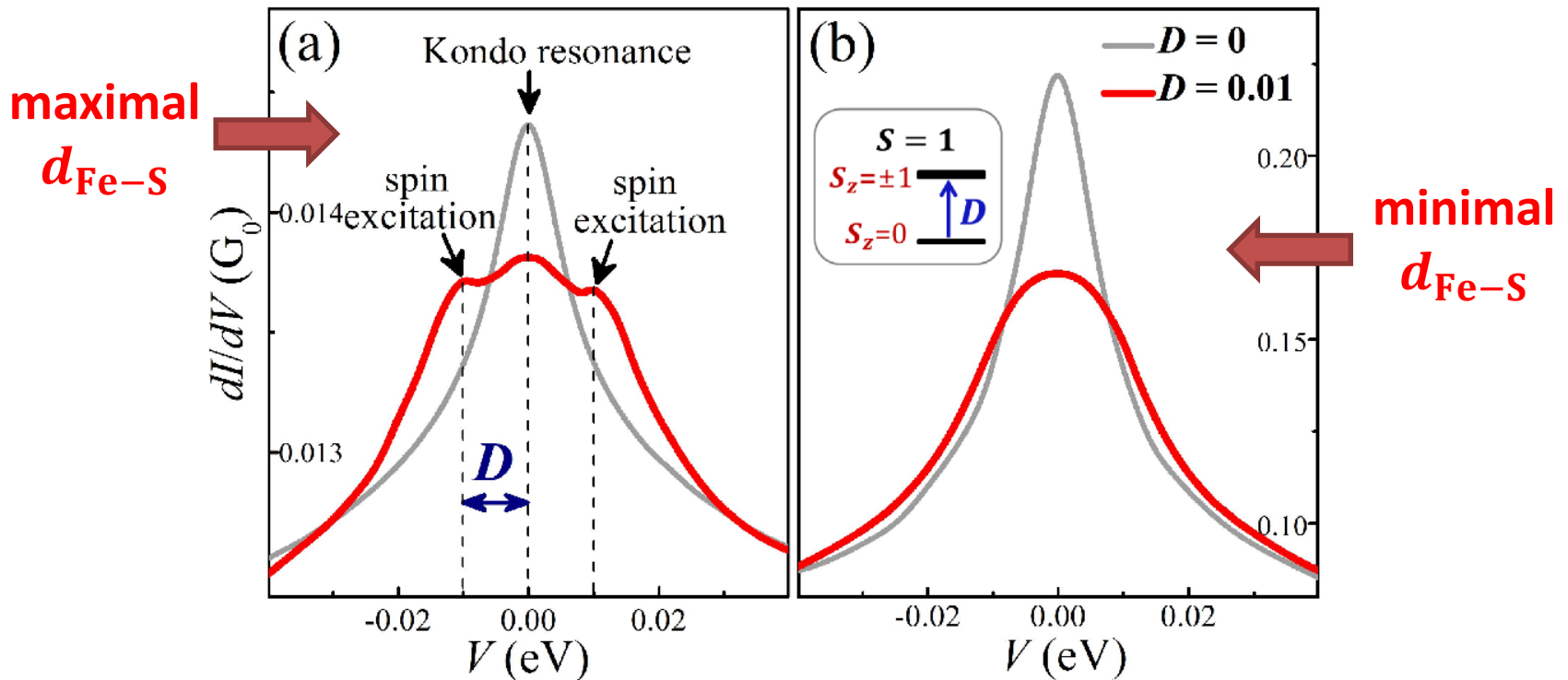
Spin excitations are suppressed by strong Kondo resonance

Experiment

Kondo resonance of a Co Atom Exchange coupled to a Ferromagnetic tip

C. Control with spin-polarized STM tip
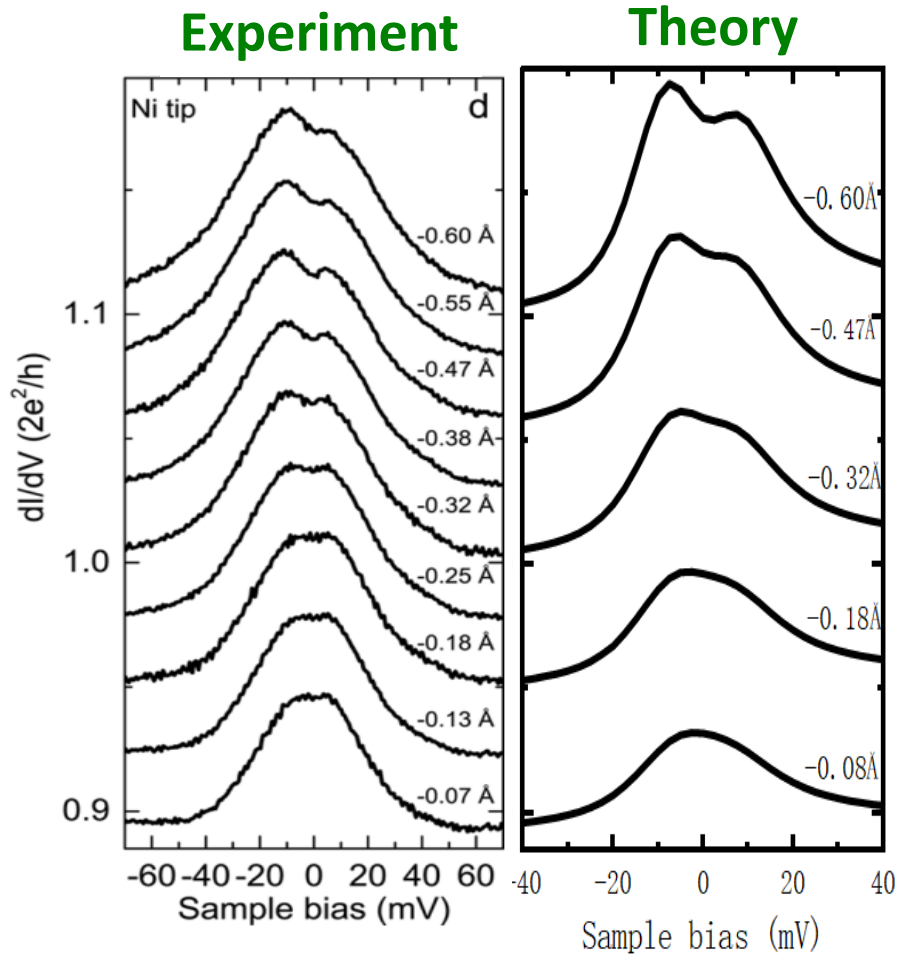
Zhuang, Wang and Zheng et al. unpublished

Outline

- Quantum mechanics of open systems: Background

- The HEOM formalism: Machineries & applications

- HEOM-QUICK package

- **The DEOM theory and applications**

- Prospects

DEOM: Statistical quasi-particle generalization of HEOM

HEOM Formalism

Bosonic: Tanimura (1990); YA Yan, JS Shao (2004); RX Xu, ..., YJ Yan (2005)
Fermionic: JS Jin, Xiao Zheng, YJ Yan (2008)
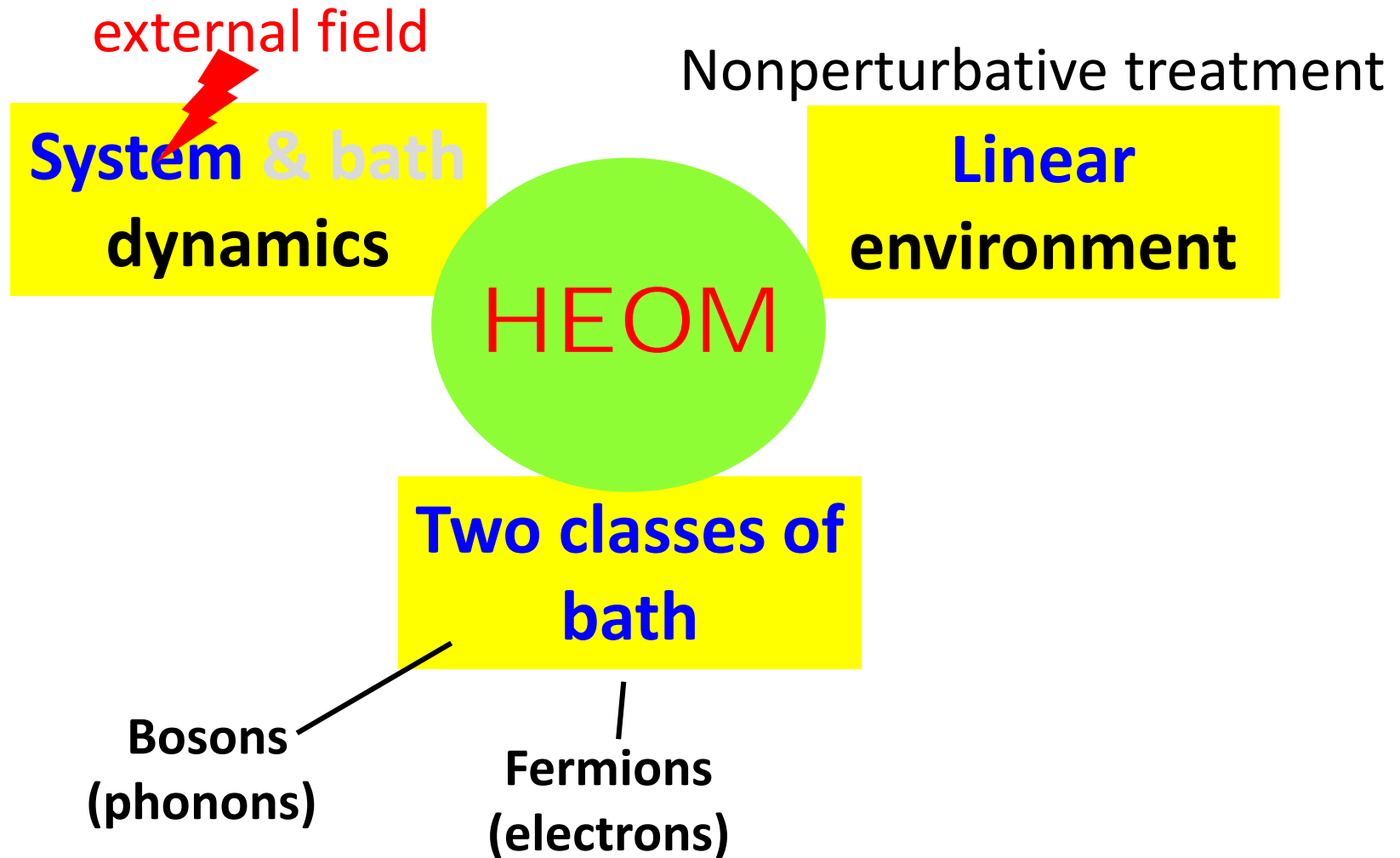
external field

Nonperturbative treatment

System & bath
dynamics

**Linear
environment**

HEOM

**Two classes of
bath**

**Bosons
(phonons)**

**Fermions
(electrons)**
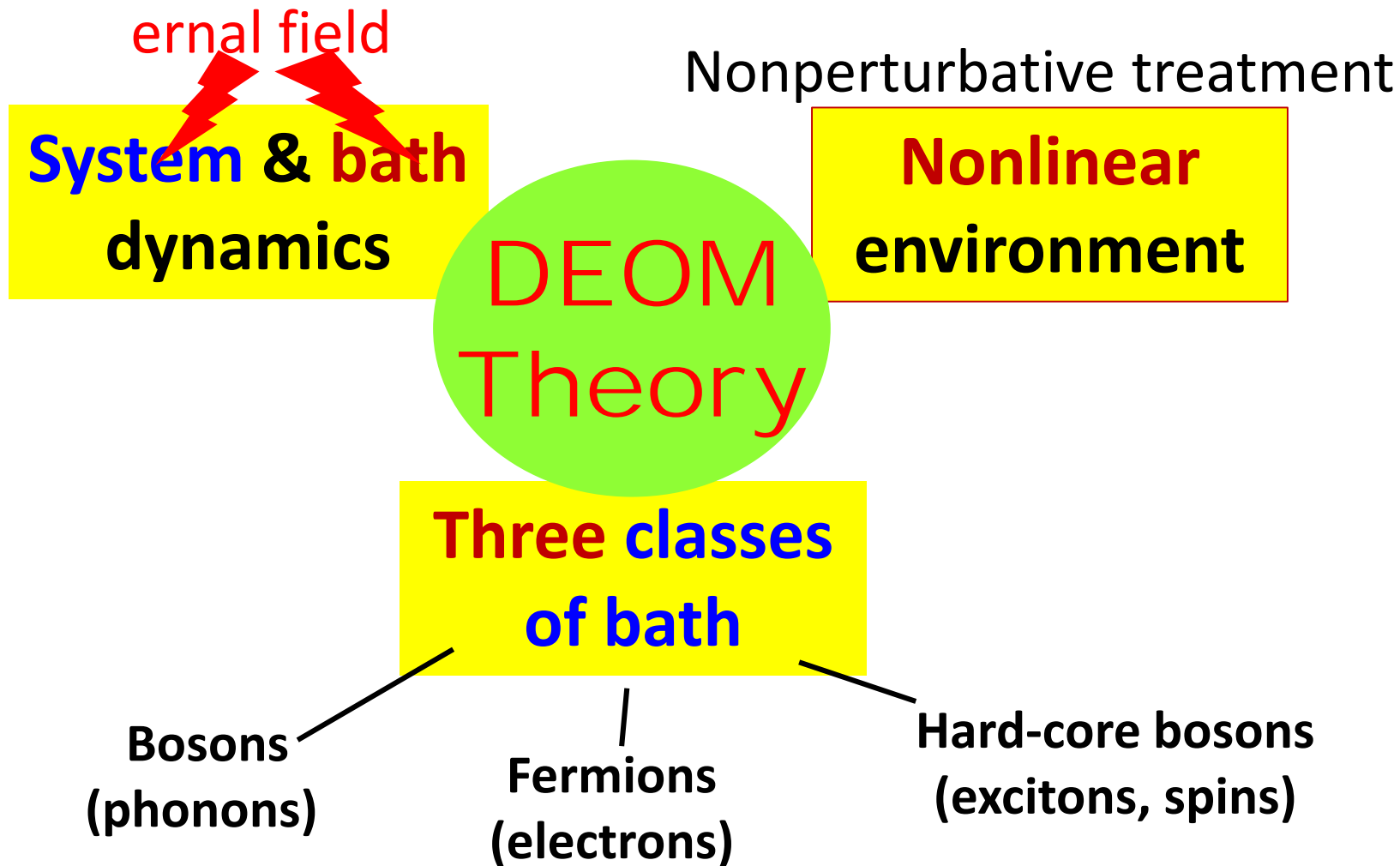
DEOM Theory: Construction

DEOM = Schrödinger Eq. + Dissipaton Algebra

1. Basic Features

$$\rho_{\mathbf{n}}^{(n)}(t) \equiv \mathrm{tr}_{\mathrm{B}}\left[\left(\hat{f}_K^{n_K} \cdots \hat{f}_1^{n_1}\right)^{\circ} \rho_{\mathrm{total}}(t)\right]$$

(HEOM)

0
1
2
3
...
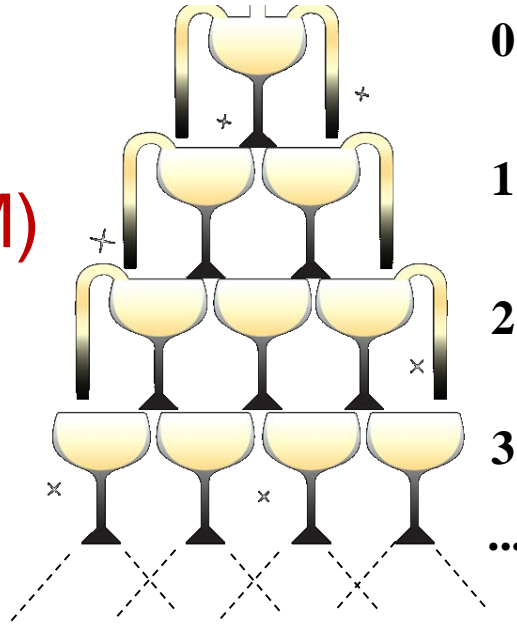
n-dissipaton excitations

- $n = n_1 + \ldots + n_K$

- $\mathbf{n} = \{n_1 \ldots n_K\}$: configuration

- $(\ldots)^{\circ}$: **irreducibility**; *i.e.*, (c-number)$^{\circ} = 0$

Environment effects are characterized with **dissipatons**, $\{\hat{f}_1, \ldots, \hat{f}_K\}$, **statistical quasi-particles**

1. Basic Features

$$\rho_{\mathbf{n}}^{(n)}(t) \equiv \text{tr}_{\text{B}}\left[\left(\hat{f}_K^{n_K}\cdots\hat{f}_1^{n_1}\right)^{\circ}\rho_{\text{total}}(t)\right]$$

Environment

Dissipatons $\{\hat{f}_j\}$	Bosonic	Fermionic	Hard-core bosonic
Occupation n_j	0, 1, 2, …	0 or 1	0 or 1
Particle Permutation	Symmetric	Anti-Sym.	Symmetric

e^-

h^+

E_{F}

Δ
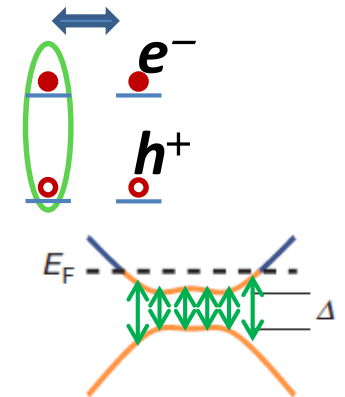
1. Basic Features

$$\rho_{\mathbf{n}}^{(n)}(t) \equiv \mathrm{tr}_{\mathrm{B}}\left[\left(\hat{f}_K^{n_K}\cdots\hat{f}_1^{n_1}\right)^{\circ}\rho_{\mathrm{total}}(t)\right]$$

Environment

Dissipatons $\{\hat{f}_j\}$	Bosonic	Fermionic	Hard-core bosonic
Occupation n_j	0, 1, 2, …	0 or 1	0 or 1
Particle Permutation	Symmetric	Anti-Sym.	Symmetric

➤ Bosonic : $\quad(\hat{f}_j\hat{f}_{j'})^{\circ} = (\hat{f}_{j'}\hat{f}_j)^{\circ}$

➤ Fermionic : $\quad(\hat{f}_j\hat{f}_{j'})^{\circ} = -(\hat{f}_{j'}\hat{f}_j)^{\circ}$

➤ Hard-core bosonic: $(\hat{f}_j\hat{f}_{j'})^{\circ} = (1-\delta_{jj'})(\hat{f}_{j'}\hat{f}_j)^{\circ}$

(c-number) $^{\circ} = 0$

1. Basic Features
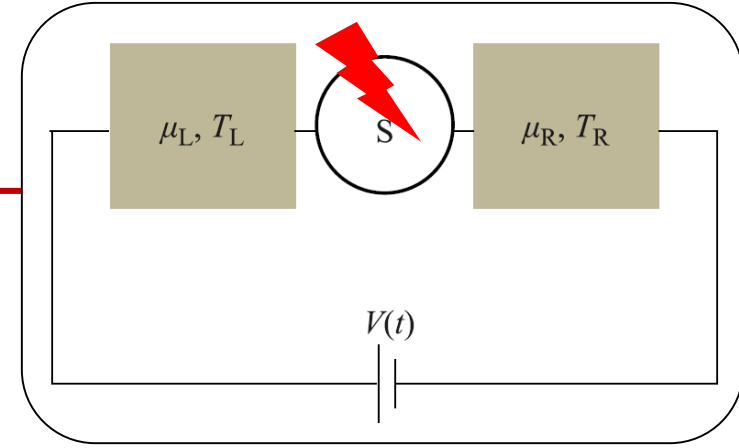
$$H_{\mathrm{T}}(t) = H(t) + \sum_{\alpha=\mathrm{L,R}} \hat{h}_\alpha^{\mathrm{eff}}(t) + H_{\mathrm{SB}}$$

$$H_{\mathrm{SB}} = \sum_{\alpha u} \left(\hat{a}_u^+ \hat{F}_{\alpha u}^- + \hat{F}_{\alpha u}^+ \hat{a}_u^- \right)$$

$$\hat{F}_{\alpha u}^+ \equiv \sum_k t_{\alpha k u} \hat{d}_{\alpha k}^+ = (\hat{F}_{\alpha u}^-)^\dagger$$

fermionic

Electrode

$$\hat{h}_\alpha^{\mathrm{eff}}(t) = \sum_k [\epsilon_{\alpha k} + \mu_\alpha(t)] \hat{d}_{\alpha k}^+ \hat{d}_{\alpha k}^-$$

Current operator

$$\hat{I}_\alpha \equiv -\frac{d}{dt}\hat{N}_\alpha = -\mathrm{i}[H_{\mathrm{SB}}, \hat{N}_\alpha]$$

$$= -\mathrm{i}\sum_u \left(\hat{a}_u^+ \hat{F}_{\alpha u}^- - \hat{F}_{\alpha u}^+ \hat{a}_u^- \right)$$

$\bar{\sigma}$: opposite sign of
$$\sigma = +,\ -$$

$$\left\langle \hat{F}_{\alpha u}^\sigma(t) \hat{F}_{\alpha v}^{\bar{\sigma}}(0) \right\rangle_{\mathrm{B}}^{\mathrm{eq}} = \frac{1}{\pi} \int_{-\infty}^{\infty} \mathrm{d}\omega\, \mathrm{e}^{\sigma \mathrm{i}\omega t} \frac{J_{\alpha u v}^\sigma(\omega)}{1 + e^{\sigma \beta_\alpha \omega}}$$

1. Basic Features

$$H_{\text{T}}(t) = H(t) + \sum_{\alpha=\text{L,R}} \hat{h}_{\alpha}^{\text{eff}}(t) + H_{\text{SB}}$$

$$H_{\text{SB}} = \sum_{\alpha u} \left(\hat{a}_u^+ \hat{F}_{\alpha u}^- + \hat{F}_{\alpha u}^+ \hat{a}_u^- \right)$$

$$\widetilde{F}_{\alpha u}^{\sigma} \equiv -\sigma \hat{F}_{\alpha u}^{\sigma} \equiv \sum_{\kappa=1}^{K} \hat{f}_{\alpha \kappa u}^{\sigma}$$

$\bar{\sigma}$: opposite sign of
$$\sigma = +\,,\ -$$

$$\left\langle \hat{F}_{\alpha u}^{\sigma}(t) \hat{F}_{\alpha v}^{\bar{\sigma}}(0) \right\rangle_{\text{B}}^{\text{eq}} = \frac{1}{\pi} \int_{-\infty}^{\infty} \mathrm{d}\omega\, \mathrm{e}^{\sigma \mathrm{i}\omega t} \frac{J_{\alpha uv}^{\sigma}(\omega)}{1 + e^{\sigma \beta_{\alpha} \omega}} = \sum_{\kappa=1}^{K} \eta_{\alpha \kappa u v}^{\sigma} \mathrm{e}^{-\gamma_{\alpha \kappa}^{\sigma} t}$$

1. Basic Features

$$\rho_{\boldsymbol{j}}^{(n)}(t) \equiv \mathrm{tr}_{\mathrm{B}}\left[\left(\hat{f}_{j_n}\cdots\hat{f}_{j_1}\right)^{\circ}\rho_{\mathrm{total}}(t)\right]$$

$$H_{\mathrm{T}}(t) = H(t) + \sum_{\alpha=\mathrm{L,R}} \hat{h}_{\alpha}^{\mathrm{eff}}(t) + \sum_{\sigma\alpha\kappa u} \hat{a}_u^{\bar{\sigma}}\hat{f}_{\alpha\kappa u}^{\sigma}$$

dissipaton's index

$$j \equiv (\sigma\alpha\kappa u)$$

$$H_{\mathrm{SB}} = \sum_{\alpha u}\left(\hat{a}_u^{+}\hat{F}_{\alpha u}^{-} + \hat{F}_{\alpha u}^{+}\hat{a}_u^{-}\right) = \sum_{\sigma\alpha\kappa u}\hat{a}_u^{\bar{\sigma}}\hat{f}_{\alpha\kappa u}^{\sigma}$$

$$\widetilde{F}_{\alpha u}^{\sigma} \equiv -\sigma\hat{F}_{\alpha u}^{\sigma} \equiv \sum_{\kappa=1}^{K}\hat{f}_{\alpha\kappa u}^{\sigma}$$

$\bar{\sigma}$: opposite sign of
$\quad\sigma = +,\ -$

$$\left\langle\hat{F}_{\alpha u}^{\sigma}(t)\hat{F}_{\alpha v}^{\bar{\sigma}}(0)\right\rangle_{\mathrm{B}}^{\mathrm{eq}} = \frac{1}{\pi}\int_{-\infty}^{\infty}\mathrm{d}\omega\,\mathrm{e}^{\sigma\mathrm{i}\omega t}\frac{J_{\alpha uv}^{\sigma}(\omega)}{1+e^{\sigma\beta_{\alpha}\omega}} = \sum_{\kappa=1}^{K}\eta_{\alpha\kappa uv}^{\sigma}\mathrm{e}^{-\gamma_{\alpha\kappa}^{\sigma}t}$$

1. Basic Features

$$\rho_{\boldsymbol{j}}^{(n)}(t) \equiv \mathrm{tr}_{\mathrm{B}}\left[(\hat{f}_{j_n}\cdots\hat{f}_{j_1})^{\circ}\rho_{\mathrm{total}}(t)\right]$$

$$H_{\mathrm{T}}(t) = H(t) + \sum_{\alpha=\mathrm{L,R}} \hat{h}_{\alpha}^{\mathrm{eff}}(t) + \sum_{\sigma\alpha\kappa u} \hat{a}_{u}^{\bar{\sigma}}\hat{f}_{\alpha\kappa u}^{\sigma}$$

$$\widetilde{F}_{\alpha u}^{\sigma} \equiv -\sigma\hat{F}_{\alpha u}^{\sigma} \equiv \sum_{\kappa=1}^{K} \hat{f}_{\alpha\kappa u}^{\sigma}$$

$$\left\langle \hat{f}_{\alpha\kappa u}^{\sigma}(t)\hat{f}_{\alpha'\kappa'v}^{\sigma'}(0)\right\rangle_{\mathrm{B}} = -\delta_{\alpha\kappa,\alpha'\kappa'}^{\sigma,\bar{\sigma}'}\eta_{\alpha\kappa uv}^{\sigma}e^{-\gamma_{\alpha\kappa}^{\sigma}t}$$

$$\left\langle \hat{f}_{\alpha'\kappa'v}^{\sigma'}(0)\hat{f}_{\alpha\kappa u}^{\sigma}(t)\right\rangle_{\mathrm{B}} = -\delta_{\alpha\kappa,\alpha'\kappa'}^{\sigma,\bar{\sigma}'}\eta_{\alpha\kappa uv}^{\bar{\sigma}*}e^{-\gamma_{\alpha\kappa}^{\sigma}t}$$

$$\left\langle \hat{B}(0)\hat{A}^{\dagger}(t)\right\rangle = \left\langle \hat{A}(t)\hat{B}^{\dagger}(0)\right\rangle^{*}$$

$\bar{\sigma}$: opposite sign of
$\sigma = +, -$

$$\left\langle \hat{F}_{\alpha u}^{\sigma}(t)\hat{F}_{\alpha v}^{\bar{\sigma}}(0)\right\rangle_{\mathrm{B}}^{\mathrm{eq}} = \frac{1}{\pi}\int_{-\infty}^{\infty}\mathrm{d}\omega\, e^{\sigma i\omega t}\frac{J_{\alpha uv}^{\sigma}(\omega)}{1+e^{\sigma\beta_{\alpha}\omega}} = \sum_{\kappa=1}^{K}\eta_{\alpha\kappa uv}^{\sigma}e^{-\gamma_{\alpha\kappa}^{\sigma}t}$$

1. Basic Features

$$\rho_{\boldsymbol{j}}^{(n)}(t) \equiv \mathrm{tr}_{\mathrm{B}}\left[\left(\hat{f}_{j_n} \cdots \hat{f}_{j_1}\right)^{\circ} \rho_{\mathrm{total}}(t)\right]$$

$$H_{\mathrm{T}}(t) = H(t) + \sum_{\alpha=\mathrm{L,R}} \hat{h}_{\alpha}^{\mathrm{eff}}(t) + \sum_{\sigma\alpha\kappa u} \hat{a}_{u}^{\bar{\sigma}} \hat{f}_{\alpha\kappa u}^{\sigma}$$

Dissipatons:

Statistically independent quasi-particles

$$\left\langle \hat{f}_{\alpha\kappa u}^{\sigma}(t)\hat{f}_{\alpha'\kappa'v}^{\sigma'}(0)\right\rangle_{\mathrm{B}} = -\delta_{\alpha\kappa,\alpha'\kappa'}^{\sigma,\bar{\sigma}'} \eta_{\alpha\kappa uv}^{\sigma} e^{-\gamma_{\alpha\kappa}^{\sigma} t}$$

$$\left\langle \hat{f}_{\alpha'\kappa'v}^{\sigma'}(0)\hat{f}_{\alpha\kappa u}^{\sigma}(t)\right\rangle_{\mathrm{B}} = -\delta_{\alpha\kappa,\alpha'\kappa'}^{\sigma,\bar{\sigma}'} \eta_{\alpha\kappa uv}^{\bar{\sigma}*} e^{-\gamma_{\alpha\kappa}^{\sigma} t}$$

2. Dissipaton Algebra

$$\rho_{\boldsymbol{j}}^{(n)}(t) \equiv \mathrm{tr_B} \left[\left(\hat{f}_{j_n} \cdots \hat{f}_{j_1} \right)^{\circ} \rho_{\mathrm{total}}(t) \right]$$

$$H_{\mathrm{T}}(t) = H(t) + \sum_{\alpha=\mathrm{L,R}} \hat{h}_{\alpha}^{\mathrm{eff}}(t) + \sum_{\sigma\alpha\kappa u} \hat{a}_u^{\bar{\sigma}} \hat{f}_{\alpha\kappa u}^{\sigma}$$

$$\left\langle \hat{f}_{\alpha\kappa u}^{\sigma}(t) \hat{f}_{\alpha'\kappa'v}^{\sigma'}(0) \right\rangle_{\mathrm{B}} = -\delta_{\alpha\kappa,\alpha'\kappa'}^{\sigma,\bar{\sigma}'} \eta_{\alpha\kappa uv}^{\sigma} e^{-\gamma_{\alpha\kappa}^{\sigma} t}$$

$$\left\langle \hat{f}_{\alpha'\kappa'v}^{\sigma'}(0) \hat{f}_{\alpha\kappa u}^{\sigma}(t) \right\rangle_{\mathrm{B}} = -\delta_{\alpha\kappa,\alpha'\kappa'}^{\sigma,\bar{\sigma}'} \eta_{\alpha\kappa uv}^{\bar{\sigma}*} e^{-\gamma_{\alpha\kappa}^{\sigma} t}$$

2.1 Generalized diffusion equation

$$\mathrm{tr_B} \left[\left(\frac{\partial \hat{f}_{\alpha\kappa u}^{\sigma}}{\partial t} \right)_{\mathrm{B}} \rho_{\mathrm{total}}(t) \right] = -\gamma_{\alpha\kappa}^{\sigma} \mathrm{tr_B} \left[\hat{f}_{\alpha\kappa u}^{\sigma} \rho_{\mathrm{total}}(t) \right]$$

$$\mathrm{i} \, \mathrm{tr_B} \left\{ \left(\hat{f}_{j_n} \cdots \hat{f}_{j_1} \right)^{\circ} [h_{\mathrm{B}}^{\mathrm{eff}}(t), \rho_{\mathrm{T}}] \right\} = \gamma_{\boldsymbol{j}}^{(n)}(t) \rho_{\boldsymbol{j}}^{(n)}$$

2. Dissipaton Algebra

$$\rho_{\boldsymbol{j}}^{(n)}(t) \equiv \mathrm{tr}_{\mathrm{B}}\left[\left(\hat{f}_{j_n}\cdots\hat{f}_{j_1}\right)^{\circ}\rho_{\mathrm{total}}(t)\right]$$

$$H_{\mathrm{T}}(t) = H(t) + \sum_{\alpha=\mathrm{L,R}} \hat{h}_{\alpha}^{\mathrm{eff}}(t) + \sum_{\sigma\alpha\kappa u} \hat{a}_u^{\bar{\sigma}}\hat{f}_{\alpha\kappa u}^{\sigma}$$

2.2 Generalized Wick's Theorem

$$\mathrm{tr}_{\mathrm{B}}\left[\left(\hat{f}_{j_n}\cdots\hat{f}_{j_1}\right)^{\circ}\hat{f}_j\rho_{\mathrm{T}}(t)\right] = \sum_{r=1}^{n}(-)^{r-1}\left\langle\hat{f}_{j_r}\hat{f}_j\right\rangle_{\mathrm{B}}^{>}\rho_{\boldsymbol{j}_r^{-}}^{(n-1)} + \rho_{j\boldsymbol{j}}^{(n+1)}$$

$$\mathrm{tr}_{\mathrm{B}}\left[\left(\hat{f}_{j_n}\cdots\hat{f}_{j_1}\right)^{\circ}\rho_{\mathrm{T}}(t)\hat{f}_j\right] = (-)^n\left[\sum_{r=1}^{n}(-)^{n-r}\left\langle\hat{f}_j\hat{f}_{j_r}\right\rangle_{\mathrm{B}}^{<}\rho_{\boldsymbol{j}_r^{-}}^{(n-1)} + \rho_{\boldsymbol{j}j}^{(n+1)}\right]$$

$$\left\langle\hat{f}_{\alpha\kappa u}^{\sigma}\hat{f}_{\alpha'\kappa'v}^{\sigma'}\right\rangle_{\mathrm{B}}^{>} = -\delta_{\alpha\kappa,\alpha'\kappa'}^{\sigma,\bar{\sigma}'}\eta_{\alpha\kappa uv}^{\sigma}, \qquad \left\langle\hat{f}_{\alpha'\kappa'v}^{\sigma'}\hat{f}_{\alpha\kappa u}^{\sigma}\right\rangle_{\mathrm{B}}^{<} = -\delta_{\alpha\kappa,\alpha'\kappa'}^{\sigma,\bar{\sigma}'}\eta_{\alpha\kappa uv}^{\bar{\sigma}*}$$

$$\mathrm{tr}_{\mathrm{B}}\left[\left(\hat{f}_{j_n}\cdots\hat{f}_{j_1}\right)^{\circ}\hat{a}_{\bar{j}}\hat{f}_j\rho_{\mathrm{T}}(t)\right] = (-)^n\hat{a}_{\bar{j}}\,\mathrm{tr}_{\mathrm{B}}\left[\left(\hat{f}_{j_n}\cdots\hat{f}_{j_1}\right)^{\circ}\hat{f}_j\rho_{\mathrm{T}}(t)\right]$$

3. DEOM Dynamics

$$\dot{\rho}_{j}^{(n)}(t) \equiv \mathrm{tr}_{\mathrm{B}} \left[(\hat{f}_{j_n} \cdots \hat{f}_{j_1})^{\circ} \dot{\rho}_{\mathrm{total}}(t) \right]$$

$$H_{\mathrm{T}}(t) = H(t) + \sum_{\alpha=\mathrm{L,R}} \hat{h}_{\alpha}^{\mathrm{eff}}(t) + \sum_{\sigma\alpha\kappa u} \hat{a}_{u}^{\bar{\sigma}} \hat{f}_{\alpha\kappa u}^{\sigma}$$

$$\dot{\rho}_{\mathrm{total}} = -i[H_{\mathrm{T}}(t), \rho_{\mathrm{total}}]$$

**Generalized
Diffusion Equation & Wick's Theorem**

$$\dot{\rho}_{\mathbf{j}}^{(n)} = -\left(i\mathcal{L}_{\mathrm{S}} + \sum_{r=1}^{n} \gamma_{j_r}\right)\rho_{\mathbf{j}}^{(n)} - i\sum_{j} \mathcal{A}_{\bar{j}} \rho_{\mathbf{j}j}^{(n+1)} - i\sum_{r=1}^{n} \mathcal{C}_{j_r} \rho_{\mathbf{j}_{r}^{-}}^{(n-1)}$$

4. DEOM Steady States

$$\rho_{j;\text{st}}^{(n)}(t) \equiv \text{tr}_{\text{B}}\left[\left(\hat{f}_{j_n}\cdots\hat{f}_{j_1}\right)^{\circ}\rho_{\text{total}}^{\text{st}}(t)\right]$$

$$H_{\text{T}}(t) = H(t) + \sum_{\alpha=\text{L},\text{R}} \hat{h}_{\alpha}^{\text{eff}}(t) + \sum_{\sigma\alpha\kappa u} \hat{a}_{u}^{\bar{\sigma}}\hat{f}_{\alpha\kappa u}^{\sigma}$$

$$\dot{\rho}_{\mathbf{j}}^{(n)} = -\left(i\mathcal{L}_{\text{S}} + \sum_{r=1}^{n}\gamma_{jr}\right)\rho_{\mathbf{j}}^{(n)} - i\sum_{j}\mathcal{A}_{\bar{j}}\rho_{\mathbf{j}j}^{(n+1)} - i\sum_{r=1}^{n}\mathcal{C}_{jr}\rho_{\mathbf{j}_r^-}^{(n-1)}$$

Steady States

$$0 = -\left(i\mathcal{L}_{\text{S}} + \sum_{r=1}^{n}\gamma_{jr}\right)\rho_{\mathbf{j};\text{st}}^{(n)} - i\sum_{j}\mathcal{A}_{\bar{j}}\rho_{\mathbf{j}j;\text{st}}^{(n+1)} - i\sum_{r=1}^{n}\mathcal{C}_{jr}\rho_{\mathbf{j}_r^-;\text{st}}^{(n-1)}$$

5. Evaluation of Experimental Observables

$$H_{\mathrm{T}}(t) = H(t) + \sum_{\alpha=\mathrm{L,R}} \hat{h}_\alpha^{\mathrm{eff}}(t) + \sum_{\sigma\alpha\kappa u} \hat{a}_u^{\bar{\sigma}} \hat{f}_{\alpha\kappa u}^{\sigma}$$

Experimental observables such as transient transport current, nonequilibrium many-particle Green's functions, & so on can be *accurately* evaluated

$$\dot{\rho}_{\mathbf{j}}^{(n)} = -\left(i\mathcal{L}_{\mathrm{S}} + \sum_{r=1}^{n} \gamma_{jr}\right)\rho_{\mathbf{j}}^{(n)} - i\sum_j \mathcal{A}_{\bar{j}}\rho_{\mathbf{j}j}^{(n+1)} - i\sum_{r=1}^{n} \mathcal{C}_{jr}\rho_{\mathbf{j}_r^-}^{(n-1)}$$

Steady States

$$0 = -\left(i\mathcal{L}_{\mathrm{S}} + \sum_{r=1}^{n} \gamma_{jr}\right)\rho_{\mathbf{j};\mathrm{st}}^{(n)} - i\sum_j \mathcal{A}_{\bar{j}}\rho_{\mathbf{j}j;\mathrm{st}}^{(n+1)} - i\sum_{r=1}^{n} \mathcal{C}_{jr}\rho_{\mathbf{j}_r^-;\mathrm{st}}^{(n-1)}$$

H. D. Zhang, Qin Qiao, R. X. Xu, X. Zheng, and YJY, *J. Chem. Phys.* **147**, 044105 (2017)

Dissipaton algebra, especially the **generalized Wick's theory**, enables DEOM/HEOM evaluation of not only system properties, but also **hybridizing bath dynamics**

2. Dissipaton Algebra

$$\rho_{\boldsymbol{j}}^{(n)}(t) \equiv \mathrm{tr}_{\mathrm{B}}\left[\left(\hat{f}_{j_n}\cdots\hat{f}_{j_1}\right)^{\circ}\rho_{\mathrm{total}}(t)\right]$$

$$H_{\mathrm{T}}(t) = H(t) + \sum_{\alpha=\mathrm{L,R}}\hat{h}_{\alpha}^{\mathrm{eff}}(t) + \sum_{\sigma\alpha\kappa u}\hat{a}_{u}^{\bar{\sigma}}\hat{f}_{\alpha\kappa u}^{\sigma}$$

2.2 Generalized Wick's Theorem

$$\mathrm{tr}_{\mathrm{B}}\left[\left(\hat{f}_{j_n}\cdots\hat{f}_{j_1}\right)^{\circ}\hat{f}_j\rho_{\mathrm{T}}(t)\right] = \sum_{r=1}^{n}(-)^{r-1}\left\langle\hat{f}_{j_r}\hat{f}_j\right\rangle_{\mathrm{B}}^{>}\rho_{\boldsymbol{j}_r^{-}}^{(n-1)} + \rho_{j\boldsymbol{j}}^{(n+1)}$$

$$\mathrm{tr}_{\mathrm{B}}\left[\left(\hat{f}_{j_n}\cdots\hat{f}_{j_1}\right)^{\circ}\rho_{\mathrm{T}}(t)\hat{f}_j\right] = (-)^{n}\left[\sum_{r=1}^{n}(-)^{n-r}\left\langle\hat{f}_j\hat{f}_{j_r}\right\rangle_{\mathrm{B}}^{<}\rho_{\boldsymbol{j}_r^{-}}^{(n-1)} + \rho_{\boldsymbol{j}j}^{(n+1)}\right]$$

$$\left\langle\hat{f}_{\alpha\kappa u}^{\sigma}\hat{f}_{\alpha'\kappa'v}^{\sigma'}\right\rangle_{\mathrm{B}}^{>} = -\delta_{\alpha\kappa,\alpha'\kappa'}^{\sigma,\bar{\sigma}'}\eta_{\alpha\kappa uv}^{\sigma}, \qquad \left\langle\hat{f}_{\alpha'\kappa'v}^{\sigma'}\hat{f}_{\alpha\kappa u}^{\sigma}\right\rangle_{\mathrm{B}}^{<} = -\delta_{\alpha\kappa,\alpha'\kappa'}^{\sigma,\bar{\sigma}'}\eta_{\alpha\kappa uv}^{\bar{\sigma}*}$$

$$\mathrm{tr}_{\mathrm{B}}\left[\left(\hat{f}_{j_n}\cdots\hat{f}_{j_1}\right)^{\circ}\hat{a}_{\bar{j}}\hat{f}_j\rho_{\mathrm{T}}(t)\right] = (-)^{n}\hat{a}_{\bar{j}}\mathrm{tr}_{\mathrm{B}}\left[\left(\hat{f}_{j_n}\cdots\hat{f}_{j_1}\right)^{\circ}\hat{f}_j\rho_{\mathrm{T}}(t)\right]$$

A. Current Noise Spectrum

J.S. Jin, S. K. Wang, Xiao Zheng, YJY, *J. Chem. Phys.* **142**, 234108 (2015)

Cotunneling:
No level within bias window
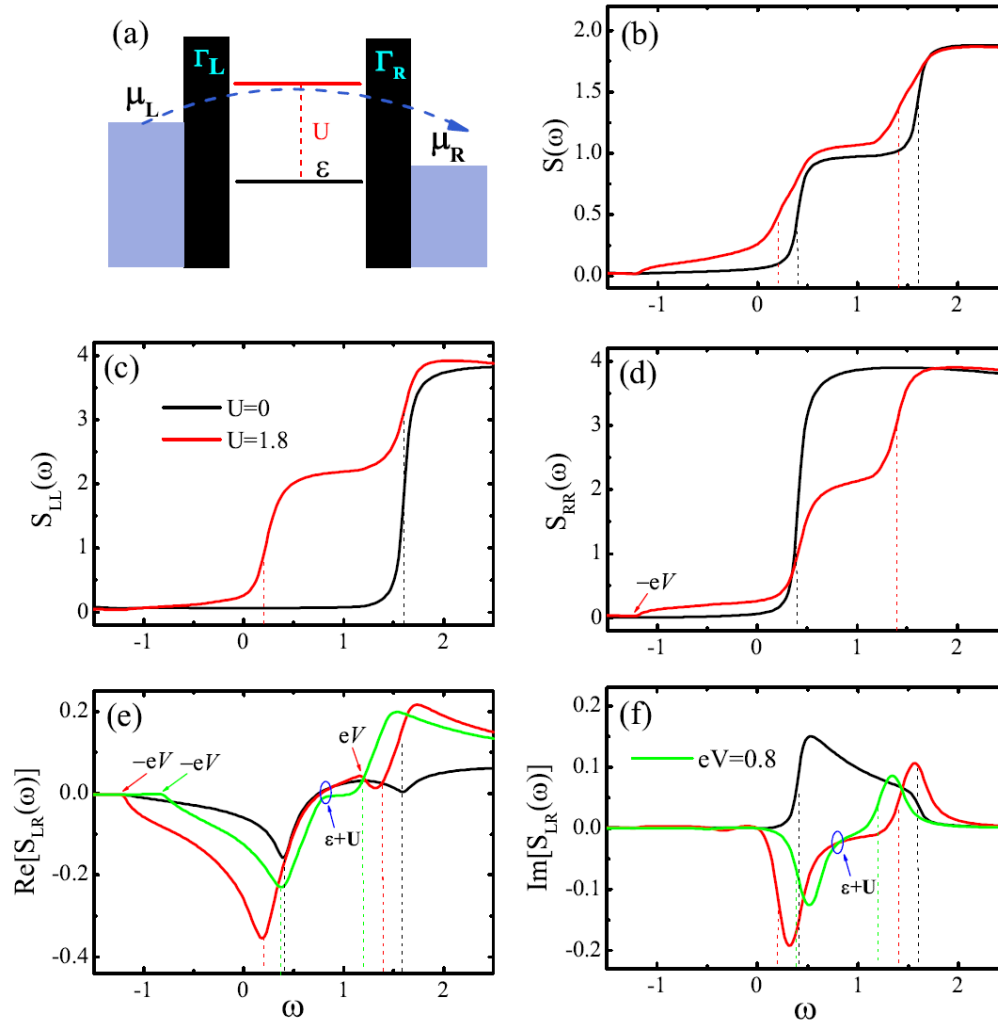
Anti-Stokes processes

Destructive interference occurs when U = 0

B. Fano Interference
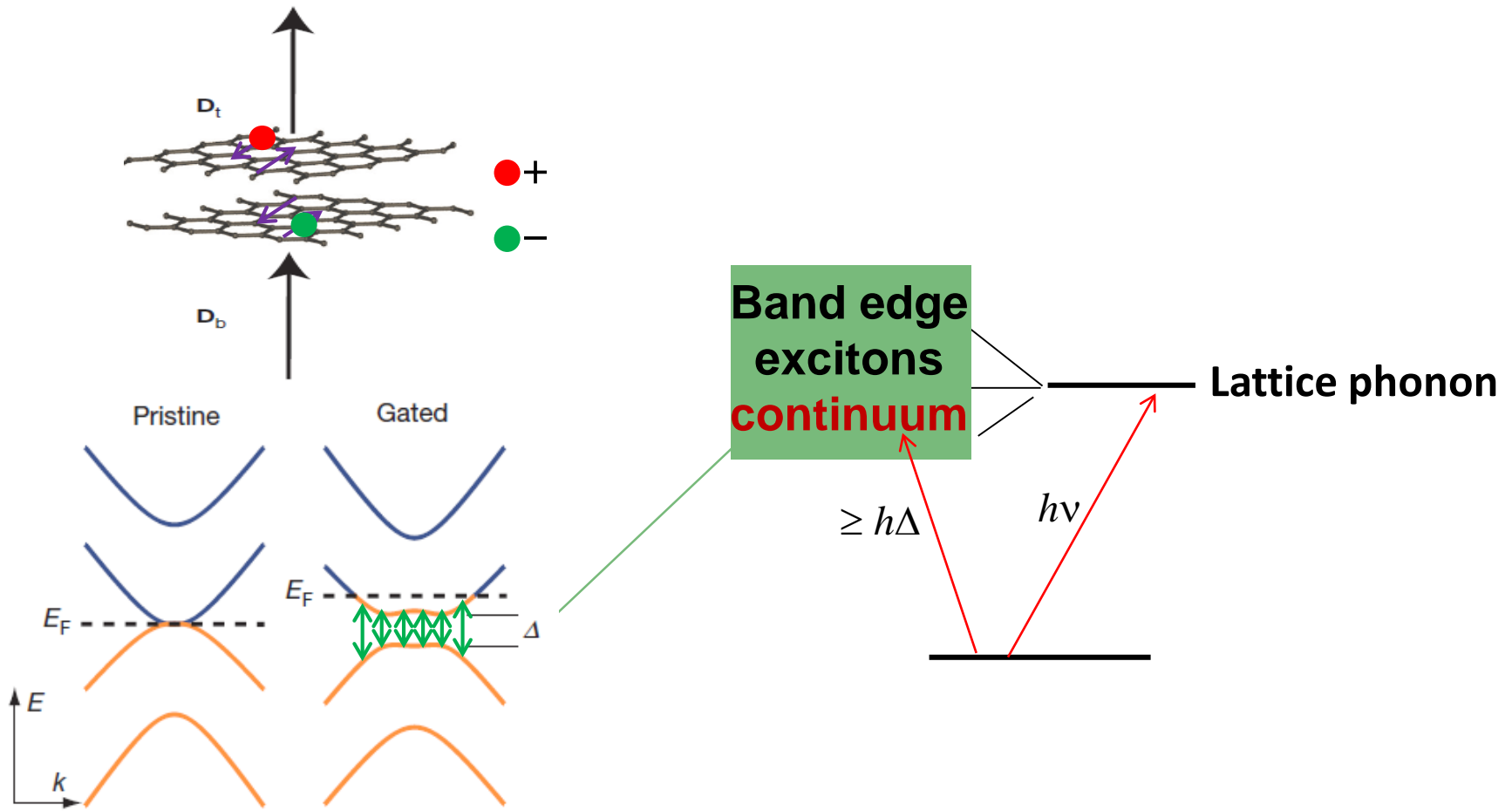
YB Zhang, et al, Nature (2009)

B. Fano Interference

YB Zhang, et al, Nature (2009)

ph. sys. / ex. bath

Fano turnover

B. Fano Interference

HD Zhang, RX Xu, X Zheng, YJ Yan, *J. Chem. Phys.* **142**, 024112 (2015)

B. Fano Interference

Bath polarization

From **Resonant peak** to **Asymmetric peak** to **Dip**

split
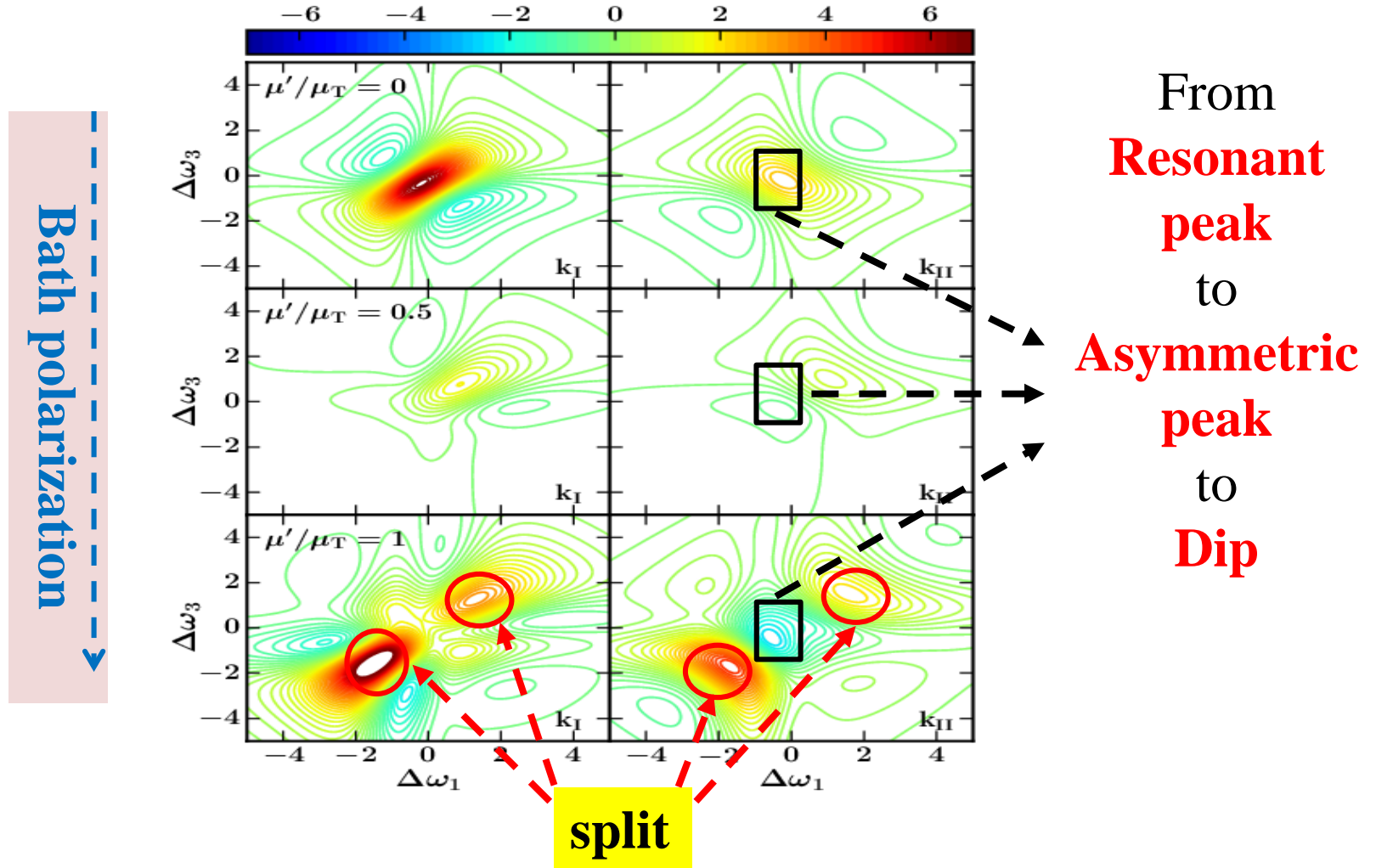
C. Herzberg-Teller Vibronic Coupling

HD Zhang, Q. Qiao, RX Xu & YJY, *J. Chem. Phys.* **145**, 204109 (2016)

$$\hat{\mu}_{\text{total}} = (\mu_0 + \mu_1 \mathbf{x})\hat{\mu}_{\text{ele}}$$
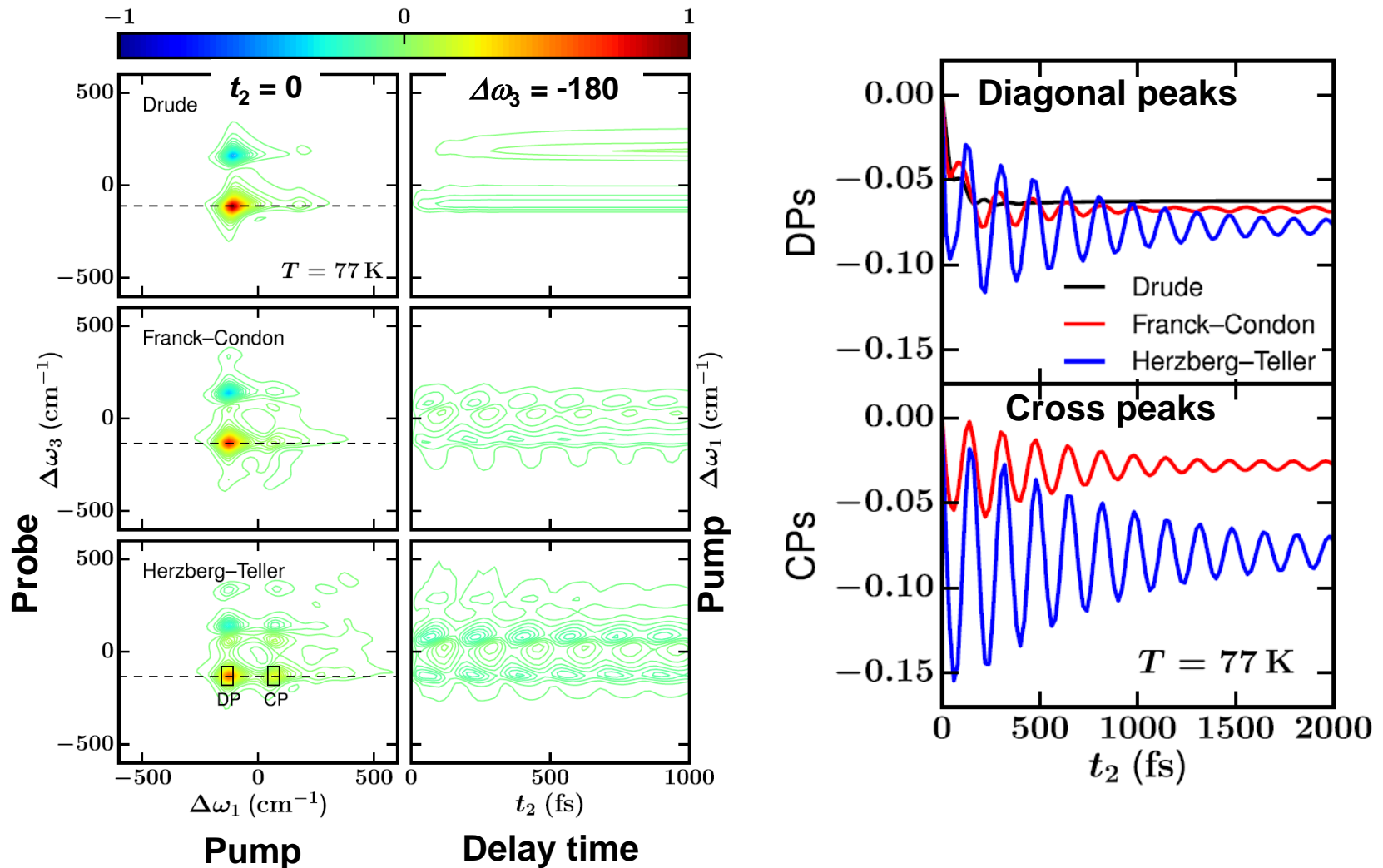
Prospects and Summary

➢ **HEOM method offers an <u>accurate</u>, <u>efficient</u>, and <u>universal</u> tool for characterization of open systems**

✓ **Equilibrium and nonequilibrium properties**

✓ **Static and dynamical properties**

✓ **Real-time electronic dynamics**

✓ **Strong electron correlation effects**

✓ **Complex non-Markovian memory effects**

• **more to discover …**

➢ **HEOM-QUICK package for <u>first-principles</u> simulation on realistic systems and processes**

Prospects and Summary

➢ **Dissipaton algebra + HEOM = DEOM**

✓ **Correlated system-bath entanglement properties: Both steady-state and transient ones**

✓ **Noise spectrum and full counting statistics analysis**

✓ **Quantum thermodynamics of impurity complex**

Acknowledgments

Prof. Xiao Zheng
Prof. Jinshuang Jin (HZNU)

Dr. LvZhou Ye (UCI)
Dr. Lu Han
Dr. Xiaoli Wang
Dr. Dong Hou (UJN)
Dr. Jinjin Ding (Nantong U)

Prof. Ninghua Tong (RMU)
Prof. Jianhua Wei (RMU)
Dr. Zhenhua Li (Lanzhou U)

Prof. RuiXue Xu
Dr. Houdao Zhang

Dr. Jian Xu (Nankai)
Dr. Jie Hu (BNU) -- PSD
Mr. Lei Cui   -- FSD
Mr. Yao Wang
Ms. Hong Gong

Prof. Qiang Shi (Inst. Chem.)

Prof. Max Di Ventra (UCSD)

REVIEW ARTICLE

Dissipation equation of motion approach to open quantum systems

YiJing Yan[1,2,†], Jinshuang Jin[3], Rui-Xue Xu[4], Xiao Zheng[4]

[1]*Hefei National Laboratory for Physical Sciences at the Microscale, iChEM (Collaborative Innovation Center of Chemistry for Energy Materials), University of Science and Technology of China, Hefei 230026, China*

[2]*Department of Chemistry, Hong Kong University of Science and Technology, Kowloon, Hong Kong, China*

[3]*Department of Physics, Hangzhou Normal University, Hangzhou 310036, China*

[4]*Hefei National Laboratory for Physical Sciences at the Microscale, Synergetic Innovation Center of Quantum Information and Quantum Physics, University of Science and Technology of China, Hefei 230026, China*

Corresponding author. E-mail: [†]*yanyj@ustc.edu.cn*

Received September 25, 2015; accepted November 13, 2015

This paper presents a comprehensive account of the dissipaton-equation-of-motion (DEOM) theory for open quantum systems. This newly developed theory treats not only the quantum dissipative systems of primary interest, but also the hybrid environment dynamics that are also experimentally measurable. Despite the fact that DEOM recovers the celebrated hierarchical-equations-of-motion (HEOM) formalism, these two approaches have some fundamental differences. To show these differences, we also scrutinize the HEOM construction via its root at the influence functional path integral formalism. We conclude that many unique features of DEOM are beyond the reach of the HEOM framework. The new DEOM approach renders a statistical quasi-particle picture to account for the environment, which can be either bosonic or fermionic. The review covers the DEOM construction, the physical meanings of dynamical variables, the underlying theorems and dissipaton algebra, and recent numerical advancements for efficient DEOM evaluations of various problems. We also address the issue of high-order many-dissipaton truncations with respect to the invariance principle of quantum mechanics of Schrödinger versus Heisenberg prescriptions. DEOM serves as a universal tool for characterizing of stationary and dynamic properties of system-and-bath interferences, as highlighted with its real-time evaluation of both linear and nonlinear current noise spectra of nonequilibrium electronic transport.

Keywords quantum dissipation, quantum transport, entangled system-and-bath dynamics

PACS numbers 03.65.Yz, 05.60.Gg, 72.10.-d

Contents

1 Introduction

Correlated system-and-bath coherence is a type of quantum entanglement which occurs whenever the quantum nature of an environment cannot be neglected. Nowadays, this type of quantum entanglement plays roles of ever-increasing importance in many fields of science. It is concerned with quantum impurities under the influence of dissipative environments that can exchange electrons (or particles) and quantum information with local impurity systems. The interplay between system anharmonicity and nonperturbative coupling with non-Markovian environments results in rich phenomena, such as Mott metal-insulator transitions and Kondo physics. In addition to quantum systems dynamics, one can manipulate and monitor certain strongly correlated collective motions of bath continuum. Examples include Fano interference spectroscopy, correlated dynamics between chromophores and surface plasmons, quantum rate fluctuations, and electronic transport current shot noise spectrum and counting statistics. To address these diversified issues, a fundamental (Schrödinger-equation-like) theory of open quantum systems, governing both systems and hybrid bath dynamics, is needed.

The quantum mechanics of open systems had been substantially developed in the context of dissipative dynamics, with the focus primarily only on reduced system density operators, $\rho_{\mathrm{S}}(t) \equiv \mathrm{tr}_{\mathrm{B}}\rho_{\mathrm{T}}(t)$; i.e., the bath-subspace trace of the total composite density operator. Quantum dissipation theories cover topics ranging from various second-order quantum master equations [1–6] to the Feynman–Vernon influence functional path integral formalism [7, 8]. For the influences of Gaussian bath on reduced systems, the path integral approach is exact, except for the initial factorization ansatz [7–9]. The celebrated hierarchical-equations-of-motion (HEOM) formalism, with either bosonic [10–17] or fermionic [18] bath influence, involves a set of auxiliary density operators that are known to be relevant to the hybrid bath dynamics [19, 20]. Nevertheless, they appear rather as mathematical auxiliaries, irrespective of whether the HEOM is constructed via the stochastic field method [10, 11] or the calculus-on-path-integral approach [12–18].

In this paper, we present a comprehensive account of the recently developed theory of the dissipaton equation of motion (DEOM) [21]. It not only recovers HEOM but also identifies the physical meanings of all involved dynamical quantities as many-dissipaton configurations. More importantly, it renders a *statistical quasi-particle* (dissipaton) picture to account for the environment, which can be either bosonic or fermionic. In this sense, DEOM is a type of "second-quantization" theory of the quantum mechanics of open systems. It consists of not only the law of governing dynamics of evolving variables but also the underlying statistical quasi-particle picture as well as novel dissipaton algebra [21–23]. Particularly important is the generalized Wick's theorem [21], which provides DEOM with a versatile means for the accurate evaluation of various experimentally measurable quantities of system-and-bath interference dynamics.

This paper is organized as follows. After an overview

110306-2

YiJing Yan, et al., Front. Phys. 11(4), 110306 (2016)

of the general features in Section 2, we present in detail the constructions of bosonic and fermionic DEOM theories, in Section 3 and Section 4, respectively. As the DEOM dynamical generators recover their HEOM correspondences, we scrutinize the fermionic HEOM construction in Section 5, following which we conclude that many unique features of DEOM are beyond the reach of the HEOM framework. However, all numerical HEOM techniques developed recently can be directly used in the present DEOM evaluations. In Section 6, we present some recent advancements in this aspect. In Section 7, we discuss the quantum mechanics on the DEOM-space algebra, considering DEOM as a universal theory for the stationary and dynamic properties of both systems and hybrid bath environments. We also derive the Heisenberg prescription of the DEOM formalism, which confirms that the derivative-resum truncation scheme, presented in Section 3.5 and Section 4.5, does preserve the invariance principle of the prescriptions. We conclude the paper in Section 8.

2 General remarks on DEOM theory

2.1 Remarks on Gaussian bath

The DEOM approach is formally exact for the linear hybridization noninteracting bath model, referred to as Gaussian bath hereafter. The details of the Gaussian bath model are as follows. (i) The bath (h_{B}) consists of practically infinite number of *noninteracting* (quasi) particles, which are either fermionic or bosonic; (ii) The system-bath coupling H_{SB} is modeled at the linear bath hybridization level. Gaussian bath covers the Caldeira-Leggett model, which is widely adopted in the study of decoherence problems, and also the electronic transfer coupling model commonly used in quantum transport and quantum impurity physics research.

The simplification of Gaussian bath is rooted at its underlying Gaussian statistics of Wick's theorem. It is concerned with the thermodynamical average, $\langle \hat{O} \rangle_{\mathrm{B}} \equiv \mathrm{tr}_{\mathrm{B}}(\hat{O}\rho_{\mathrm{B}}^{\mathrm{eq}})$, over the equilibrium canonical ensembles of the *bare* bath at a given temperature [8, 9]. The extension to nonequilibrium grand canonical ensembles for bath reservoirs in the presence of bias chemical potentials is rather trivial. This will be considered in the context of quantum transport (cf. Section 4). Apparently, $\langle H_{\mathrm{SB}} \rangle_{\mathrm{B}} = 0$ automatically holds in the present bath model. More importantly, the Gaussian statistical dynamics with zero-means is completely characterized by its second cumulants. These are simply the hybridization bath correlation functions, which can be further related

to the hybridizing bath spectral density functions via the fluctuation-dissipation theorem [8, 9], owing to the underlying detailed balance relation [6]. In other words, the above bath characterization completely determines the bath influences on the reduced system dynamics. This is also the reason why the Feynman-Vernon influence functional path integral formalism [7, 8] is exact in the present bath model; for further details see Section 5.

It is worth noting that the initial factorization ansatz, $\rho_{\mathrm{T}}(t_0) = \rho_{\mathrm{S}}(t_0)\rho_{\mathrm{B}}^{\mathrm{eq}}$, for the total system-and-bath density operator is adopted in deriving the influence functionals in the path integral formalism. Its differential-equation counterpart, the HEOM formalism, would in principle also suffer this problem. On the other hand, the DEOM construction formally starts with an arbitrary initial $\rho_{\mathrm{T}}(t_0)$.

2.2 Remarks on total composite Hamiltonian

The total composite Hamiltonian tractable with the DEOM formalism has the following generic form,

$$H_{\mathrm{T}}(t) = [H_{\mathrm{S}} - \hat{D}_{\mathrm{S}}E(t)] + h_{\mathrm{B}} + H_{\mathrm{SB}} + \hat{D}_{\mathrm{B}}E'(t). \quad (2.1)$$

Here, h_{B} and H_{SB} were modeled with the Gaussian bath, as detailed in Section 2.1. The first term of Eq. (2.1) is the system Hamiltonian, $H(t) = H_{\mathrm{S}} - \hat{D}_{\mathrm{S}}E(t)$, under the local classical electromagnetic field $E(t)$ interrogation. Both H_{S} and $\hat{D}_{\mathrm{S}}$ are arbitrary Hermitian operators in the system subspace. Define system Liouvillian superoperator $\mathcal{L}(t)$ via

$$\mathcal{L}(t)\hat{O} \equiv [H(t), \hat{O}] \equiv [H_{\mathrm{S}} - \hat{D}_{\mathrm{S}}E(t), \hat{O}]. \quad (2.2)$$

The last term in Eq. (2.1), $\hat{D}_{\mathrm{B}}E'(t)$, represents the interaction between the environment (bath) and external classical field $E'(t)$, which can be arbitrary. It highlights the fact that various experimentally accessible bath dynamics, including system-and-bath interference phenomena, are also within the reach of the DEOM framework in this review article. The interrogated bath operator $\hat{D}_{\mathrm{B}}$ is chosen to modify either h_{B} or H_{SB}, without altering the underlying Gaussian statistics, as stipulated in Section 2.1. Some details are as follows. (i) The bosonic DEOM will be considered with the quantum dissipation setup (cf. Fig. 1), where the bath polarization gives rise to $\hat{D}_{\mathrm{B}}E'(t)$ that effectively modifies H_{SB} [cf. Eq. (3.1)]. (ii) The fermionic DEOM will be considered with a quantum transport setup (cf. Fig. 2), where a local quantum impurity is coupled with electrodes that serve as bath reservoirs. In this case, $\hat{D}_{\mathrm{B}}E'(t)$ represents the modifications to the individual bath reservoirs bath [cf. Eq. (4.4)], due to the applied external bias electric potential field, which can be time-dependent.

2.3 General features of DEOM

The DEOM approach provides a statistical quasi-particle (dissipaton) picture to account for the environment, which can be either bosonic or fermionic. In this approach, the linear hybridizing bath operators are decomposed into a set of statistically independent dissipaton operators $\{\hat{f}_k\}$, with certain well-defined features to support rather simple but novel dissipaton algebra. This includes the generalized diffusion equation and the generalized Wick's theorem for dissipatons.

Dynamical variables in DEOM are the so-called dissipaton density operators (DDOs) [21–23], with the generic form of

$$\rho_{\boldsymbol{n}}^{(n)}(t) \equiv \rho_{n_1 \cdots n_K}^{(n)}(t) \equiv \text{tr}_{\text{B}}\left[\left(\hat{f}_1^{n_1} \cdots \hat{f}_K^{n_K}\right)^{\circ} \rho_{\text{T}}(t)\right]. \quad (2.3)$$

The product of dissipaton operators inside $(\cdots)^{\circ}$ is *irreducible*. Note that $(\text{c} - \text{number})^{\circ} \equiv 0$. Moreover, bosonic/fermionic dissipatons satisfy $[\hat{f}_k, \hat{f}_j]_{\mp} = \text{c} - \text{number}$, with $[\cdot, \cdot]_- \equiv [\cdot, \cdot]$ and $[\cdot, \cdot]_+ \equiv \{\cdot, \cdot\}$ being commutator and anti-commutator, respectively. Therefore,

$$\begin{aligned}\left(\hat{f}_k \hat{f}_j\right)^{\circ} &= \left(\hat{f}_j \hat{f}_k\right)^{\circ} & \text{(bosonic)};\\ \left(\hat{f}_k \hat{f}_j\right)^{\circ} &= -\left(\hat{f}_j \hat{f}_k\right)^{\circ} & \text{(fermionic)}.\end{aligned} \quad (2.4)$$

Each DDO of Eq. (2.3), where $n = n_1 + \cdots + n_K$, specifies an n-dissipaton configuration, with n_k being the participation number of a specified dissipaton: $n_k \geqslant 0$ if $\hat{f}_k$ is bosonic, and $n_k = 0$ or 1 if $\hat{f}_k$ is fermionic [cf. Eq. (2.4)]. Apparently, the reduced system density operator is simply $\rho_{\text{s}}(t) = \rho^{(0)}(t)$, a special member of Eq. (2.3).

The DEOM formalism assumes the generic form of

$$\dot{\rho}_{\boldsymbol{n}}^{(n)} = -\left[\text{i}\mathcal{L}(t) + \gamma_{\boldsymbol{n}}^{(n)}\right]\rho_{\boldsymbol{n}}^{(n)} + \left\{\rho_{\boldsymbol{n}^-}^{(n-1)}\right\} + \left\{\rho_{\boldsymbol{n}^+}^{(n+1)}\right\}. (2.5)$$

It is constructed by applying the Liouville-von Neumann equation, $\dot{\rho}_{\text{T}}(t) = -\text{i}\left[H(t) + h_{\text{B}} + H_{\text{SB}}, \rho_{\text{T}}(t)\right]$, to the total composite density operator in Eq. (2.3), followed by applying the novel dissipaton algebra [21–23]. In general, the system $H(t)$ gives rise to $\mathcal{L}(t)$ of Eq. (2.2). The h_{B}-commutator action is evaluated via the generalized diffusion equation, resulting in the $\gamma_{\boldsymbol{n}}^{(n)}$-term in Eq. (2.5). The diffusion parameter $\gamma_{\boldsymbol{n}}^{(n)}$ is usually complex, and it represents the memory-frequency contents of the n-body DDO under study. It can even be time-dependent, if the underlying bath Hamiltonian is an effective $h_{\text{B}}^{\text{eff}}(t)$ [cf. Eq. (4.1)]. This is the case in transient quantum transport studies, in which a time-dependent external bias electric field is applied across the contacting bath reservoirs. The H_{SB}-commutator action is evaluated via the generalized Wick's theorem [21], resulting in the dependence on the associating $(n \pm 1)$-body DDOs, as denoted

by $\left\{\rho_{\boldsymbol{n}^{\pm}}^{(n\pm1)}\right\}$ in Eq. (2.5).

It is worth re-emphasizing here that the DEOM theory does not just describe how the DDOs evolve in time, as governed by Eq. (2.5), it also describes the underlying statistical quasi-particle picture and the novel dissipaton algebra [21]. In particular, the notion of irreducibility, $(\cdots)^{\circ}$ in Eq. (2.3), is closely related to a novel Wick's-like theorem [21]. It enables DEOM to address not only the system but also the bath dynamics and the interferences between them.

Throughout this paper, we adopt the units of $\hbar = e = 1$, where $\hbar$ is the Planck constant and e is the electron charge. Denote $\beta \equiv 1/(k_{\text{B}}T)$, with k_B being the Boltzmann constant and T the temperature.

Hereafter, the time variable $t > 0$, unless specified otherwise. The correlation functions of the type,

$$\langle \hat{A}^{\dagger}(t)\hat{B}(0)\rangle \equiv \text{Tr}\left[\hat{A}^{\dagger}(t)\hat{B}(0)\rho_{\text{T}}^{\text{eq}}\right], \quad (2.6)$$

associate physically with the Keldysh forward $(>)$ path. The backward $(<)$ path counterpart is

$$\langle \hat{B}(0)\hat{A}^{\dagger}(t)\rangle \equiv \text{Tr}\left[\hat{A}^{\dagger}(t)\rho_{\text{T}}^{\text{eq}}\hat{B}(0)\right]. \quad (2.7)$$

Here, $\hat{A}(t) = \text{e}^{\text{i}H_{\text{T}}t}\hat{A}\text{e}^{-\text{i}H_{\text{T}}t}$, with the total composite Hamiltonian H_{T}, in the absence of an external field, and $\rho_{\text{T}}^{\text{eq}} \equiv \text{e}^{-\beta H_{\text{T}}}/Z_{\text{T}}$ with Z_{T} being the canonical thermal equilibrium partition function. Both $\hat{A}$ and $\hat{B}$ are also defined within the total space, involved both system and environment. The above definitions readily lead to the time-reversal and detailed-balance relations [6], respectively, of

$$\langle \hat{B}(0)\hat{A}^{\dagger}(t)\rangle = \langle \hat{A}(t)\hat{B}^{\dagger}(0)\rangle^{*} = \langle \hat{A}^{\dagger}(t - \text{i}\beta)\hat{B}(0)\rangle. \quad (2.8)$$

2.4 Basic algebra for superoperators and tensors

Some superoperators, defined in the system subspace, are involved in the DEOM formalism. A superoparator maps an operator, such as a DDO of Eq. (2.3), to another operator. Throughout this work, we define superoperators via their actions on an arbitrary operator. For completeness, we also represent the basic superoperator algebra, as follows.

(i) Superoperators are also referred to as Liouville-space operators. They are tensors with respect to a given Hilbert-space basis-set representation, $\{|m\rangle\}$. The Liouville-space basis set elements are then $\{|mn\rangle\rangle\}$, with each $|mn\rangle\rangle = |m\rangle\langle n|$ being an ordinary Hilbert-space projection-type state operator. Here, we adopt the so-called *tetradic bra-and-ket notation*. The orthonormality and completeness of a Liouville-space basis set read [24, 25]

$$\langle\langle mn|m'n'\rangle\rangle \equiv \text{tr}_{\text{s}}\left[(|n\rangle\langle m|)(|m'\rangle\langle n'|)\right] = \delta_{mm'}\delta_{n'n},$$

$$\sum_{mn} |mn\rangle\rangle\langle\langle mn| = \mathcal{I}. \tag{2.9}$$

The tensor elements of a superoperator $\mathcal{O}$ are then

$$\mathcal{O}_{mn,m'n'} \equiv \langle\langle mn|\mathcal{O}|m'n'\rangle\rangle \equiv \langle m|\big[\mathcal{O}(|m'\rangle\langle n'|)\big]|n\rangle.$$

The tetradic bra-ket notation [24, 25] is convenient for the superoperator/tensor algebra, because

$$(\mathcal{O}\hat{A})_{mn} = \sum_{m'n'} \mathcal{O}_{mn,m'n'} A_{m'n'}, \tag{2.10}$$

where $A_{m'n'} = \langle m'|\hat{A}|n'\rangle$.

(ii) Hermitian superoperators, $\mathcal{O}$, are defined, via their actions on an arbitrary operator, as $(\mathcal{O}\hat{A})^\dagger = \mathcal{O}\hat{A}^\dagger$. It is equivalent to state that a Hermitian superoperator maps a Hermitian operator to another Hermitian operator. From this definition, it immediately follows that the *product of Hermitian superoperators remains Hermitian*. The tensor elements of a Hermitian superoperator satisfy

$$\mathcal{O}_{mn,m'n'} = \mathcal{O}^*_{nm,n'm'}. \tag{2.11}$$

Note that the diagonal elements, following Eq. (2.9) or (2.10), are $\mathcal{O}_{mn,mn}$, which are complex in general. For example, $i\mathcal{L}_S$ is Hermitian. Its tetradic tensor elements, in the diagonal H_S-representation, are $(i\mathcal{L}_S)_{mn,m'n'} = i\omega_{mn}\delta_{mm'}\delta_{nn'}$, with $\omega_{mn} = \epsilon_m - \epsilon_n$ being the transition frequency between two eigenstates of the bare system Hamiltonian. The diagonal elements of $(i\mathcal{L}_S)$ are purely imaginary in the above tetradic convention.

(iii) Another is the so-called "chemistry" convention. It arranges the tensor $\{\mathcal{O}_{mn,m'n'} \equiv \langle\langle mn|\mathcal{O}|m'n'\rangle\rangle\}$ in an ordinary matrix form, $\{\mathcal{O}_{pq}\}$, such that a Hermitian superoperator satisfies

$$\mathcal{O}_{pq} = \mathcal{O}^*_{qp}. \tag{2.12}$$

This can be achieved via

$$\mathcal{O}_{pq} \equiv (p|\mathcal{O}|q) = (mm'|\mathcal{O}|nn') \equiv \langle\langle mn|\mathcal{O}|m'n'\rangle\rangle. \tag{2.13}$$

The Hermitian matrix indexes are then $p = mM + m'$ and $q = nM + n'$, provided the Hilbert-space basic set in use is $\{|m\rangle; m = 0, \cdots, M-1\}$. This convention is numerically useful, when the eigenvalues of a Hermitian superoperator are needed to be explicitly evaluated.

3 Bosonic DEOM theory

3.1 Statistical description of bosonic bath

3.1.1 Fluctuation-dissipation theorem for bosonic bath

For a quantum dissipation setup such as that in Fig. 1,
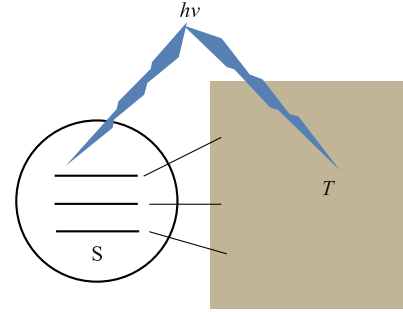
Fig. 1 Schematic representation of a quantum dissipation setup, in which a mesoscopic system S is coupled to a macroscopic bath, under temperature T. The external light field interrogates both the discrete system and bath continuum.

we specify the total composite Hamiltonian of Eq. (2.1) as

$$H_T(t) = H(t) + h_B + \sum_a [\hat{Q}^S_a - \zeta^B_a E(t)]\hat{F}^B_a, \tag{3.1}$$

with the Caldeira–Leggett bath model of [26, 27]

$$h_B = \frac{1}{2}\sum_j \omega_j(p_j^2 + x_j^2) \quad \text{and} \quad \hat{F}^B_a = \sum_j c_{aj} x_j. \tag{3.2}$$

The last two terms in Eq. (2.1) are now combined into the single last term in Eq. (3.1), with the self-explained forms of H_{SB} and $\hat{D}_B$, in terms of the hybridizing bath operators $\{\hat{F}^B_a\}$. Involved in the system-bath coupling, H_{SB}, are also the hybridizing system modes $\{\hat{Q}^S_a\}$, which are usually set to be dimensionless. We also set a same electromagnetic field, $E'(t) = E(t)$, to act on both system and bath continuum, so that Fano interference is anticipated.

Equation (3.2) is a type of linear hybridization noninteracting bath. The bath influence on the system dynamics satisfies the aforementioned Gaussian statistics (cf. Section 2.1). The characterizing hybridization bath spectral density functions, as described microscopically via Eq. (3.2), are

$$J_{ab}(\omega) = \frac{\pi}{2}\sum_j c_{aj} c_{bj} \delta(\omega - \omega_j), \quad \text{with } \omega \geqslant 0. \tag{3.3}$$

The equivalent thermodynamical description, covering all real ω, reads [6]

$$J_{ab}(\omega) = \frac{1}{2}\int_{-\infty}^{\infty} dt\, e^{i\omega t}\langle [\hat{F}^B_a(t), \hat{F}^B_b(0)]\rangle_B. \tag{3.4}$$

Here, $\hat{F}^B_a(t) \equiv e^{ih_B t/\hbar}\hat{F}^B_a e^{-ih_B t/\hbar}$, and $\langle\hat{O}\rangle_B$ denotes an average over the unperturbed *bare bath* thermal equilibrium ensemble at a given temperature. Apparently, the relations in Eq. (2.8) hold for the isolated bath quantities above. It is easy to show that bosonic bath spectral density functions satisfy the Hermitian anti-symmetric

YiJing Yan, et al., Front. Phys. 11(4), 110306 (2016)

110306-5

relations [6]:

$$J_{ab}^*(\omega) = -J_{ab}(-\omega) = J_{ba}(\omega). \qquad (3.5)$$

Moreover, the underlying detailed-balance relation, as inferred from Eqs. (2.8) and (3.4), leads to [6]

$$\left\langle \hat{F}_a^{\mathrm{B}}(t)\hat{F}_b^{\mathrm{B}}(0)\right\rangle_{\mathrm{B}} = \frac{1}{\pi}\int_{-\infty}^{\infty}\mathrm{d}\omega\,\mathrm{e}^{-\mathrm{i}\omega t}\frac{J_{ab}(\omega)}{1-\mathrm{e}^{-\beta\omega}}. \qquad (3.6)$$

This is the bosonic fluctuation-dissipation theorem [6, 9].

3.1.2 Sum-over-poles decomposition of bath correlation functions

We will see later that the form of exponential expansion of $\left\langle \hat{F}_a^{\mathrm{B}}(t)\hat{F}_b^{\mathrm{B}}(0)\right\rangle_{\mathrm{B}}$ in Eq. (3.6) actually dictates the explicit expressions of either the DEOM or HEOM formalism. Some related properties of this expansion are as described here.

Firstly, the prerequisite on a form of exponential expansion for bare bath correlation functions is rather generally achievable, as shown in what follows. Consider the Fourier integrand of Eq. (3.6), i.e., the spectrum, represented by the product of $J_{ab}(\omega)$ and $f^{\mathrm{Bose}}(\omega) = 1/(1-\mathrm{e}^{-\beta\omega})$. After exploiting certain sum-over-poles decompositions on $J_{ab}(\omega)$ and $f^{\mathrm{Bose}}(\omega)$, the Cauchy's contour integration technique is applied for the formal evaluation of Eq. (3.6). Let $\{z = -\mathrm{i}\gamma_{abj}; j = 1,\cdots,N_J\}$ be the poles of $J_{ab}(z)$ in the lower-half plane, and $\{z = -\mathrm{i}\check{\gamma}_m; m = 1,\cdots,\infty\}$ be those of the Bose function $f^{\mathrm{Bose}}(z)$, with $\check{\gamma}_m = 2\pi m/\beta$ being the Matsubara frequencies. The resulting infinite exponential series has the general form,

$$\left\langle \hat{F}_a^{\mathrm{B}}(t)\hat{F}_b^{\mathrm{B}}(0)\right\rangle_{\mathrm{B}} = \sum_{j=1}^{N_J}\eta_{abj}\mathrm{e}^{-\gamma_{abj}t} + \sum_{m=1}^{\infty}\check{\eta}_{abm}\mathrm{e}^{-\check{\gamma}_m t}. \qquad (3.7)$$

Two properties of the involved parameters will be of some non-essential but practical relevance to the final DEOM/HEOM expressions. Both these properties are related to Eq. (3.5).

One is related to the pre-exponential coefficients $\{\check{\eta}_{abm}\}$, originating from the Bose function, being entirely real [15]; i.e.,

$$\check{\eta}_{abm} = \check{\eta}_{abm}^*. \qquad (3.8)$$

In fact, the Matsubara expansion of the Bose function leads to $\check{\eta}_{abm} = -\mathrm{i}(2/\beta)J_{ab}(-\mathrm{i}\check{\gamma}_m)$. Now, by applying the Hermitian and anti-symmetry relations of Eq. (3.5), we conclude that while $J_{ab}(\omega)$ can be complex when $a \neq b$, its analytical continuation $J_{ab}(\mathrm{i}\omega)$ is purely imaginary; thus, $\check{\eta}_{abm}$ is real. This property remains with those op-

timal sum-over-poles expansions, the Padé spectrum decompositions of the Bose function [28, 29].

Another property is that the exponents $\{\gamma_{abj}\}$, originating from $J_{ab}(\omega)$, appear either real or in *complex conjugate pairs.* This property can be expressed as

$$\gamma_{ab\bar{j}} \equiv \gamma_{abj}^* \in \{\gamma_{abj}; j = 1,\cdots,N_J\}, \qquad (3.9)$$

which is also related to Eq. (3.5).

Without loss of generality, we hereafter assume all those $\{\gamma_{abj} = \gamma_j\}$ independent of the indexes (ab). For an accuracy controllable optimal DEOM construction, [16, 17, 28–31] consider Eq. (3.7) as a finite exponential-plus-residue expansion form of

$$\left\langle \hat{F}_a^{\mathrm{B}}(t)\hat{F}_b^{\mathrm{B}}(0)\right\rangle_{\mathrm{B}} = \sum_{k=1}^{K}\eta_{abk}\mathrm{e}^{-\gamma_k t} + 2\Delta_{ab}\delta(t). \qquad (3.10)$$

Here, $K = N_J + N_{\mathrm{Bose}}$ is the total number of poles, chosen by taking into account both $J_{ab}(\omega)$ and the Bose function. The last term, if it were expressed exactly, would be the residue from all remaining $(m > N_{\mathrm{Bose}})$ components in Eq. (3.7), which are not included in the first term of Eq. (3.10). The resulting residue spectra must be real and symmetric functions, as inferred from the fact that all $\check{\gamma}_m$ and $\check{\eta}_{abm}$ are real. This fact supports the last term of Eq. (3.10) the white-noise-residue (WNR) ansatz, in close relation to the accuracy controllable optimal DEOM/HEOM constructions [16, 17, 28–31]. Apparently, $\Delta_{ab} = \Delta_{ab}^*$, in line with Eq. (3.8).

Moreover, the time-reversal (backward) counterpart to Eq. (3.10), as inferred from Eq. (2.8), can be expressed as

$$\left\langle \hat{F}_b^{\mathrm{B}}(0)\hat{F}_a^{\mathrm{B}}(t)\right\rangle_{\mathrm{B}} = \sum_{k=1}^{K}\eta_{ab\bar{k}}^*\mathrm{e}^{-\gamma_k t} + 2\Delta_{ab}\delta(t). \qquad (3.11)$$

The index $\bar{k} \in \{k = 1,\cdots,K\}$, defined in line with Eq. (3.9) via $\gamma_{\bar{k}} \equiv \gamma_k^*$. Apparently, $\bar{k} = k$ if γ_k is real.

3.2 Dissipatons decomposition scheme and generalized diffusion equation

Consider now the hybridizing bath operators $\{\hat{F}_a^{\mathrm{B}}\}$ in the dissipaton decomposition, as follows [21]:

$$\hat{F}_a^{\mathrm{B}} \equiv \sum_{k=1}^{K}\hat{f}_{ak} + \delta\hat{F}_a. \qquad (3.12)$$

The involved $\{\hat{f}_{ak}, \delta\hat{F}_a\}$ are called dissipatons that support a statistical quasi-particle picture to account for the influence of a Gaussian environment. Dissipatons are defined via their correlation functions in relation to the individual components in Eq. (3.7) or (3.11). These are

$(t > 0)$

$$\langle \hat{f}_{ak}(t)\hat{f}_{bj}(0)\rangle_{\mathrm{B}} = \delta_{kj}\eta_{abk}\mathrm{e}^{-\gamma_k t},$$

$$\langle \hat{f}_{bj}(0)\hat{f}_{ak}(t)\rangle_{\mathrm{B}} = \delta_{kj}\eta^*_{ab\bar{k}}\mathrm{e}^{-\gamma_k t}; \qquad (3.13)$$

$\langle \hat{f}_{ak}(t)\delta\hat{F}_b(0)\rangle_{\mathrm{B}} = 0$, and

$$\langle \delta\hat{F}_a(t)\delta\hat{F}_b(0)\rangle_{\mathrm{B}} = \langle \delta\hat{F}_b(0)\delta\hat{F}_a(t)\rangle_{\mathrm{B}} = 2\Delta_{ab}\delta(t). \quad (3.14)$$

Both Eqs. (3.10) and (3.11) are strictly preserved. We have thus verified that the above statistical quasi-particles or dissipatons decomposition scheme is exact for Gaussian bath interactions (cf. Section 2.1).

As inferred from Eq. (3.13), where $\gamma_{\bar{k}} \equiv \gamma^*_k$, in general, we obtain

$$\langle \hat{f}_{bj}(0)\hat{f}_{ak}(t)\rangle_{\mathrm{B}} = \langle \hat{f}_{a\bar{k}}(t)\hat{f}_{b\bar{j}}(0)\rangle^*_{\mathrm{B}}. \quad (3.15)$$

This is the time-reversal relation for bosonic dissipatons, which also implies that $\hat{f}_{a\bar{k}} = \hat{f}^\dagger_{ak}$, as inferred from Eq. (2.8).

Equation (3.13) highlights two important features of dissipatons: (i) Dissipatons with different "color-γ_k" are statistically independent with respective to the k-index; (ii) each individual dissipaton is of a *single-exponential* correlation function, with a *same exponent* for both the forward and the backward paths. These features are closely related to the dissipaton algebra used in the DEOM construction. In particular, the feature (ii) above leads to [21]

$$\mathrm{tr}_{\mathrm{B}}\left[\left(\frac{\partial}{\partial t}\hat{f}_{ak}\right)_{\mathrm{B}}\rho_{\mathrm{T}}(t)\right] = -\gamma_k \mathrm{tr}_{\mathrm{B}}\left[\hat{f}_{ak}\rho_{\mathrm{T}}(t)\right]. \quad (3.16)$$

This is the *generalized diffusion equation* for dissipatons, where γ_k can be complex and the total system-and-bath composite $\rho_{\mathrm{T}}(t)$ is non-Gaussian in general.

To complete the description of dissipatons, we are also interested in their variances in the bare bath canonical ensembles. Start again from Eq. (3.6) for the variance of

$$\langle \hat{F}^{\mathrm{B}}_a \hat{F}^{\mathrm{B}}_b \rangle_{\mathrm{B}} = \frac{1}{\pi}\mathrm{Re}\int_{-\infty}^{\infty}\mathrm{d}\omega\frac{J_{ab}(\omega)}{1-\mathrm{e}^{-\beta\omega}}. \quad (3.17)$$

Note also that $[\hat{f}_{ak}, \hat{f}_{bj}] = 0$, as $\hat{F}^{\mathrm{B}}_a$ in Eq. (3.2) is simply a collection of bath coordinates. Consider now Eq. (3.13). We have

$$\langle \hat{f}_{ak}\hat{f}_{bj}\rangle_{\mathrm{B}} = \delta_{kj}(\eta_{abk} + \eta_{bak} + \eta^*_{ab\bar{k}} + \eta^*_{ba\bar{k}})/4. \quad (3.18)$$

Together with Eq. (3.12), we obtain

$$\langle \delta\hat{F}_a\delta\hat{F}_b\rangle_{\mathrm{B}} = \langle \hat{F}^{\mathrm{B}}_a\hat{F}^{\mathrm{B}}_b\rangle_{\mathrm{B}} - \frac{1}{2}\mathrm{Re}\sum_k(\eta_{abk} + \eta_{bak}). \quad (3.19)$$

3.3 Bosonic DEOM formalism and generalized Wick's theorem

Dynamically independent DDOs explicitly contain only those colored-dissipatons, involved in the first term of Eq. (3.12). These are the active dynamical variables, explicitly engaged in the DEOM formalism [cf. Eq. (3.24)]. Those involved WNR dissipatons are also physically important, but they can be expressed in terms of the active ones [cf. Eq. (3.28)].

The active bosonic DDOs, which satisfy symmetric permutation [cf. Eqs. (2.3) and (2.4)], now read [21]

$$\rho^{(n)}_{\boldsymbol{n}}(t) \equiv \mathrm{tr}_{\mathrm{B}}\left[\left(\prod_{ak}\hat{f}^{n_{ak}}_{ak}\right)^\circ\rho_{\mathrm{T}}(t)\right]. \quad (3.20)$$

Here, $\boldsymbol{n} \equiv \{n_{ak}\}$ is the collective indexes, and

$$n = \sum_{ak}n_{ak}, \quad \text{with } n_{ak} = 0, 1, 2, \cdots$$

being the participation number for each individual $\hat{f}_{ak}$-dissipaton. Thus, $\rho^{(n)}_{\boldsymbol{n}}$ of Eq. (3.20) specifies the "configuration" of the n bosonic dissipatons involved. Denote also $\rho^{(n\pm1)}_{\boldsymbol{n}^\pm_{ak}}$ as the associated $(n\pm1)$-dissipatons configuration, with $\boldsymbol{n}^\pm_{ak}$ differing from $\boldsymbol{n}$ only at the specified $\hat{f}_{ak}$-dissipaton participation number, n_{ak}, by ±1. Apparently, the reduced system density operator is simply $\rho_{\mathrm{S}} \equiv \rho^{(0)}$.

The most important ingredient of the dissipaton algebra is the generalized Wick's theorem, which satisfies the notion of irreducibility, $(\cdots)^\circ$, as follows:

$$\mathrm{tr}_{\mathrm{B}}\left[\left(\prod_{ak}\hat{f}^{n_{ak}}_{ak}\right)^\circ\hat{f}_{bj}\rho_{\mathrm{T}}(t)\right]$$
$$= \sum_{ak}n_{ak}\langle \hat{f}_{ak}\hat{f}_{bj}\rangle^>_{\mathrm{B}}\rho^{(n-1)}_{\boldsymbol{n}^-_{ak}}(t) + \rho^{(n+1)}_{\boldsymbol{n}^+_{bj}}(t), \quad (3.21)$$

and

$$\mathrm{tr}_{\mathrm{B}}\left[\left(\prod_{ak}\hat{f}^{n_{ak}}_{ak}\right)^\circ\rho_{\mathrm{T}}(t)\hat{f}_{bj}\right]$$
$$= \sum_{ak}n_{ak}\langle \hat{f}_{bj}\hat{f}_{ak}\rangle^<_{\mathrm{B}}\rho^{(n-1)}_{\boldsymbol{n}^-_{ak}}(t) + \rho^{(n+1)}_{\boldsymbol{n}^+_{bj}}(t). \quad (3.22)$$

Here [cf. Eq. (3.13)],

$$\langle \hat{f}_{ak}\hat{f}_{bj}\rangle^>_{\mathrm{B}} \equiv \langle \hat{f}_{ak}(0+)\hat{f}_{bj}\rangle = \delta_{kj}\eta_{abk},$$
$$\langle \hat{f}_{bj}\hat{f}_{ak}\rangle^<_{\mathrm{B}} \equiv \langle \hat{f}_{bj}\hat{f}_{ak}(0+)\rangle = \delta_{kj}\eta^*_{ab\bar{k}}. \quad (3.23)$$

The generalized Wick's theorem above holds for Gaussian bath influences, regardless of the fact that the total system-and-bath composite $\rho_{\mathrm{T}}(t)$ is generally non-Gaussian and non-factorizable.

The DEOM formalism is summarized as follows [21, 22]:

$$\dot{\rho}^{(n)}_{\boldsymbol{n}} = -\left(\mathrm{i}\mathcal{L}(t) + \sum_{ak}n_{ak}\gamma_k + \delta\mathcal{R}\right)\rho^{(n)}_{\boldsymbol{n}}$$
$$-\mathrm{i}\sum_{ak}\left(n_{ak}\mathcal{C}^{\mathrm{eff}}_{ak}(t)\rho^{(n-1)}_{\boldsymbol{n}^-_{ak}} + \mathcal{A}_a\rho^{(n+1)}_{\boldsymbol{n}^+_{ak}}\right), \quad (3.24)$$

with [cf. the total Hamiltonian $H_{\text{T}}(t)$ of Eq. (3.1)]

$$\delta\mathcal{R}\hat{O} \equiv \sum_{a,b}\Delta_{ab}\big[\hat{Q}_a^{\text{S}},[\hat{Q}_b^{\text{S}},\hat{O}]\big], \tag{3.25}$$

$$\mathcal{C}_{ak}^{\text{eff}}(t) \equiv \mathcal{C}_{ak} - E(t)\sum_b(\eta_{abk}-\eta_{ab\bar{k}}^*)\zeta_b^{\text{B}}, \tag{3.26}$$

and

$$\mathcal{A}_a\hat{O} \equiv [\hat{Q}_a^{\text{S}},\hat{O}],$$

$$\mathcal{C}_{ak}\hat{O} \equiv \sum_b\big(\eta_{abk}\hat{Q}_b^{\text{S}}\hat{O} - \eta_{ab\bar{k}}^*\hat{O}\hat{Q}_b^{\text{S}}\big). \tag{3.27}$$

Note that the second term of Eq. (3.26) is responsible for the Fano interference. An individual $(\eta_{abk}-\eta_{ab\bar{k}}^*)$ is nonzero only when its corresponding γ_k arises from the poles of $J_{ab}(\omega)$. Those associated with the poles of the Bose function are all zeros [cf. Eq. (3.8)].

The DEOM theory also includes the single-WNR-dissipaton-containing DDOs (SW-DDOs) [21]:

$$\varrho_{\bm{n},a'}^{(n)}(t) \equiv \text{tr}_{\text{B}}\Big[\delta\hat{F}_{a'}\Big(\prod_{ak}\hat{f}_{ak}^{n_{ak}}\Big)^{\circ}\rho_{\text{T}}(t)\Big]$$

$$= -\text{i}\sum_b\Delta_{a'b}\big[\hat{Q}_b^{\text{S}},\rho_{\bm{n}}^{(n)}(t)\big]. \tag{3.28}$$

The first identity is simply the mathematical definition of SW-DDO, $\varrho_{\bm{n};a'}^{(n)}$, which is actually an irreducible $(n+1)$-body quantity, since the involved WNR $\delta\hat{F}_{a'}$ do not correlate with the colored $\{\hat{f}_{ak}\}$-dissipatons. The second expression of Eq. (3.28) is exactly what we need for the WNR dissipaton dynamics.

Note also that there is the so-called WNR dissipaton lemma: *No more than single irreducible white-noise-dissipatons can physically participate in dynamics* [21]. Therefore, SW-DDOs of Eq. (3.28) are all we need for the WNR dissipaton dynamics, including the $\delta\mathcal{R}$-term in Eq. (3.24). In fact, the second identity of Eq. (3.28) leads to Eq. (3.25) and the expression

$$\delta\mathcal{R}\rho_{\bm{n}}^{(n)} = \text{i}\sum_a\mathcal{A}_a\varrho_{\bm{n},a}^{(n)}. \tag{3.29}$$

Actually, Eq. (3.24), in the absence of external-field induced bath polarization, where $\mathcal{C}_{ak}^{\text{eff}}(t) = \mathcal{C}_{ak}$, reduces to the celebrated HEOM formalism; see Ref. [17], for example. The latter is rooted at the Feynman–Vernon influence functional path integral formalism [7]. The HEOM theory offers no physical meanings to all $\{\rho_{\bm{n}}^{(n>0)}\}$ that were used to be just mathematical auxiliaries [12–17]. The DEOM framework, which consists of all equations in this subsections, is much more rich. The underlying picture of DDOs, Eq. (3.20), and the algebra of dissipatons, especially the generalized Wick's theorem of Eqs. (3.21) and (3.22), renders DEOM a novel theory, for not only

system but also hybrid bath dynamics. The important observations above will be further illustrated in Section 7.

We will terminate the infinite hierarchy of Eq. (3.24) to complete the DEOM framework in Section 3.5. Before doing so, we present the detailed derivations of Eqs. (3.24)–(3.28).

3.4 Derivations of bosonic DEOM formalism

3.4.1 Basic applications of dissipaton algebra

Evidently, derivations are only needed for Eq. (3.24) and the second expression of Eq. (3.28). We start by applying $\dot{\rho}_{\text{T}} = -\text{i}[H_{\text{T}}(t),\rho_{\text{T}}]$ to the total composite density operator in Eq. (3.20), and we then examine the contributions of different components in the total composite $H_{\text{T}}(t)$. Following the dissipaton decomposition of $\{\hat{F}_a^{\text{B}}\}$, Eq. (3.12), the total composite Hamiltonian, $H_{\text{T}}(t)$ of Eq. (3.1), can be recast as

$$H_{\text{T}}(t) = H(t) + h_{\text{B}} + H_{\text{SB}}'(t) + \delta H_{\text{SB}}(t), \tag{3.30}$$

with

$$H_{\text{SB}}'(t) = \sum_{ak}\big[\hat{Q}_a^{\text{S}} - \zeta_b^{\text{B}}E(t)\big]\hat{f}_{ak}, \tag{3.31}$$

$$\delta H_{\text{SB}}(t) = \sum_a\big[\hat{Q}_a^{\text{S}} - \zeta_b^{\text{B}}E(t)\big]\delta\hat{F}_a^{\text{B}}. \tag{3.32}$$

The commutator actions of h_{B}, $H_{\text{SB}}'(t)$ and $\delta H_{\text{SB}}(t)$, are evaluated, respectively, with the three aforementioned ingredients of dissipaton algebra, as follows.

The h_{B}-commutator action is evaluated via the generalized diffusion equation (3.16). Together with the Heisenberg equation of motion in the bare bath,

$$\Big(\frac{\partial}{\partial t}\hat{O}^{\text{B}}\Big)_{\text{B}} = -\text{i}[\hat{O}^{\text{B}},h_{\text{B}}], \tag{3.33}$$

we readily obtain

$$\text{i}\,\text{tr}_{\text{B}}\Big\{\Big(\prod_{ak}\hat{f}_{ak}^{n_{ak}}\Big)^{\circ}[h_{\text{B}},\rho_{\text{T}}]\Big\}$$

$$= \text{i}\,\text{tr}_{\text{B}}\Big\{\Big[\Big(\prod_{ak}\hat{f}_{ak}^{n_{ak}}\Big)^{\circ},h_{\text{B}}\Big]\rho_{\text{T}}\Big\}$$

$$= -\text{tr}_{\text{B}}\Big\{\Big[\frac{\partial}{\partial t}\Big(\prod_{ak}\hat{f}_{ak}^{n_{ak}}\Big)^{\circ}\Big]_{\text{B}}\rho_{\text{T}}\Big\}$$

$$= \Big(\sum_{ak}n_{ak}\gamma_k\Big)\rho_{\bm{n}}^{(n)}. \tag{3.34}$$

This contributes to the second term in the first parentheses of Eq. (3.24).

The $H_{\text{SB}}'(t)$-commutator action is evaluated readily via the generalized Wick's theorem, Eqs. (3.21) and (3.22),

with Eq. (3.23). With the $H'_{SB}(t)$ expression of Eq. (3.31), first evaluate

$$\text{tr}_{B}\Big\{\Big(\prod_{ak}\hat{f}_{ak}^{n_{ak}}\Big)^{\circ}\big[\hat{Q}_{b}^{S}\hat{f}_{bj},\rho_{T}\big]\Big\}$$
$$=\sum_{ak}\delta_{kj}n_{ak}\Big(\eta_{abk}\hat{Q}_{b}^{S}\rho_{\boldsymbol{n}_{ak}^{-}}^{(n-1)}-\eta_{ab\bar{k}}^{*}\rho_{\boldsymbol{n}_{ak}^{-}}^{(n-1)}\hat{Q}_{b}^{S}\Big)$$
$$+\big[\hat{Q}_{b}^{S},\rho_{\boldsymbol{n}_{bj}^{+}}^{(n+1)}\big]. \qquad (3.35)$$

It immediately follows that

$$\text{tr}_{B}\Big\{\Big(\prod_{ak}\hat{f}_{ak}^{n_{ak}}\Big)^{\circ}\big[H'_{SB}(t),\rho_{T}\big]\Big\}$$
$$=\sum_{bj}\text{tr}_{B}\Big\{\Big(\prod_{ak}\hat{f}_{ak}^{n_{ak}}\Big)^{\circ}\big[(\hat{Q}_{b}^{S}-\zeta_{b}^{B}E(t))\hat{f}_{bj},\rho_{T}\big]\Big\}$$
$$=\sum_{abk}n_{ak}\Big(\eta_{abk}\hat{Q}_{b}^{S}\rho_{\boldsymbol{n}_{ak}^{-}}^{(n-1)}-\eta_{ab\bar{k}}^{*}\rho_{\boldsymbol{n}_{ak}^{-}}^{(n-1)}\hat{Q}_{b}^{S}\Big)$$
$$-E(t)\sum_{abk}n_{ak}(\eta_{abk}-\eta_{ab\bar{k}}^{*})\zeta_{b}^{B}\rho_{\boldsymbol{n}_{ak}^{-}}^{(n-1)}$$
$$+\sum_{bj}\big[\hat{Q}_{b}^{S},\rho_{\boldsymbol{n}_{bj}^{+}}^{(n+1)}\big], \qquad (3.36)$$

which can be recast as [cf. Eq. (3.26) and (3.27)]

$$\text{tr}_{B}\Big\{\Big(\prod_{ak}\hat{f}_{ak}^{n_{ak}}\Big)^{\circ}\big[H'_{SB}(t),\rho_{T}\big]\Big\}$$
$$=\sum_{ak}\big[n_{ak}\mathcal{C}_{ak}^{\text{eff}}(t)\rho_{\boldsymbol{n}_{ak}^{-}}^{(n-1)}+\mathcal{A}_{a}\rho_{\boldsymbol{n}_{ak}^{+}}^{(n+1)}\big]. \qquad (3.37)$$

This contributes to the last term in Eq. (3.24).

Turn now to the influence of $\delta H_{SB}(t)$, Eq. (3.31), on the DDOs of Eq. (3.20). Its contribution is an analogue to Eq. (3.37) but contains no contraction terms, since $\langle\hat{f}_{ak}(t)\delta\hat{F}_{b}(0)\rangle_{B}=0$. That is,

$$\text{tr}_{B}\Big\{\Big(\prod_{ak}\hat{f}_{ak}^{n_{ak}}\Big)^{\circ}\big[\delta H_{SB}(t),\rho_{T}\big]\Big\}=\sum_{a}\mathcal{A}_{a}\varrho_{\boldsymbol{n};a}^{(n)}. \quad (3.38)$$

It can be recast as

$$\text{i}\,\text{tr}_{B}\Big\{\Big(\prod_{ak}\hat{f}_{ak}^{n_{ak}}\Big)^{\circ}\big[\delta H_{SB}(t),\rho_{T}\big]\Big\}=\delta\mathcal{R}\rho_{\boldsymbol{n}}^{(n)}. \quad (3.39)$$

Adopted here is Eq. (3.29), the trivial result of the second identity of Eq. (3.28), which is the remaining equation to be derived, as below.

3.4.2 *Treatment of white-noise-residue dissipatons*

Recall the SW-DDO lemma: *No more than single irreducible white-noise-dissipatons can physically participate in dynamics* [21]. Consequently, the SW-DDOs, $\varrho_{\boldsymbol{n},a}^{(n)}(t)$ of Eq. (3.28), are all we need for the WNR dissipaton dynamics, including the $\delta H_{SB}(t)$-contribution to the

DEOM formalism, Eq. (3.24).

The first identity of Eq. (3.28) is simply the mathematical definition of $\varrho_{\boldsymbol{n};a'}^{(n)}$, which is actually an irreducible $(n+1)$-body quantity, since the involved WNR $\{\delta\hat{F}_{a}\}$ does not correlate with the colored $\{\hat{f}_{ak}\}$-dissipatons. The second expression of Eq. (3.28) is exactly what we need for the WNR dissipaton dynamics.

To derive the second expression of Eq. (3.28), we recast Eq. (3.14) as

$$\langle\delta\hat{F}_{a}(t)\delta\hat{F}_{b}(0)\rangle_{B}=2\Delta_{ab}\delta(t)=\Delta_{ab}\lim_{\Lambda\to\infty}\big(\Lambda e^{-\Lambda t}\big).$$

We then evaluate $\dot{\varrho}_{\boldsymbol{n};a}^{(n)}$, with a finite but large Λ in the SW-DDO lemma limit, following the same procedure as that from Eq. (3.34) to Eq. (3.37). The resulting $\dot{\varrho}_{\boldsymbol{n};a}^{(n)}$ exclusively contains the following Λ-dependent terms:

$$-\Lambda\varrho_{\boldsymbol{n};a}^{(n)}-\text{i}\Lambda\sum_{b}\Delta_{ab}\big[\hat{Q}_{b}^{S},\rho_{\boldsymbol{n}}^{(n)}\big]\to 0,$$

which should vanish when $\Lambda\to\infty$, since $\dot{\varrho}_{\boldsymbol{n};a}^{(n)}$ does not diverge in this limit. Therefore,

$$\varrho_{\boldsymbol{n};a}^{(n)}(t)=-\text{i}\sum_{b}\Delta_{ab}\big[\hat{Q}_{b}^{S},\rho_{\boldsymbol{n}}^{(n)}(t)\big]. \qquad (3.40)$$

This is the second expression of Eq. (3.28). It also completes the derivation of Eq. (3.24). The fact that Eq. (3.24) recovers the path integral-based HEOM formalism *de facto* validates the dissipaton algebra discussed throughout this section.

3.5 Derivative-resum truncation scheme

The DEOM formalism, Eq. (3.24), consists of an infinite hierarchy and needs to be truncated. This issue can be addressed via practical aspects as well as some principles of elementary quantum mechanics. Various schemes have been proposed [13–15], all from the practical aspect, with a focus on the approximate treatments of $\{\rho_{\boldsymbol{n}}^{(n>L)}\}$. The standard method is to set all $\{\rho_{\boldsymbol{n}}^{(n>L)}=0\}$. This simplest scheme is usually sufficient and reliable, owing to the nonperturbative nature of the DEOM/HEOM formalism [14]. As inferred from the DDOs expression, Eq. (3.20), the standard truncation scheme treats all L-body dissipatons exactly. The higher level many-body effects would have been accounted for via the generalized Wick's contraction approximation. This fact may explain why a variety of other $\{\rho_{\boldsymbol{n}}^{(n>L)}\}$-based schemes [13–15] hardly show improvement when implemented; see Ref. [32] for numerical demonstrations.

Note that the total number of active bosonic DDOs participating in Eq. (3.24) is

Frontiers of Physics

$$\mathcal{N}(L, \tilde{K}) = \sum_{n=0}^{L} \frac{(n + \tilde{K} - 1)!}{n!(\tilde{K} - 1)!} = \frac{(L + \tilde{K})!}{L!\tilde{K}!}, \qquad (3.41)$$

where $\tilde{K} = N_a K$, with a fixed number N_a of the $\{\hat{Q}_a^{\mathrm{s}} \hat{F}_a^{\mathrm{B}}\}$-decomposition terms in H_{SB} of the study [33]. The optimal DEOM/HEOM construction goes with a minimum number of K-space basis-set dissipatons [cf. Eq. (3.10) and comments therein]. It should also have an efficient L-space truncation scheme. The number of $\{\rho_{\boldsymbol{n}}^{(L+1)}\}$ is often comparable to or even greater than that of $\{\rho_{\boldsymbol{n}}^{(n \leqslant L)}\}$ in total. It would be practically important to have a truly improved resum scheme to retrieve the influence of $\{\rho_{\boldsymbol{n}}^{(L+1)}\}$ in the final DEOM dynamics.

In this paper, we treat the issue of truncation, not only from the aforementioned practical aspect, but, more fundamentally, also from the invariance principle of *quantum mechanics prescriptions* [32]. It demands that a proper truncation scheme in the Schrödinger picture be transferable to a Heisenberg-picture equivalent to Eq. (3.24), without further approximations. We will see in Section 7.4 that the standard $\{\rho_{\boldsymbol{n}}^{(n > L)} = 0\}$-based scheme [6, 13–15, 34, 35] fails in this formal requirement. Considered below is the so-called derivative-resum scheme [32, 36].

To this end, we scrutinize the $\dot{\rho}_{\boldsymbol{n}_{ak}^+}^{(L+1)}$ expression, with the general form of Eq. (3.24). To simplify the notation, we denote the quantity inside the first parentheses of Eq. (3.24)

$$\mathcal{L}_{\boldsymbol{n}}^{(n)}(t) \equiv i\mathcal{L}(t) + \sum_{ak} n_{ak}\gamma_k + \delta\mathcal{R}. \qquad (3.42)$$

We then have [cf. Eq. (3.24)]

$$\dot{\rho}_{\boldsymbol{n}_{ak}^+}^{(L+1)} = -\mathcal{L}_{\boldsymbol{n}_{ak}^+}^{(L+1)}(t)\rho_{\boldsymbol{n}_{ak}^+}^{(L+1)} - i\sum_{bj}\mathcal{A}_b\rho_{\boldsymbol{n}_{ak,bj}^{+,+}}^{(L+2)}$$
$$- i\sum_{bj}(n_{bj} + \delta_{ab}\delta_{kj})\mathcal{C}_{bj}^{\mathrm{eff}}(t)\rho_{\boldsymbol{n}_{ak,bj}^{+,-}}^{(L)}. \qquad (3.43)$$

The derivative-resum truncation goes [32, 36]

$$\dot{\rho}_{\boldsymbol{n}_{ak}^+}^{(L+1)} \approx -i\sum_{bj}\mathcal{A}_b\rho_{\boldsymbol{n}_{ak,bj}^{+,+}}^{(L+2)}. \qquad (3.44)$$

It leads to the following relation between the other two terms in Eq. (3.43),

$$\rho_{\boldsymbol{n}_{ak}^+}^{(L+1)} = -i\sum_{bj}\frac{n_{bj} + \delta_{ab}\delta_{kj}}{\mathcal{L}_{\boldsymbol{n}_{ak}^+}^{(L+1)}(t)}\mathcal{C}_{bj}^{\mathrm{eff}}(t)\rho_{\boldsymbol{n}_{ak,bj}^{+,-}}^{(L)}. \qquad (3.45)$$

This closes the bosonic DEOM formalism with

$$\dot{\rho}_{\boldsymbol{n}}^{(L)} = -\mathcal{L}_{\boldsymbol{n}}^{(L)}(t)\rho_{\boldsymbol{j}}^{(L)} - i\sum_{ak} n_{ak}\mathcal{C}_{ak}^{\mathrm{eff}}(t)\rho_{\boldsymbol{n}_{ak}^-}^{(L-1)}$$
$$- \sum_{ak,bj}\mathcal{A}_a\frac{n_{bj} + \delta_{ab}\delta_{kj}}{\mathcal{L}_{\boldsymbol{n}_{ak}^+}^{(L+1)}(t)}\mathcal{C}_{bj}^{\mathrm{eff}}(t)\rho_{\boldsymbol{n}_{ak,bj}^{+,-}}^{(L)}. \qquad (3.46)$$

Explicitly used here is Eq. (3.45), which is equivalent to Eq. (3.44). The latter is related directly to the equivalent Heisenberg prescription of DEOM truncation; cf. Section 7.4. The involved superoperator inverse, $1/\mathcal{L}_{\boldsymbol{n}_{ak}^+}^{(L+1)}(t)$ in Eq. (3.46), can be evaluated with tensor algebra, as detailed in Section 2.4. The Dyson equation would also be useful to facilitate the evaluation.

The bosonic DEOM framework is now complete. It consists of all equations in Section 3.3, including the generalized Wick's theorem, which enables DEOM to be a theory for not only systems but also hybrid bath dynamics. The DEOM formalism, Eq. (3.24) with $n \leqslant L$ and the terminal expression (3.45) or Eq. (3.46), governs how the DDOs evolve in time as well as the steady-state solutions for structural properties; cf. Section 7.1 for further comments. Note that $\{\rho_{\boldsymbol{n}}^{(L+1)}\}$ via Eq. (3.45) is also a useful part of the complete theory. The derivative-resum scheme presented in this subsection does obey the invariance principle of quantum mechanics prescriptions (cf. Section 7.4), with the overall best performance, by far, among all resum schemes we have tested; cf. Section 6.4 and also Ref. [32].

Note that a variation of Eq. (3.45), developed originally by Tanimura and Wolynes [37], supports also a prescription invariant correspondence. However, the derivation there involved a local classical treatment, which replaces individual $\mathcal{L}_{\boldsymbol{n}_{ak}^+}^{(L+1)}$ with its damping constant only [32, 37]. This comprises the numerical efficiency to about the same as the standard $\{\rho_{\boldsymbol{n}}^{(n \geqslant L+1)} = 0\}$–based truncation; see Ref. [32] for numerical demonstrations.

4 Fermionic DEOM theory

4.1 Bath hybridization functions and setup

4.1.1 Quantum transport setup

The fermionic DEOM will be constructed in contact with an electron transport setup such as in Fig. 2, where a mesoscopic electronic impurity system is in contact with electrodes ($\alpha = $ L and R), which are represented by bath reservoirs here. Throughout this paper, we set $\mu_{\mathrm{L}}^{\mathrm{eq}} = \mu_{\mathrm{R}}^{\mathrm{eq}} = 0$ for equilibrium chemical potentials in the absence of an external field. Also denote $\beta_\alpha \equiv 1/(k_{\mathrm{B}}T_\alpha)$, with k_{B} being the Boltzmann constant and T_α the temperature of the α-electrode.

The total composite Hamiltonian $H_{\mathrm{T}}(t)$, in the presence of external fields, has the generic form of Eq. (2.1), where the impurity system $H(t)$ is arbitrary, and the reservoir environment belongs to a Gaussian bath model,

110306-10

YiJing Yan, et al., Front. Phys. 11(4), 110306 (2016)
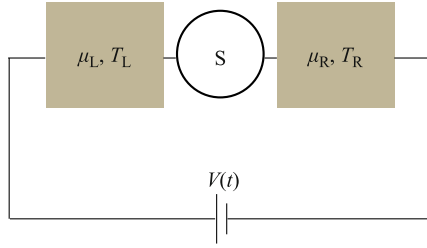
Fig. 2 Schematic representation of a quantum electron transport setup, where a mesoscopic system S is coupled to two macroscopic electrodes, L and R, under temperatures T_L and T_R, respectively. The difference in chemical potential between L and R is controlled by a time-dependent bias voltage, $V(t)$, applied across the two electrodes.

cf. Section 2.1. The specifications of h_B and H_{SB} for the electron transport setup are as follows.

The bare reservoirs bath (electrodes) Hamiltonian is modeled as noninteracting electrons,

$$h_B = \sum_\alpha \hat{h}_\alpha; \quad \text{with} \quad \hat{h}_\alpha = \sum_k \epsilon_{\alpha k} \hat{d}^+_{\alpha k} \hat{d}^-_{\alpha k}. \quad (4.1)$$

Here, $\hat{d}^-_{\alpha k} \equiv \hat{d}_{\alpha k}$ ($\hat{d}^+_{\alpha k} \equiv \hat{d}^\dagger_{\alpha k}$) denotes the annihilation (creation) operator for the kth single-electron spin-orbital state with energy $\epsilon_{\alpha k}$ in the α-electrode. Denote also $\hat{a}^-_u \equiv \hat{a}_u$ ($\hat{a}^+_u \equiv \hat{a}^\dagger_u$), the electron annihilation (creation) operator in the specified system spin-orbital $|u\rangle$-state.

The system-reservoirs interaction Hamiltonian assumes the standard transfer coupling form,

$$H_{SB} = \sum_{\alpha u} \left(\hat{a}^+_u \hat{F}^-_{\alpha u} + \hat{F}^+_{\alpha u} \hat{a}^-_u \right), \quad (4.2)$$

with the linear hybridizing bath operators of

$$\hat{F}^+_{\alpha u} \equiv \sum_k t_{\alpha k u} \hat{d}^+_{\alpha k} = (\hat{F}^-_{\alpha u})^\dagger. \quad (4.3)$$

For bookkeeping, introduce the sign symbols $\sigma = +, -$ and $\bar{\sigma}$ with the sign opposite to that of σ.

To manipulate and control the electronic dynamics in the central system, the external fields are, in general, time-dependent, such as the laser pulses applied to the system. This case had been implied via the time-dependent $H(t)$ for system; cf. Eq. (2.2). The quantum transport setup naturally includes a time-dependent external bias electric (voltage) potential, $eV(t) = \mu_L(t) - \mu_R(t)$. Its effect can be described by rigid homogeneous time-dependent shifts of the conduction bands of electrodes such that the occupation on each electronic state is unchanged [38]. The shifted $\hat{h}_\alpha$ reads

$$\hat{h}^{eff}_\alpha(t) = \sum_k [\epsilon_{\alpha k} + \mu_\alpha(t)] \hat{d}^+_{\alpha k} \hat{d}^-_{\alpha k} = \hat{h}_\alpha + \mu_\alpha(t) \hat{N}_\alpha. \quad (4.4)$$

The electron number operator $\hat{N}_\alpha$ in the α-electrode satisfies $[\hat{h}_\alpha, \hat{N}_\alpha] = 0$, in line with the electron number con-

servation in an isolated electrode. The transport current operator, with a specified flux from the bath α-reservoir to the system, is then $\hat{I}_\alpha \equiv -\frac{d}{dt}\hat{N}_\alpha = -i[H_{SB}, \hat{N}_\alpha]$. Together with Eq. (4.2), we obtain

$$\hat{I}_\alpha = -i \sum_u \left(\hat{a}^+_u \hat{F}^-_{\alpha u} - \hat{F}^+_{\alpha u} \hat{a}^-_u \right). \quad (4.5)$$

The DEOM-based evaluations of transport current and current-current correlation functions will be discussed in Section 7.2.

The total composite Hamiltonian to be treated with the fermionic DEOM theory, including the last term of Eq. (2.1), can now be expressed as

$$H_T(t) = H(t) + \sum_\alpha \hat{h}^{eff}_\alpha(t) + H_{SB}. \quad (4.6)$$

The last two terms remain in the framework of the linear hybridization noninteracting bath model that obeys the Wick's Gaussian statistics, as elaborated in Section 2.1. For later use, also denote the bath Hamiltonians,

$$h^{st}_B \equiv \sum_\alpha \hat{h}^{st}_\alpha \quad \text{and} \quad h^{eff}_B(t) \equiv \sum_\alpha \hat{h}^{eff}_\alpha(t), \quad (4.7)$$

in the presence of time-independent and time-dependent bias voltage potentials, respectively.

4.1.2 Bath hybridization and equilibrium correlation functions

The hybridizing bath spectral density functions, which characterize the influence of $\{\hat{F}^\sigma_{\alpha u}\}$, Eq. (4.3), are defined with the bare bath h_B of Eq. (4.1). They read

$$J_{\alpha u v}(\omega) \equiv J^-_{\alpha u v}(\omega) = \pi \sum_k t^*_{\alpha k u} t_{\alpha k v} \delta(\omega - \epsilon_{\alpha k}). \quad (4.8)$$

Its equivalent thermodynamics definition is given by [cf. the bosonic Eq. (3.4)]

$$J^\sigma_{\alpha u v}(\omega) \equiv \frac{1}{2} \int_{-\infty}^\infty dt \, e^{i\omega t} \left\langle \left\{ \hat{F}^\sigma_{\alpha u}(t), \hat{F}^{\bar{\sigma}}_{\alpha v}(0) \right\} \right\rangle^{eq}_B. \quad (4.9)$$

It is easy to verify that [cf. the bosonic Eq. (3.5)]

$$J^\sigma_{\alpha v u}(\omega) = [J^\sigma_{\alpha u v}(\omega)]^* = J^{\bar{\sigma}}_{\alpha u v}(\omega). \quad (4.10)$$

Moreover,

$$\left\langle \hat{F}^\sigma_{\alpha u}(t) \hat{F}^{\bar{\sigma}}_{\alpha v}(0) \right\rangle^{eq}_B = \frac{1}{\pi} \int_{-\infty}^\infty d\omega \, e^{\sigma i \omega t} \frac{J^\sigma_{\alpha u v}(\omega)}{1 + e^{\sigma \beta_\alpha \omega}}. \quad (4.11)$$

This is the fermionic fluctuation-dissipation theorem [6, 8, 9]. Both Eqs. (4.9) and (4.11) follow the so-called $\hat{h}_\alpha$-based thermodynamic prescription: $\hat{F}^\sigma_{\alpha u}(t) = e^{i\hat{h}_\alpha t} \hat{F}^\sigma_{\alpha u} e^{-i\hat{h}_\alpha t}$ and $\langle \hat{O} \rangle^{eq}_B = \text{tr}_B(\hat{O} e^{-\beta_\alpha \hat{h}_\alpha})/Z^{eq}_\alpha$, with $Z^{eq}_\alpha = \text{tr}_B e^{-\beta_\alpha \hat{h}_\alpha}$, the canonical ($\mu^{eq}_\alpha = 0$) ensembles partition function at temperature T_α.

4.2 Steady-state versus nonstationary bath correlation functions

4.2.1 Steady-state bath correlation functions

Consider the nonequilibrium steady-state case, in which the applied bias potential, $eV = \mu_{\mathrm{L}} - \mu_{\mathrm{R}}$, is time-independent. The effective α-electrode Hamiltonian of Eq. (4.4) reads

$$\hat{h}_\alpha^{\mathrm{st}} \equiv \hat{h}_\alpha + \mu_\alpha \hat{N}_\alpha = \sum_k (\epsilon_{\alpha k} + \mu_\alpha) \hat{d}_{\alpha k}^+ \hat{d}_{\alpha k}^-. \quad (4.12)$$

Nonequilibrium steady-state $\langle \hat{F}_{\alpha u}^\sigma(t) \hat{F}_{\alpha v}^{\bar{\sigma}}(0) \rangle_{\mathrm{B}}$ follows the $\hat{h}_\alpha^{\mathrm{st}}$-based thermodynamic prescription. It involves the partition function of grand canonical ensembles, $Z_\alpha(\beta_\alpha, \mu_\alpha) = \mathrm{tr}_{\mathrm{B}} e^{-\beta_\alpha(\hat{h}_\alpha + \mu_\alpha \hat{N}_\alpha)}$, at a specified temperature T_α and chemical potential μ_α. The underlying statistical thermodynamics average is completely characterized by $1/[1 + e^{\sigma \beta_\alpha(\omega - \mu_\alpha)}]$, the Fermi function for electrons ($\sigma = +$) or holes ($\sigma = -$). In parallel, the steady-state hybridizing bath spectral density functions are $J_{\alpha uv}^{\mathrm{st}}(\omega) = J_{\alpha uv}(\omega - \mu_\alpha)$, in relation to their μ_α-free equilibrium counterparts, Eq. (4.9). Consequently, the nonequilibrium steady-state correlation functions are related to the equilibrium ones as

$$\langle \hat{F}_{\alpha u}^\sigma(t) \hat{F}_{\alpha v}^{\bar{\sigma}}(0) \rangle_{\mathrm{B}} = e^{\sigma i \mu_\alpha t} \langle \hat{F}_{\alpha u}^\sigma(t) \hat{F}_{\alpha v}^{\bar{\sigma}}(0) \rangle_{\mathrm{B}}^{\mathrm{eq}}. \quad (4.13)$$

The equilibrium $\langle \cdots \rangle_{\mathrm{B}}^{\mathrm{eq}}$ in the right-hand-side of the above expression follows the μ_α-free $\hat{h}_\alpha$-based thermodynamic prescription, as specified following Eq. (4.11).

It is easy to show that the time-reversal counterpart to the nonequilibrium steady-state $\langle \hat{F}_{\alpha u}^\sigma(t) \hat{F}_{\alpha v}^{\bar{\sigma}}(0) \rangle_{\mathrm{B}}$ satisfies [cf. the first identity of Eq. (2.8)]

$$\langle \hat{F}_{\alpha v}^{\bar{\sigma}}(0) \hat{F}_{\alpha u}^\sigma(t) \rangle_{\mathrm{B}} = \langle \hat{F}_{\alpha u}^\sigma(t) \hat{F}_{\alpha v}^{\bar{\sigma}}(0) \rangle_{\mathrm{B}}^*. \quad (4.14)$$

We also have [cf. the second identity of Eq. (2.8)]

$$\langle \hat{F}_{\alpha u}^\sigma(t - i\beta) \hat{F}_{\alpha v}^{\bar{\sigma}}(0) \rangle_{\mathrm{B}} = e^{\sigma \beta \mu_\alpha} \langle \hat{F}_{\alpha v}^{\bar{\sigma}}(t) \hat{F}_{\alpha v}^{\bar{\sigma}}(0) \rangle_{\mathrm{B}}^*. \quad (4.15)$$

This is the grand canonical detailed-balance relation. However, there is no simple relation if it involves flux.

4.2.2 Nonstationary bath correlation functions

In the presence of time-dependent $\mu_\alpha(t) \equiv \mu_\alpha + \Delta_\alpha(t)$, the hybridizing bath correlation functions,

$$C_{\alpha uv}^\sigma(t, \tau) \equiv \langle \hat{F}_{\alpha u}^\sigma(t) \hat{F}_{\alpha v}^{\bar{\sigma}}(\tau) \rangle_{\mathrm{B}}^{\mathrm{nst}}, \quad (4.16)$$

are nonstationary and do not have time-translational invariance. While $\langle \cdots \rangle_{\mathrm{B}}^{\mathrm{nst}}$ remains in the $\hat{h}_\alpha^{\mathrm{st}}$-based prescription of the average of grand canonical ensembles, those $\{\hat{F}_{\alpha u}^\sigma(t)\}$ inside $\langle \cdots \rangle_{\mathrm{B}}^{\mathrm{nst}}$ are governed by $\hat{h}_\alpha^{\mathrm{eff}}(t) \equiv$

$\hat{h}_\alpha^{\mathrm{st}} + \Delta_\alpha(t) \hat{N}_\alpha$. That is

$$\frac{\partial}{\partial t} \hat{F}_{\alpha u}^\sigma(t) = -i [\hat{F}_{\alpha u}^\sigma(t), \hat{h}_\alpha^{\mathrm{eff}}(t)], \quad (4.17)$$

or

$$\hat{F}_{\alpha u}^\sigma(t) = \exp_- \left[i \int_{t_0}^t d\tau \hat{h}_\alpha^{\mathrm{eff}}(\tau) \right]$$
$$\times \hat{F}_{\alpha u}^\sigma \exp_+ \left[-i \int_{t_0}^t d\tau \hat{h}_\alpha^{\mathrm{eff}}(\tau) \right].$$

The initial t_0 can be at any time prior to the time-dependent $\Delta_\alpha(t)$ taking action. The resulting nonstationary bath correlation functions are then expressed as ($t \geqslant \tau$)

$$C_{\alpha uv}^\sigma(t, \tau) = \exp \left[\sigma i \int_\tau^t dt' \Delta_\alpha(t') \right] C_{\alpha uv}^{\sigma;\mathrm{st}}(t - \tau), \quad (4.18)$$

Note that $\Delta_\alpha(t)$ is the time-dependent chemical potential, in addition to the constant part μ_α, applied on the α-electrode. The stationary $C_{\alpha uv}^{\sigma;\mathrm{st}}(t)$ simply represents the steady-state Eq. (4.13). Apparently, Eq. (4.18) can be considered the generalization of Eq. (4.13), in line with the homogeneous-conduction-band-shift ansatz, as described above Eq. (4.4).

4.3 Dissipatons decomposition scheme and generalized diffusion equation

4.3.1 Onset of exponential expansions

Consider now an exponential series expansion of the steady-state [cf. Eq. (3.7) and the remarks therein]

$$C_{\alpha uv}^{\sigma;\mathrm{st}}(t) = \sum_{k=1}^{N_J} \eta_{\alpha k uv}^\sigma e^{-\gamma_{\alpha k uv}^\sigma t} + \sum_{m=1}^\infty \check{\eta}_{\alpha m uv}^\sigma e^{-\check{\gamma}_{\alpha m}^\sigma t}. \quad (4.19)$$

The exponents are related to the poles of $J_{\alpha uv}^\sigma(\omega)$ and the Fermi function,

$$\gamma_{\alpha k uv}^\sigma = \gamma_{\alpha k uv}^{\sigma;\mathrm{eq}} - \sigma i \mu_\alpha,$$
$$\check{\gamma}_{\alpha m}^\sigma = (2m - 1)\pi/\beta_\alpha - \sigma i \mu_\alpha. \quad (4.20)$$

While $\{\check{\gamma}_{\alpha m}^{\sigma;\mathrm{eq}} = (2m - 1)\pi/\beta_\alpha\}$, the fermionic Matsubara frequencies, are all real, those from $J_{\alpha uv}^\sigma(\omega)$ have the property of $\gamma_{\alpha k uv}^{\sigma;\mathrm{eq}} = (\gamma_{\alpha k uv}^{\bar{\sigma};\mathrm{eq}})^*$, owing to the second identity of Eq. (4.10). The above observations indicate that

$$\gamma_{\alpha k uv}^\sigma = (\gamma_{\alpha k uv}^{\bar{\sigma}})^*, \quad \check{\gamma}_{\alpha m}^\sigma = (\check{\gamma}_{\alpha m}^{\bar{\sigma}})^*. \quad (4.21)$$

This property of all involved exponents will be explicitly used in the formulations later.

Furthermore, note that the symmetry relation of $J_{\alpha uv}^\sigma(\omega)$ in Eq. (4.10) implies also [cf. Eq. (3.8)]

110306-12

YiJing Yan, et al., Front. Phys. 11(4), 110306 (2016)

$$\breve{\eta}_{\alpha kuv}^{\sigma} = -(\breve{\eta}_{\alpha kuv}^{\bar{\sigma}})^*. \tag{4.22}$$

It turns out that each individual frequency-domain component from the last term of Eq. (4.19) is, in general, an asymmetric and complex function. The dominant part is antisymmetric and imaginary. All existing nonzero residue resum treatments, including the $\dot{\delta}(t)$-type WNR ansatz proposed in the original DEOM paper [21], are rather uncontrollable and case-dependent. The situation here is very different from that of the bosonic bath. The latter does support the $\delta(t)$-type WNR ansatz, i.e., the last term in Eq. (3.10), which is generally controllable [16, 17, 28–31]. Owing to the remarkably efficient Padé spectra decomposition for the Fermi/Bose function [28, 29], we adopt the zero-residue treatment for fermions Eq. (4.19), which is always controllable and has also been proved sufficient even for a variety of Kondo problems; see Ref. [36] and references therein.

For clarity, we also assume $\gamma_{\alpha kuv}^{\sigma} = \gamma_{\alpha k}^{\sigma}$, such that Eq. (4.19) can be recast as

$$\left\langle \hat{F}_{\alpha u}^{\sigma}(t) \hat{F}_{\alpha v}^{\bar{\sigma}}(0) \right\rangle_{\mathrm{B}} = \sum_{\kappa=1}^{K} \eta_{\alpha kuv}^{\sigma} e^{-\gamma_{\alpha\kappa}^{\sigma} t}. \tag{4.23}$$

Here, $K = N_J + N_{\mathrm{Fermi}}$ is the total number of poles from both $J_{\alpha uv}^{\sigma}(\omega)$ and the Fermi function.

4.3.2 Decomposition of fermionic dissipatons

To proceed, let us recast Eq. (4.2) in a compact form, the second identity below,

$$H_{\mathrm{SB}} = \sum_{\alpha u} \left(\hat{a}_u^+ \hat{F}_{\alpha u}^- + \hat{F}_{\alpha u}^+ \hat{a}_u^- \right) \equiv \sum_{\sigma\alpha u} \hat{a}_u^{\bar{\sigma}} \widetilde{F}_{\alpha u}^{\sigma}, \tag{4.24}$$

which defines

$$\widetilde{F}_{\alpha u}^{\sigma} \equiv -\sigma \hat{F}_{\alpha u}^{\sigma} \equiv \bar{\sigma} \hat{F}_{\alpha u}^{\sigma}. \tag{4.25}$$

Apparently, $\left\langle \widetilde{F}_{\alpha u}^{\sigma}(t) \widetilde{F}_{\alpha v}^{\bar{\sigma}}(0) \right\rangle_{\mathrm{B}} = -\left\langle \hat{F}_{\alpha u}^{\sigma}(t) \hat{F}_{\alpha v}^{\bar{\sigma}}(0) \right\rangle_{\mathrm{B}}$.

The decomposition of dissipatons for the fermionic bath hybridizing operators reads

$$\widetilde{F}_{\alpha u}^{\sigma} \equiv -\sigma \hat{F}_{\alpha u}^{\sigma} \equiv \sum_{\kappa=1}^{K} \hat{f}_{\alpha\kappa u}^{\sigma}, \tag{4.26}$$

with [cf. Eq. (3.13)]

$$\left\langle \hat{f}_{\alpha\kappa u}^{\sigma}(t) \hat{f}_{\alpha'\kappa'v}^{\sigma'}(0) \right\rangle_{\mathrm{B}} = -\delta_{\alpha\kappa,\alpha'\kappa'}^{\sigma,\bar{\sigma}'} \eta_{\alpha\kappa uv}^{\sigma} e^{-\gamma_{\alpha\kappa}^{\sigma} t},$$
$$\left\langle \hat{f}_{\alpha'\kappa'v}^{\sigma'}(0) \hat{f}_{\alpha\kappa u}^{\sigma}(t) \right\rangle_{\mathrm{B}} = -\delta_{\alpha\kappa,\alpha'\kappa'}^{\sigma,\bar{\sigma}'} \eta_{\alpha\kappa uv}^{\bar{\sigma}*} e^{-\gamma_{\alpha\kappa}^{\sigma} t}, \tag{4.27}$$

where

$$\delta_{\alpha\kappa,\alpha'\kappa'}^{\sigma,\bar{\sigma}'} \equiv \delta_{\sigma\bar{\sigma}'} \delta_{\alpha\alpha'} \delta_{\kappa\kappa'}. \tag{4.28}$$

The time-reversal relation for fermionic dissipatons reads [noting that $\gamma_{\alpha m}^{\bar{\sigma}*} = \gamma_{\alpha m}^{\sigma}$; cf. Eq. (4.21)]

$$\left\langle \hat{f}_{\alpha'\kappa'v}^{\bar{\sigma}'}(0) \hat{f}_{\alpha\kappa u}^{\sigma}(t) \right\rangle_{\mathrm{B}} = \left\langle \hat{f}_{\alpha\kappa u}^{\bar{\sigma}}(t) \hat{f}_{\alpha'\kappa'v}^{\sigma'}(0) \right\rangle_{\mathrm{B}}^*. \tag{4.29}$$

It is easy to verify that the above decomposition preserves the bath correlation function of Eq. (4.23).

4.3.3 Generalized diffusion equation with extension

The extension to the nonstationary case is rather straightforward. In line with Section 4.1.2, the nonstationary counterpart of Eq. (4.27), exemplified with the nonzero and forward-path one, reads $(-\infty < \tau < t < \infty)$

$$\left\langle \hat{f}_{\alpha\kappa u}^{\sigma}(t) \hat{f}_{\alpha\kappa v}^{\bar{\sigma}}(\tau) \right\rangle_{\mathrm{B}}^{\mathrm{nst}} = -\eta_{\alpha\kappa uv}^{\sigma} \exp\left[-\int_{\tau}^{t} \mathrm{d}t' \gamma_{\alpha\kappa}^{\sigma}(t') \right],$$
$$\left\langle \hat{f}_{\alpha\kappa v}^{\bar{\sigma}}(\tau) \hat{f}_{\alpha\kappa u}^{\sigma}(t) \right\rangle_{\mathrm{B}}^{\mathrm{nst}} = -\eta_{\alpha\kappa uv}^{\bar{\sigma}*} \exp\left[-\int_{\tau}^{t} \mathrm{d}t' \gamma_{\alpha\kappa}^{\sigma}(t') \right]. \tag{4.30}$$

Here,

$$\gamma_{\alpha\kappa}^{\sigma}(t) \equiv \gamma_{\alpha\kappa}^{\sigma;\mathrm{eq}} - \sigma\mathrm{i}\mu_{\alpha} - \sigma\mathrm{i}\Delta_{\alpha}(t). \tag{4.31}$$

The same-and-single-exponent nature remains; cf. the last paragraph in Section 3.2. The generalized diffusion equation [cf. Eq. (3.16)] now reads

$$\mathrm{tr}_{\mathrm{B}}\left[\left(\frac{\partial}{\partial t} \hat{f}_{\alpha\kappa u}^{\sigma} \right)_{\mathrm{B}} \rho_{\mathrm{T}}(t) \right] = -\gamma_{\alpha\kappa}^{\sigma}(t) \mathrm{tr}_{\mathrm{B}}\left[\hat{f}_{\alpha\kappa u}^{\sigma} \rho_{\mathrm{T}}(t) \right]. \tag{4.32}$$

It is to be used together with the Heisenberg equation of motion,

$$\left(\frac{\partial}{\partial t} \hat{O}^{\mathrm{B}} \right)_{\mathrm{B}} = -\mathrm{i}[\hat{O}^{\mathrm{B}}, h_{\mathrm{B}}^{\mathrm{eff}}(t)], \tag{4.33}$$

for the evaluations of the $h_{\mathrm{B}}^{\mathrm{eff}}(t)$ effect on the fermionic DDOs [cf. Eq. (3.34)].

Moreover, the fermionic counterparts to Eq. (3.23) are also rooted at the correlation functions for nonstationary dissipatons, such as Eq. (4.30), defined with $t - \tau = 0+$.

$$\left\langle \hat{f}_{\alpha\kappa u}^{\sigma} \hat{f}_{\alpha'\kappa'v}^{\sigma'} \right\rangle_{\mathrm{B}}^{>} = -\delta_{\alpha\kappa,\alpha'\kappa'}^{\sigma,\bar{\sigma}'} \eta_{\alpha\kappa uv}^{\sigma},$$
$$\left\langle \hat{f}_{\alpha'\kappa'v}^{\sigma'} \hat{f}_{\alpha\kappa u}^{\sigma} \right\rangle_{\mathrm{B}}^{<} = -\delta_{\alpha\kappa,\alpha'\kappa'}^{\sigma,\bar{\sigma}'} \eta_{\alpha\kappa uv}^{\bar{\sigma}*}. \tag{4.34}$$

4.4 Fermionic DEOM formalism and generalized Wick's theorem

For bookkeeping, we adopt the abbreviations,

$$j \equiv (\sigma\alpha\kappa u), \qquad \bar{j} \equiv (\bar{\sigma}\alpha\kappa u), \tag{4.35}$$

for the collective indexes in fermionic dissipatons, such that $\hat{f}_j \equiv \hat{f}_{\alpha\kappa u}^{\sigma}$ and so on. The fermionic DDOs are therefore [cf. Eq. (2.3) and remarks therein]

$$\rho_{\boldsymbol{j}}^{(n)}(t) \equiv \rho_{j_1\cdots j_n}^{(n)}(t) \equiv \mathrm{tr}_{\mathrm{B}}\left[\left(\hat{f}_{j_n} \cdots \hat{f}_{j_1} \right)^{\circ} \rho_{\mathrm{T}}(t) \right]. \tag{4.36}$$

YiJing Yan, et al., Front. Phys. 11(4), 110306 (2016)

110306-13

The indexes in $\rho_{\boldsymbol{j}}^{(n)}$ are self-explanatory. Note that the participating number for each fermionic dissipaton $\hat{f}_j$ can only be $n_j = 0$ or 1. The product of dissipaton operators dissipatons operator product inside $(\cdots)^{\circ}$ is also ordered. A swap of any two irreducible fermionic dissipatons causes a minus sign, such as $(\hat{f}_j \hat{f}_{j'})^{\circ} = -(\hat{f}_{j'} \hat{f}_j)^{\circ}$ [cf. Eq. (2.4)].

From Eqs. (4.32) and (4.33), we immediately obtain [cf. Eq. (3.34)]

$$\mathrm{i}\,\mathrm{tr}_{\mathrm{B}}\Big\{ \big(\hat{f}_{j_n} \cdots \hat{f}_{j_1}\big)^{\circ}[h_{\mathrm{B}}^{\mathrm{eff}}(t), \rho_{\mathrm{T}}]\Big\} = \gamma_{\boldsymbol{j}}^{(n)}(t)\rho_{\boldsymbol{j}}^{(n)}. \quad (4.37)$$

Here [noting $\gamma_j(t) \equiv \gamma_{\alpha\kappa u}^{\sigma}(t) = \gamma_{\alpha\kappa}^{\sigma}(t)$ of Eq. (4.31)],

$$\gamma_{\boldsymbol{j}}^{(n)}(t) = \sum_{r=1}^{n} \gamma_{j_r}(t). \quad (4.38)$$

The effect of H_{SB} on $\rho_{\boldsymbol{j}}^{(n)}(t)$ is to be evaluated with the generalized fermionic Wick's theorem [cf. the bosonic counterparts of Eqs. (3.21) and (3.21)]. Apparently, H_{SB} of Eq. (4.24), now reads (noting $\hat{a}_{\bar{j}} \equiv \hat{a}_{\alpha\kappa u}^{\bar{\sigma}} = \hat{a}_u^{\bar{\sigma}}$)

$$H_{\mathrm{SB}} = \sum_j \hat{a}_{\bar{j}} \hat{f}_j. \quad (4.39)$$

It will give rise to $\big\{\rho_{\boldsymbol{j}_r^-}^{(n-1)} \equiv \rho_{j_1 \cdots j_{r-1} j_{r+1} \cdots j_n}^{(n-1)}\big\}$ and $\big\{\rho_{\boldsymbol{jj}}^{(n+1)} \equiv \rho_{j_1 \cdots j_n j}^{(n+1)}\big\}$. Note also

$$\rho_{j\boldsymbol{j}}^{(n+1)} = (-)^n \rho_{\boldsymbol{j}j}^{(n+1)}. \quad (4.40)$$

It highlights the fact that the product of irreducible fermionic dissipaton operators inside the $(\cdots)^{\circ}$ in Eq. (4.36) is ordered.

The generalized Wick's theorem for fermionic dissipatons results in [cf. Eqs. (3.21) and (3.22)]

$$\mathrm{tr}_{\mathrm{B}}\Big[\big(\hat{f}_{j_n} \cdots \hat{f}_{j_1}\big)^{\circ} \hat{f}_j \rho_{\mathrm{T}}(t)\Big]$$
$$= \sum_{r=1}^{n} (-)^{r-1}\langle \hat{f}_{j_r}\hat{f}_j\rangle_{\mathrm{B}}^{>}\rho_{\boldsymbol{j}_r^-}^{(n-1)} + \rho_{j\boldsymbol{j}}^{(n+1)}, \quad (4.41)$$

and

$$\mathrm{tr}_{\mathrm{B}}\Big[\big(\hat{f}_{j_n} \cdots \hat{f}_{j_1}\big)^{\circ} \rho_{\mathrm{T}}(t)\hat{f}_j\Big]$$
$$= (-)^n \mathrm{tr}_{\mathrm{B}}\Big[\hat{f}_j\big(\hat{f}_{j_n} \cdots \hat{f}_{j_1}\big)^{\circ} \rho_{\mathrm{T}}(t)\Big]$$
$$= (-)^n \Big[\sum_{r=1}^{n}(-)^{n-r}\langle \hat{f}_j\hat{f}_{j_r}\rangle_{\mathrm{B}}^{<}\rho_{\boldsymbol{j}_r^-}^{(n-1)} + \rho_{\boldsymbol{j}j}^{(n+1)}\Big]. \quad (4.42)$$

The first identity in Eq. (4.42) highlights the *fermionic cyclic partial-trace relation*, as detailed in to the end of Appendix A of Ref. [21]. Note also

$$\mathrm{tr}_{\mathrm{B}}\Big[\big(\hat{f}_{j_n} \cdots \hat{f}_{j_1}\big)^{\circ} \hat{a}_{\bar{j}} \hat{f}_j \rho_{\mathrm{T}}(t)\Big]$$

$$= (-)^n \hat{a}_{\bar{j}} \mathrm{tr}_{\mathrm{B}}\Big[\big(\hat{f}_{j_n} \cdots \hat{f}_{j_1}\big)^{\circ} \hat{f}_j \rho_{\mathrm{T}}(t)\Big]. \quad (4.43)$$

Equations (4.39)–(4.43), together with Eq. (4.34) for the values of $\langle \hat{f}_{j_r}\hat{f}_j\rangle_{\mathrm{B}}^{>}$ and $\langle \hat{f}_j\hat{f}_{j_r}\rangle_{\mathrm{B}}^{<}$, lead readily to [21, 23]

$$\mathrm{tr}_{\mathrm{B}}\Big\{\big(\hat{f}_{j_n} \cdots \hat{f}_{j_1}\big)^{\circ}[H_{\mathrm{SB}}, \rho_{\mathrm{T}}]\Big\}$$
$$= \sum_{r=1}^{n}(-)^{n-r}\mathcal{C}_{j_r}\rho_{\boldsymbol{j}_r^-}^{(n-1)} + \sum_j \mathcal{A}_{\bar{j}}\rho_{\boldsymbol{jj}}^{(n+1)}. \quad (4.44)$$

Together with Eq. (4.37), we obtain the final DEOM formalism, as follows [21, 23].

$$\dot{\rho}_{\boldsymbol{j}}^{(n)} = -\big[\mathrm{i}\mathcal{L}(t) + \gamma_{\boldsymbol{j}}^{(n)}(t)\big]\rho_{\boldsymbol{j}}^{(n)} - \mathrm{i}\sum_j \mathcal{A}_{\bar{j}}\rho_{\boldsymbol{jj}}^{(n+1)}$$
$$- \mathrm{i}\sum_{r=1}^{n}(-)^{n-r}\mathcal{C}_{j_r}\rho_{\boldsymbol{j}_r^-}^{(n-1)}. \quad (4.45)$$

Here, $\mathcal{A}_{\bar{j}} \equiv \mathcal{A}_{\alpha\kappa u}^{\bar{\sigma}} = \mathcal{A}_u^{\bar{\sigma}}$ and $\mathcal{C}_j \equiv \mathcal{C}_{\alpha\kappa u}^{\sigma}$ are *Grassmannian* superoperators defined via

$$\mathcal{A}_u^{\sigma}\hat{O}_{\pm} \equiv \hat{a}_u^{\sigma}\hat{O}_{\pm} \pm \hat{O}_{\pm}a_u^{\sigma} \equiv \big[\hat{a}_u^{\sigma}, \hat{O}_{\pm}\big]_{\pm},$$
$$\mathcal{C}_{\alpha\kappa u}^{\sigma}\hat{O}_{\pm} \equiv \sum_v \big(\eta_{\alpha\kappa uv}^{\sigma}\hat{a}_v^{\sigma}\hat{O}_{\pm} \mp \eta_{\alpha\kappa uv}^{\bar{\sigma}*}\hat{O}_{\pm}\hat{a}_v^{\sigma}\big). \quad (4.46)$$

Here, $\hat{O}_{\pm}$ denotes an arbitrary operator, with even $(+)$ or odd $(-)$ fermionic parity, such as $\rho^{(2m)}$ or $\rho^{(2m+1)}$ in Eq. (4.36), respectively.

In Section 5, we present the HEOM formalism that also assumes the form of Eq. (4.45) but is rooted at the Feynman–Vernon influential functional path integral formulations. The close comparison between DEOM and HEOM will be scrutinized in due course.

4.5 Derivative-resum truncation scheme

We address the issue of truncation, in parallel to Section 3.5, with respect to the invariance principle of quantum mechanics prescriptions [32]. Note that various commonly used truncation schemes [13–15, 33], including the resultant quantum master equations and self-consistent Born approximations [6, 34, 35], are concerned only with the practical implementation aspect. The common feature among these conventional schemes is to set $\big\{\rho_{\boldsymbol{j}}^{(n>L)}\big\}$, all or some, to be zeroes explicitly. It will be evident in Section 7.4 that all these $\big\{\rho_{\boldsymbol{j}}^{(n>L)} = 0\big\}$-based schemes, if transferred to the Heisenberg prescriptions, require additional approximations, at least formally. The derivative-resum scheme, similar to Eq. (3.44), which preserves the invariance of the prescriptions, is to be adopted as follows.

Let us recast $\dot{\rho}_{\boldsymbol{jj}}^{(L+1)}$ via Eq. (4.45) as

$$\dot{\rho}_{\boldsymbol{j}j}^{(L+1)} = -\big[\mathrm{i}\mathcal{L}(t) + \gamma_{\boldsymbol{j}j}^{(L+1)}(t)\big]\rho_{\boldsymbol{j}j}^{(L+1)}$$

$$-\mathrm{i}\sum_{j'}\mathcal{A}_{\bar{j}'}\rho_{\boldsymbol{j}jj'}^{(L+2)} - \mathrm{i}\sum_{r=1}^{L+1}\mathcal{C}_{j_r}\rho_{\boldsymbol{j}_r}^{(L)}, \qquad (4.47)$$

where

$$\rho_{\boldsymbol{j}_r}^{(L)} \equiv \rho_{j_1\cdots j_{r-1}jj_{r+1}\cdots j_L}^{(L)}. \qquad (4.48)$$

The derivative-resum scheme, the counterpart to the bosonic Eq. (3.44), now reads

$$\dot{\rho}_{\boldsymbol{j}j}^{(L+1)} \approx -\mathrm{i}\sum_{j'}\mathcal{A}_{\bar{j}'}\rho_{\boldsymbol{j}jj'}^{(L+2)}. \qquad (4.49)$$

The other two terms in Eq. (4.47) are then related via

$$\rho_{\boldsymbol{j}j}^{(L+1)} = \frac{-\mathrm{i}}{\mathrm{i}\mathcal{L}(t)+\gamma_{\boldsymbol{j}j}^{(L+1)}(t)}\sum_{r=1}^{L+1}\mathcal{C}_{j_r}\rho_{\boldsymbol{j}_r}^{(L)}. \qquad (4.50)$$

It closes the DEOM formalism, Eq. (4.45), with [36]

$$\dot{\rho}_{\boldsymbol{j}}^{(L)} = -\Big[\mathrm{i}\mathcal{L}(t)+\sum_{r=1}^{L}\gamma_{j_r}(t)\Big]\rho_{\boldsymbol{j}}^{(L)} - \mathrm{i}\sum_{r=1}^{L}(-)^{L-r}\mathcal{C}_{j_r}\rho_{\boldsymbol{j}_r^-}^{(L-1)}$$

$$-\sum_{j}\mathcal{A}_{\bar{j}}\frac{1}{\mathrm{i}\mathcal{L}(t)+\gamma_{\boldsymbol{j}j}^{(L+1)}(t)}\Big(\sum_{r=1}^{L+1}\mathcal{C}_{j_r}\rho_{\boldsymbol{j}_r}^{(L)}\Big). \qquad (4.51)$$

In the absence of a time-dependent laser field applied to the local system, $\mathcal{L}(t) = \mathcal{L}_{\mathrm{s}}$, which is diagonal in the H_{s}-representation; see the tetradic bra-ket notation described in Section 2.4. That is $(\mathcal{L}_{\mathrm{s}})_{mn,m'n'} = \omega_{mn}\delta_{mm'}\delta_{nn'}$, with $\omega_{mn} = \epsilon_m - \epsilon_n$ being the transition frequency between two eigenstates of the bare system Hamiltonian. The superoperator inversion involved in the above equations are also diagonal and can be readily evaluated. For the case of the time-dependent $\mathcal{L}(t)$, we may use the Dyson equation to facilitate the evaluation.

Actually, Eq. (4.50) had been proposed before, as an efficient HEOM truncation method [36]. However, the previous work addressed only the numerical aspect of truncation, with setting individual $\dot{\rho}_{\boldsymbol{j}j}^{(L+1)}$ and $\rho_{\boldsymbol{j}jj'}^{(L+2)}$ be zeroes. Apparently, this double setting is overkilled. The derivative–resum, Eq. (4.49), with its equivalence Eq. (4.50), is preferred for the prescription invariance requirement [32]. While it is Eq. (4.50) that is used in Eq. (4.51), its equivalent Eq. (4.49) is reflected directly in the Heisenberg prescription of the truncation; cf. Section 7.4. The derivative-resum scheme does follow Eq. (4.49) without setting $\{\rho_{\boldsymbol{j}jj'}^{(L+2)}(t)\}$ to be zero. This observation implies that Eq. (4.51) would have effectively taken certain nonzero $\{\rho_{\boldsymbol{j}jj'}^{(L+2)}(t)\}$ dynamical influences into account. Note that for stationary states, Eq. (4.49) gives $\{\rho_{\boldsymbol{j}jj'}^{(L+2);\mathrm{st}} = 0\}$. The numerical performance of the derivative-resum scheme will be detailed later in Section

6; cf. Table 1.

The fermionic DEOM theory is now complete. It consists of a closed set of equations of motion, Eqs. (4.45), and (4.51) for $\rho_{\boldsymbol{j}}^{(n\leqslant L)}(t)$, and also Eq. (4.50) for $\rho_{\boldsymbol{j}}^{(L+1)}(t)$. The underlying dissipaton algebra, especially the generalized Wick's theorem, Eqs. (4.41) and (4.42), is also very important. It enables DEOM to be a theory for both systems and hybrid bath dynamics; see Section 7 for details.

5 Fermionic HEOM via path integral influence functionals

The DEOM formalism, either bosonic, Eq. (3.24), or fermionic, Eq. (4.45), had been constructed before in the HEOM framework [12–15, 18], where the dynamical variables were mainly just mathematical auxiliaries. As we will see later in Section 7, the crucially important ingredients of the DEOM theory include also the expression of DDOs, Eq. (3.20) or Eq. (4.36), and the generalized Wick's theorems, Eqs. (3.21) and (3.22) or Eqs. (4.41) and (4.42). In this section, we revisit the HEOM construction, from its root at the Feynman-Vernon influence functional path integral formalism [7, 8], and closely compare the involved key steps with their DEOM correspondences, if any. It will be evident that, except for Eq. (3.24) or Eq. (4.45), the aforementioned additional crucially important ingredients of the DEOM theory are hardly within the reach of the HEOM framework. Without loss of generality, we focus on the fermionic HEOM formalism.

5.1 Path integral influence functional formalism

Let us start by recasting the total composite Hamiltonian in Eq. (4.6) with Eqs. (4.7) and (4.24) in the $h_{\mathrm{B}}^{\mathrm{eff}}(t)$-interaction picture:

$$\tilde{H}_{\mathrm{T}}(t) = H(t) + \sum_{\sigma\alpha u}\hat{a}_u^{\bar{\sigma}}\widetilde{F}_{\alpha u}^{\sigma}(t). \qquad (5.1)$$

Here, $\widetilde{F}_{\alpha u}^{\sigma}(t) \equiv U_{\mathrm{B}}^{\dagger}(t;t_0)\widetilde{F}_{\alpha u}^{\sigma}(t)U_{\mathrm{B}}(t;t_0)$. It satisfies [cf. Eq. (4.17)]

$$\frac{\partial}{\partial t}\widetilde{F}_{\alpha u}^{\sigma}(t) = -\mathrm{i}[\widetilde{F}_{\alpha u}^{\sigma}(t), \hat{h}_{\mathrm{B}}^{\mathrm{eff}}(t)], \qquad (5.2)$$

with $\hat{h}_{\mathrm{B}}^{\mathrm{eff}}(t)$ specified in Section 4.1.1 as

$$\hat{h}_{\mathrm{B}}^{\mathrm{eff}}(t) \equiv \sum_{\alpha}\big\{\hat{h}_{\alpha} + [\mu_{\alpha} + \Delta_{\alpha}(t)]\hat{N}_{\alpha}\big\}. \qquad (5.3)$$

The initial t_0 in Eq. (5.2), and also hereafter, can be at any time prior to the time-dependent $\Delta_{\alpha}(t)$. In the $\hat{h}_{\mathrm{B}}^{\mathrm{eff}}(t)$-interaction picture, the total composite density

operator, $\tilde{\rho}_{\mathrm{T}}(t) = U_{\mathrm{B}}^{\dagger}(t;t_0)\rho_{\mathrm{T}}(t)U_{\mathrm{B}}(t;t_0)$, reads

$$\tilde{\rho}_{\mathrm{T}}(t) = \tilde{U}_{\mathrm{T}}(t,t_0;\{\widetilde{F}_{\alpha u}^{\sigma}(t)\})\rho_{\mathrm{T}}(t_0)\tilde{U}_{\mathrm{T}}^{\dagger}(t,t_0;\{\widetilde{F}_{\alpha u}^{\sigma}(t)\}), \tag{5.4}$$

where [cf. Eq. (5.1)]

$$\tilde{U}_{\mathrm{T}}(t,t_0;\{\widetilde{F}_{\alpha u}^{\sigma}(t)\}) = \exp_{+}\left[-\mathrm{i}\int_{t_0}^{t}\mathrm{d}\tau\tilde{H}_{\mathrm{T}}(\tau)\right], \tag{5.5}$$

with $\tilde{H}_{\mathrm{T}}(\tau)$ of Eq. (5.1).

The influence functional path integral theory targets at the reduced system density operator, which reads now as $\rho_{\mathrm{S}}(t) = \mathrm{tr}_{\mathrm{B}}[\tilde{\rho}_{\mathrm{T}}(t)]$. For its formal evaluation, the initial value in Eq. (5.4) has to be of either the steady-state total composite density operator [39], or the following factorization form [18],

$$\rho_{\mathrm{T}}(t_0) = \rho_{\mathrm{S}}(t_0)\rho_{\mathrm{B}}^{\mathrm{st}}, \tag{5.6}$$

with

$$\rho_{\mathrm{B}}^{\mathrm{st}} = \prod_{\alpha}\frac{\mathrm{e}^{-\beta_{\alpha}(\hat{h}_{\alpha}+\mu_{\alpha}\hat{N}_{\alpha})}}{Z_{\alpha}(\beta_{\alpha},\mu_{\alpha})}. \tag{5.7}$$

Here, $Z_{\alpha}(\beta_{\alpha},\mu_{\alpha})$ denotes the grand canonical partition function of electrons in the α-reservoir under the time-independent nonequilibrium potential μ_{α}. Under the homogeneous-conduction-band-shift ansatz, as described above Eq. (4.4), an additional time-dependent potential $\Delta_{\alpha}(t)$ will not change the distribution of electrons in the conduction bands of the α-electrode. Together with Eq. (5.4), we have [18]

$$\begin{aligned}\rho_{\mathrm{S}}(t) &= \langle\tilde{U}_{\mathrm{T}}(t,t_0;\{\widetilde{F}_{\alpha u}^{\sigma}(t-\mathrm{i}\beta)\})\rho_{\mathrm{S}}(t_0)\\ &\quad\times\tilde{U}_{\mathrm{T}}^{\dagger}(t,t_0;\{\widetilde{F}_{\alpha u}^{\sigma}(t)\})\rangle_{\mathrm{B}}^{\mathrm{nst}}\\ &\equiv \mathcal{U}(t,t_0)\rho_{\mathrm{S}}(t_0),\end{aligned} \tag{5.8}$$

with $\langle\cdots\rangle_{\mathrm{B}}^{\mathrm{nst}}$, the nonstationary-state reservoirs bath average, defined in Eq. (4.16).

In Eq. (5.8), $\mathcal{U}(t,t_0)$ is symbolically introduced as the reduced Liouville-space propagator. It only has a concrete expression in the path integral "space-time" representation [8, 40]. Let $\{|\psi\rangle\}$ be a generic basis set in the system subspace such that $\rho_{\mathrm{S}}(\boldsymbol{\psi},t) \equiv \rho_{\mathrm{S}}(\psi,\psi',t) \equiv \langle\psi|\rho_{\mathrm{S}}(t)|\psi'\rangle$. The reduced Liouville-space propagator in the path integral representation reads [7, 8]

$$\mathcal{U}(\boldsymbol{\psi},t;\boldsymbol{\psi}_0,t_0) = \int_{\boldsymbol{\psi}_0[t_0]}^{\boldsymbol{\psi}[t]}\mathcal{D}\boldsymbol{\psi}\mathrm{e}^{\mathrm{i}S[\psi]}\mathcal{F}[\boldsymbol{\psi}]\mathrm{e}^{-\mathrm{i}S[\psi']}. \tag{5.9}$$

Here, $S[\psi]$ is the classical action functional of the reduced system, evaluated along a path $\psi(\tau)$, subject to the constraint that the two ending points $\psi(t_0) = \psi_0$ and $\psi(t) = \psi$ are fixed. The influence functional $\mathcal{F}[\boldsymbol{\psi}]$ in Eq. (5.9) can be evaluated using Eq. (5.8), together

with the Gaussian statistics for the stochastic linear bath operators $\{\widetilde{F}_{\alpha u}^{\sigma}(t)\}$. The final result reads [18]

$$\mathcal{F}[\boldsymbol{\psi}] = \exp\left\{-\int_{t_0}^{t}\mathrm{d}\tau\mathcal{R}\big[\tau;\{\boldsymbol{\psi}\}\big]\right\}, \tag{5.10}$$

with the dissipation functional of

$$\mathcal{R}\big[t;\{\boldsymbol{\psi}\}\big] = \mathrm{i}\sum_{\sigma\alpha u}\mathcal{A}_{u}^{\bar{\sigma}}[\boldsymbol{\psi}(t)]\tilde{\mathcal{B}}_{\alpha u}^{\sigma}\big[t;\{\boldsymbol{\psi}\}\big]. \tag{5.11}$$

Here,

$$\mathcal{A}_{u}^{\sigma}[\boldsymbol{\psi}(t)] = a_{u}^{\sigma}[\psi(t)] + a_{u}^{\sigma}[\psi'(t)], \tag{5.12}$$

and

$$\tilde{\mathcal{B}}_{\alpha u}^{\sigma}[t;\{\boldsymbol{\psi}\}] = -\mathrm{i}\big\{\tilde{B}_{\alpha u}^{\sigma;>}[t;\{\psi\}] - \tilde{B}_{\alpha u}^{\sigma;<}[t;\{\psi'\}]\big\}, \tag{5.13}$$

with

$$\begin{aligned}\tilde{B}_{\alpha u}^{\sigma;>}[t;\{\psi\}] &\equiv \sum_{v}\int_{t_0}^{t}\mathrm{d}\tau C_{\alpha uv}^{\sigma}(t,\tau)a_{v}^{\sigma}[\psi(\tau)],\\ \tilde{B}_{\alpha u}^{\sigma;<}[t;\{\psi'\}] &\equiv \sum_{v}\int_{t_0}^{t}\mathrm{d}\tau\big[C_{\alpha uv}^{\bar{\sigma}}(t,\tau)\big]^{*}a_{v}^{\sigma}[\psi'(\tau)].\end{aligned} \tag{5.14}$$

The above two expressions are specified with the "forward" ($>$) and "backward" ($<$) notations that are used throughout this paper. They involve the nonstationary bath correlation functions [cf. Eq. (4.16)], along the forward and backward paths, respectively; i.e.,

$$\begin{aligned}C_{\alpha uv}^{\sigma}(t,\tau) &= \big\langle\hat{F}_{\alpha u}^{\sigma}(t)\hat{F}_{\alpha v}^{\bar{\sigma}}(\tau)\big\rangle_{\mathrm{B}}^{\mathrm{nst}},\\ \big[C_{\alpha uv}^{\bar{\sigma}}(t,\tau)\big]^{*} &= \big\langle\hat{F}_{\alpha v}^{\bar{\sigma}}(\tau)\hat{F}_{\alpha u}^{\sigma}(t)\big\rangle_{\mathrm{B}}^{\mathrm{nst}}.\end{aligned} \tag{5.15}$$

While the $\mathcal{A}$-functionals in Eq. (5.12) depend on $\{a_{u}^{\sigma}[\psi(t)]\}$ at a fixed local terminal time t, the $\tilde{\mathcal{B}}$-functionals in Eq. (5.13) are of time nonlocal memory. The involved $\{a_{u}^{\sigma}[\cdot]\}$, the path-integral representations of the fermionic $\{\hat{a}_{u}^{\sigma}\}$ operators, are *not* c-numbers, but rather *Grassmann* variables [8, 40]. Consequently, the quantities defined in Eqs. (5.12)–(5.13) are all Grassmann variables, satisfying the algebraic rule of $xy = -yx$.

5.2 Fermionic HEOM formalism

From Eqs. (5.10) and (5.11), we have

$$\frac{\partial}{\partial t}\mathcal{F} = -\mathrm{i}\Big(\sum_{\sigma\alpha u}\mathcal{A}_{u}^{\bar{\sigma}}[\boldsymbol{\psi}(t)]\tilde{\mathcal{B}}_{\alpha u}^{\sigma}[t;\{\boldsymbol{\psi}\}]\Big)\mathcal{F}. \tag{5.16}$$

This equation is not closed, because of the time-nonlocal nature of the $\tilde{\mathcal{B}}$-functionals.

The HEOM construction is to resolve the memory contents in the $\tilde{\mathcal{B}}$-functionals of Eq. (5.13) with Eq. (5.14). It follows the same exponential series expansion as in Section 4.3 for the involved correlation functions of reser-

voirs. By combining Eqs. (4.18) and (4.23), we have Eq. (5.15) the expressions [cf. Eq. (4.30)]

$$C_{\alpha uv}^{\sigma}(t,\tau) = \sum_{\kappa=1}^{K} \eta_{\alpha\kappa uv}^{\sigma} \exp\left[-\int_{\tau}^{t} dt' \gamma_{\alpha\kappa}^{\sigma}(t')\right],$$

$$\left[C_{\alpha uv}^{\bar{\sigma}}(t,\tau)\right]^{*} = \sum_{\kappa=1}^{K} \eta_{\alpha\kappa uv}^{\bar{\sigma}*} \exp\left[-\int_{\tau}^{t} dt' \gamma_{\alpha\kappa}^{\sigma}(t')\right]. \quad (5.17)$$

We can then recast Eq. (5.13) with Eq. (5.14) as

$$\tilde{\mathcal{B}}_{\alpha u}^{\sigma}[t;\{\psi\}] \equiv \sum_{\kappa=1}^{K} \mathcal{B}_{\alpha\kappa u}^{\sigma}[t;\{\psi\}], \quad (5.18)$$

where

$$\mathcal{B}_{\alpha\kappa u}^{\sigma}[t;\{\psi\}] = -i \sum_{v} \left\{\eta_{\alpha\kappa uv}^{\sigma} B_{\alpha\kappa u}^{\sigma;>}[t;\{\psi\}]\right.$$
$$\left. -\eta_{\alpha\kappa uv}^{\bar{\sigma}*} B_{\alpha\kappa u}^{\sigma;<}[t;\{\psi'\}]\right\}, \quad (5.19)$$

with

$$B_{\alpha\kappa u}^{\sigma;>}[t;\{\psi\}] = \int_{t_0}^{t} d\tau \left\{a_v^{\sigma}[\psi(\tau)] e^{-\int_{\tau}^{t} dt' \gamma_{\alpha\kappa}^{\sigma}(t')}\right\},$$

$$B_{\alpha\kappa u}^{\sigma;<}[t;\{\psi'\}] = \int_{t_0}^{t} d\tau \left\{a_v^{\sigma}[\psi'(\tau)] e^{-\int_{\tau}^{t} dt' \gamma_{\alpha\kappa}^{\sigma}(t')}\right\}. \quad (5.20)$$

The above $\mathcal{B}$-functionals satisfy the memory-resolved, time-local equation of motion,

$$\frac{\partial}{\partial t} \mathcal{B}_{\alpha\kappa u}^{\sigma}[t;\{\psi\}] = -i \sum_{v} \left\{\eta_{\alpha\kappa uv}^{\sigma} a_v^{\sigma}[\psi(t)]\right.$$
$$\left. -\eta_{\alpha\kappa uv}^{\bar{\sigma}*} a_v^{\sigma}[\psi'(t)]\right\} - \gamma_{\alpha\kappa}^{\sigma}(t) \mathcal{B}_{\alpha\kappa u}^{\sigma}[t;\{\psi\}]. \quad (5.21)$$

Substituting Eq. (5.18) in Eq. (5.16) leads to

$$\frac{\partial}{\partial t}\mathcal{F} = -i\left(\sum_{j} \mathcal{A}_{\bar{j}}[\psi(t)]\mathcal{B}_{j}[t;\{\psi\}]\right)\mathcal{F}. \quad (5.22)$$

Note that $j \equiv (\sigma\alpha\kappa u)$ and $\bar{j} \equiv (\bar{\sigma}\alpha\kappa u)$, were defined in Eq. (4.35). Introduce a set of auxiliary influence functionals,

$$\mathcal{F}_{\mathbf{j}}^{(n)} = \mathcal{F}_{j_1 j_2 \cdots j_n}^{(n)} = \mathcal{B}_{j_n} \cdots \mathcal{B}_{j_2} \mathcal{B}_{j_1} \mathcal{F}. \quad (5.23)$$

Their equations of motion are all time-local, but hierarchically coupled. In parallel to Eq. (5.9), we introduce

$$\mathcal{U}_{\mathbf{j}}^{(n)}(\psi, t; \psi_0, t_0) = \int_{\boldsymbol{\psi}_0[t_0]}^{\boldsymbol{\psi}[t]} \mathcal{D}\psi e^{iS[\psi]} \mathcal{F}_{\mathbf{j}}^{(n)}[\psi] e^{-iS[\psi']}, \quad (5.24)$$

to define the auxiliary density operators (ADOs),

$$\rho_{\mathbf{j}}^{(n)}(t) \equiv \mathcal{U}_{\mathbf{j}}^{(n)}(t, t_0)\rho_{\mathrm{S}}(t_0). \quad (5.25)$$

The above equations, (5.21)–(5.25), readily lead to [18]

$$\dot{\rho}_{\mathbf{j}}^{(n)} = -\left[i\mathcal{L}(t) + \sum_{r=1}^{n} \gamma_{j_r}(t)\right]\rho_{\mathbf{j}}^{(n)} - i\sum_{j} \mathcal{A}_{\bar{j}}\rho_{\mathbf{j}j}^{(n+1)}$$
$$-i\sum_{r=1}^{n}(-)^{n-r}\mathcal{C}_{j_r}\rho_{\mathbf{j}_r}^{(n-1)}. \quad (5.26)$$

This is the fermionic HEOM formalism, which identical to the fermionic DEOM (4.45). It *de facto* verifies the important dissipaton algebra presented in Section 3 and Section 4. However, these two approaches are of some fundamental differences, as elaborated below.

5.3   Comments on HEOM versus DEOM

The main drawback of the HEOM formalism is the lack of physical meanings of all its dynamical variables, except for $\rho^{(0)}(t) = \rho_{\mathrm{S}}(t)$. Those $\{\rho_{\mathbf{j}}^{(n>0)}(t)\}$ are simply mathematical auxiliaries, referred to as the ADOs in the HEOM literature. They were introduced as intermediate quantities, with the definition being given in Eqs. (5.23)–(5.25), together with Eqs. (5.19) and (5.20). This definition works only for the purpose of obtaining Eq. (5.26), and it has hardly any relation to various HEOM applications. Strictly speaking, it is more harmful than useful, as it may limit the use of HEOM (5.26), with the initial conditions of $\{\rho_{\mathbf{j}}^{(n>0)}(t_0) = 0\}$, the manifestations of ADOs of the initial factorization of Eq. (5.6).

Nevertheless, the HEOM construction is exact, and the resulting formalism, Eq. (5.26), should be applicable to a broad range of initial values of $\{\rho_{\mathbf{j}}^{(n)}(t = 0)\}$ that are dynamically accessible from those uncorrelated ADOs in the past, say $t_0 \to -\infty$. Therefore, the HEOM formalism has been widely used in characterizing the properties of reduced systems, both static structures and dynamical behaviors, in the presence of couplings of a non-Markovian and nonperturbative environment. There had also been some efforts toward identifying the physical meanings of ADOs, with clear indications that they are related to correlated system-and-bath interferences [19, 20, 41]. The most important identification may be the relation of the first-tier ADOs, $\{\rho_j^{(1)}(t)\}$, with the transient transport current [18, 36, 42–48]. However, the transport current fluctuations, such as current correlation functions and noise spectra, are beyond reach. The main drawback remains. Because the HEOM framework is rooted at the influence functional path integral formalism, it is concerned mainly with reduced systems [49, 50].

The DEOM theory is different. All $\{\rho_{\mathbf{j}}^{(n)}\}$ are now the physically well defined DDOs, with Eq. (4.36) that is free of the puzzle of initial values. The underlying dissipaton algebra, especially the generalized Wick's theorem, renders the DEOM a unique theory for not only sys-

YiJing Yan, et al., Front. Phys. 11(4), 110306 (2016)

110306-17

tems but also hybrid bath dynamics. The DEOM-based evaluations of nonlinear Fano interferences and transport current noise spectra have been reported recently [22, 23]. Neither the expressions of DDOs, Eq. (4.36), nor the dissipaton algebra are within the reach of the HEOM framework.

Nevertheless, the dynamical generators of two approaches, i.e., Eq. (4.45) and Eq. (5.26), are identical. All artilleries developed before for HEOM can be used directly in the present DEOM approach. For our previous reviews on this aspect, see for example, Ref. [36] and Ref. [33]. As far the numerical implementations are concerned, "DEOM" and "DDO" used in the next section, are completely exchangeable with "HEOM" and "ADO", respectively.

6 Onsets of efficient DEOM methods

6.1 General remarks

Let us start with the indexing algorithm for DDOs. For fermionic dissipatons, $\{\hat{f}_{\alpha\kappa u}^{\sigma}\}$, the total number of DDOs participating in the DEOM formalism, truncated at the L-body level, is [cf. Eq. (3.41)]

$$\mathcal{N}(L, \tilde{K}) = \sum_{n=0}^{L} \frac{\tilde{K}!}{n!(\tilde{K} - n)!}; \quad \tilde{K} \equiv 2N_\alpha N_u K. \quad (6.1)$$

Here, N_α and N_u are the numbers of bath reservoirs and system orbitals, respectively, and the factor of 2 accounts for the two signs of $\sigma = +, -$. Thus, $\tilde{K}$ defined above is the number of the distinct fermionic dissipatons, $\{\hat{f}_{\alpha\kappa u}^{\sigma}\}$.

To locate individual DDOs in a numerical DEOM code, we map the multiple indices in $\rho_{\boldsymbol{j}}^{(n)}$ to an integer $\mathrm{j}(n, \boldsymbol{j}) \in [0, \mathcal{N}]$, i.e., $\rho_{\boldsymbol{j}}^{(n)} = \rho_{\mathrm{j}(n,\boldsymbol{j})}$. To proceed, let $\rho_{\boldsymbol{j}}^{(n)} \equiv \rho_{j_1 \cdots j_n}^{(n)} \equiv \rho_{n_1 \cdots n_{\tilde{K}}}^{(n)}$, with $n_k = \delta_{k_{j_r} k}$. The ordered set $\boldsymbol{j} = j_1 \cdots j_n$ follows the same order as in $\boldsymbol{n} = (n_1 \cdots n_{\tilde{K}})$. The indexing algorithm for DDOs, for $\mathrm{j}(\boldsymbol{n}) \equiv \mathrm{j}(n, \boldsymbol{j})$, can be chosen as [33]

$$\mathrm{j}(\boldsymbol{n}) = \mathcal{N}(n-1, \tilde{K}) + \sum_{k=1}^{\tilde{K}} (1 - n_k)\mathcal{N}(N_k - 1, \tilde{K} - k).$$

Here, $N_k = n_{k+1} + \cdots + n_{\tilde{K}}$ and $\mathcal{N}(m < 0, M) = 0$. This algorithm sorts DDOs into n-based blocks, followed by the sub-indices $\boldsymbol{n} = (n_1 \cdots n_{\tilde{K}})$ of a same n-dissipaton level. For example, $\mathrm{j}(0 \cdots 0) = 0$; $\mathrm{j}(10 \cdots 0) = 1, \cdots,$ $\mathrm{j}(0 \cdots 01) = \tilde{K}$; and $\mathrm{j}(110 \cdots 0) = \tilde{K} + 1$.

Currently, the major challenge of the DEOM approach is the rapidly increasing memory space for storing and computing these DDOs. Reducing such memory cost will dramatically enhance the efficiency of this approach. We

tackle this problem from both the optimal DEOM formalism and efficient numerical implementation aspects, as presented in the two subsequent subsections, respectively.

6.2 Minimum basis-set dissipatons

The optimal DEOM formalism deals with the so-called K-space and L-space issues. The latter is concerned with efficient L-body dissipaton-level truncations. The derivative-resum scheme, presented in Section 3.5 and Section 4.5 is by far the best; see Section 6.4 for numerical verifications.

The K-space issue is to minimize the number of distinct dissipatons, exemplified with the fermionic $\{\hat{f}_{\alpha\kappa u}^{\sigma}\}$, cf. Section 4.4, where $\kappa_{\max} = K = N_J + N_{\mathrm{Fermi}}$. For the given problems under study, the number N_J of the poles from the bath hybridization function is fixed. Thus, the basis-set issue may simply refer to the minimal N_{Fermi}, as required from the Fermi function. Apparently, every one-increment of N_{Fermi} results in the increase of the size of basis-set dissipatons by $2N_\alpha N_u$; see Eq. (6.1). The curse of the dimensionality problem would quickly appear. The very best minimal N_{Fermi} is in demand.

In the following, we denote the "best" $N_{\mathrm{Fermi}}^{\min} \equiv P$, as it follows the Padé spectral decomposition [28, 29, 51]. This scheme is not only the $[P-1/P]$ Padé approximant of the Fermi function, but also the fact that all involving parameters in the sum-over-poles decomposition form are determined at machine precision via simple algorithms [28, 29, 51].

The number P of Padé terms determines the accuracy of the correlation functions of the bath reservoirs in exponential expansion, Eq. (4.23), that leads to the basis-set dissipatons for the DEOM construction. Note that the discrepancy of $\Delta f_{\mathrm{Fermi}}^{[P-1/P]}(\omega) \equiv \left| f_{\mathrm{Fermi}}(\omega) - f_{\mathrm{Fermi}}^{[P-1/P]}(\omega) \right|$ is on the order of $(\beta\omega)^{4P+1}$. However, the challenge occurs at a lower temperature, especially in the Kondo regime, where the optimal number of Padé terms, P, sensitively varies with temperature T. For a convenient implementation of the DEOM approach, it would be helpful to have an *a priori* estimate of the required P value. To this end, we define the relative error of dissipaton-decomposition as follows:

$$E_{\mathrm{c}} = \int \mathrm{d}\omega \Delta f_{\mathrm{Fermi}}^{[P-1/P]}(\omega) J(\omega) \bigg/ \int \mathrm{d}\omega f_{\mathrm{Fermi}}(\omega) J(\omega).$$

Here, $J(\omega)$ denotes the function form of $J_{\alpha uv}(\omega)$. We adopt $J(\omega) = 1/(\omega^2 + W^2)$ for the illustrations below.

Figure 3 plots the minimal P that gives an error less than the preset E_{c} for different temperatures, aiming at the DEOM evaluations in the Kondo regime. Appar-
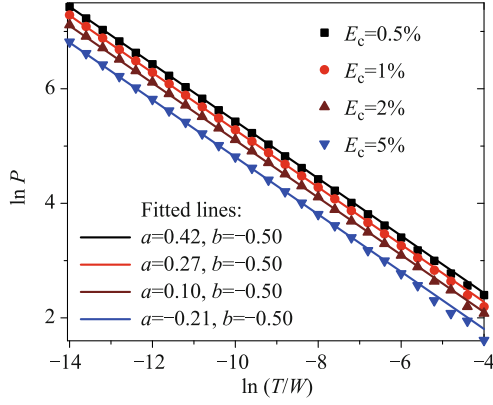
Fig. 3 The scattered data are the minimal number of Padé terms P versus the temperature T corresponding to different preset errors E_c. The scatters are determined using the $[P-1/P]$ Padé spectral decomposition of the Fermi function, and the lines are the least squared fits to the relation $\ln P = a + b \ln(T/W)$. The values of fitting parameters a and b for each line are listed in the figure. Reproduced with permission from Ref. [36], Copyright © 2015 AIP Publishing LLC.

ently, a larger P is required for a lower T or to reach a smaller error E_c. It is found that the data fit remarkably well to a linear relation $\ln P = a + b \ln(T/W)$. Here, the reservoir band width W is taken as a reference energy scale. The parameter a depends on the preset E_c via $a = 1.10 \ln(-0.28 \ln E_c)$, while b is nearly constant in all cases; see Fig. 3. This leads to [36]

$$\ln P = 1.10 \ln(-0.28 \ln E_c) - 0.50 \ln(T/W). \qquad (6.2)$$

This quantitative relation, reliable at $T/W < 0.004$, provides an *a priori* estimate of P such that the somewhat tedious trial-and-error search process can be avoided. Such a quantitative relation helps to reach an optimal balance between the accuracy and efficiency of DEOM.

6.3   Utilizing the sparsity feature

In the previous implementation of DEOM, all matrix elements of all the DDOs were stored in physical memory. Consequently, the memory cost rapidly increases with the number of system spin-orbitals N_u or as the temperature decreases. It is important to note that DDOs are often sparse matrixes; a large percentage of the elements are exactly zero owing to physical constraints. The sparsity feature is completely determined by the interactions among electrons on different dot orbitals. In the DEOM approach, this involves the system Hamiltonian H_s and the reservoir spectral functions $J_{\alpha uv}(\omega)$.

Take a quantum dot (QD) system consisting of only one orbital as an example. Such a system is often described by the single-impurity Anderson model (SIAM) [52, 53]. The dot Hamiltonian is $H_s = \epsilon(\hat{n}_\uparrow + \hat{n}_\downarrow) + U\hat{n}_\uparrow\hat{n}_\downarrow$. Here, $\hat{n}_s = \hat{a}_s^\dagger \hat{a}_s$ and U is the on-dot electron-electron

Coulomb repulsion energy. The physical space of the QD is spanned by four Fock states, $|0\rangle$, $|\uparrow\rangle$, $|\downarrow\rangle$, and $|\uparrow\downarrow\rangle$. Usually, the direct spin-flip term $\hat{a}_\uparrow^\dagger \hat{a}_\downarrow$ and its Hermitian conjugate are absent from H_s. Consequently, there is no coherence between the two states $|\uparrow\rangle$ and $|\downarrow\rangle$. Therefore, the reduced density matrix element $\langle\uparrow|\rho|\downarrow\rangle$ is exactly zero, and its contribution to all the associated first-tier DDOs is also zero.

In many cases, up to 90% or even more DDO-matrix elements are zero, owing to the intrinsic system configuration. Therefore, utilizing the sparsity of the DDOs will lead to a substantial reduction in the memory cost of DEOM. The challenge is that the zero elements are located at different positions of different DDOs. An efficient algorithm is needed to identify and screen these zero elements quickly. Such an algorithm has been proposed in Ref. [36], which consists of the following two ansatzs:

(i) The sparsity of the reduced density matrix $\rho_s = \rho^{(0)}$ of the system is determined by an effective Hamiltonian as $\rho^{(0)} \sim e^{-\beta H_{\text{eff}}}$, with $H_{\text{eff}} = H_s + H_\Sigma$. Here, H_Σ originates from the reservoir spectral functions, since an off-diagonal $J_{\alpha uv}(\omega)$ may introduce a nonzero coupling between dot orbitals $|u\rangle$ and $|v\rangle$ mediated by α-reservoir. Note that the reservoir correlation functions are equivalent to the "embedding" self-energies in the nonequilibrium Green's function theory: $\langle\hat{F}_{\alpha u}^-(t)\hat{F}_{\alpha v}^+(0)\rangle_{\text{B}} = i\Sigma_{\alpha uv}^>(t)$ and $\langle\hat{F}_{\alpha v}^+(0)\hat{F}_{\alpha u}^-(t)\rangle_{\text{B}} = -i\Sigma_{\alpha uv}^<(t)$. As inferred from Eqs. (4.9) and (4.13), $J_{\alpha uv}(\omega - \mu_\alpha)$ is simply the spectrum of $i[\Sigma_{\alpha uv}^>(t) - \Sigma_{\alpha uv}^<(t)]$. For any pair of u and v that gives $J_{\alpha uv}(\omega) \neq 0$, we add a nonzero term $(t_{uv}\hat{a}_u^\dagger\hat{a}_v + \text{H.c.})$ to H_Σ. In this manner, the reservoir mediated couplings among different dot orbitals are properly accounted for.

(ii) The sparsity of any n-body DDO $\rho_{\bm{j}}^{(n)}$ is completely determined by H_{eff} and all its associated $(n-1)$-body DDOs via $[H_{\text{eff}}, \rho_{\bm{j}}^{(n)}] + \sum_{r=1}^n \mathcal{C}_{j_r}\rho_{\bm{j}_r}^{(n-1)}$. Therefore, by scanning through all $\{\rho_{\bm{j}}^{(n)}; n = 0, \cdots, L\}$, the sparsity of all the DDOs can be deduced.

Although not rigorously proved, the above two ansatzs have been validated by our extensive numerical tests on a variety of systems with diversified H_s and $J_{\alpha uv}(\omega)$. In our present implementation of fermionic DEOM, both the above sparse mode and the derivative-resum truncation (cf. Section 4.5) are included, leading to significant enhancement in numerical efficiency, while maintaining accuracy.

6.4   Numerical verifications

In the following, we denote the original implementation

of DEOM as the "standard mode" which exploits neither the sparsity feature nor the derivative-resum scheme. It stores and computes all DDOs appearing in the DEOM formalism of Eq. (4.45), with $n = 0, \cdots, L$, and setting all $\{\rho_j^{(n>L)}\} = 0$. The "sparse mode" exploits the sparsity pre-screening algorithm, as described above, to store and compute only those surviving nonzero elements of DDOs. Usually, the memory space required by the "sparse mode" is only 5%–10% of that needed in the "standard mode", while the numerical outcomes are exactly the same. Therefore, the use of the "sparse mode" dramatically reduces the memory cost, and hence substantially enhances the efficiency of the DEOM approach. The "derivative mode" itself refers to the use of the derivative-resum truncation scheme in Section 4.5, whereas the "derivative+sparse mode" combines those two advanced techniques. It should be emphasized that all these four modes yield exactly the same numerical results, if all converge.

The benchmark is performed on a SIAM system, $H_s = \epsilon(\hat{n}_\uparrow + \hat{n}_\downarrow) + U\hat{n}_\uparrow\hat{n}_\downarrow$, where $\hat{n}_u = \hat{a}_u^\dagger\hat{a}_u$, in the quantum transport setup (cf. Fig. 2), with $\mu_L = \mu_L^{eq} + V/2$ and $\mu_R = \mu_R^{eq} - V/2$, under the bias potential. Set $\mu_\alpha^{eq} = 0$ as energy zero. The equilibrium reservoir spectral function assumes the form of $J_\alpha(\omega) = \frac{\Delta}{2}\frac{W^2}{\omega^2 + W^2}$. The hybridization strength Δ is taken as an energy unit below. The parameters $\epsilon = -U/2 = -6\Delta$ are adopted, such that the dot is exactly half-filling, and the reservoir band width is $W = 20\Delta$. The system is in a nonequilibrium steady state under a bias voltage $V = 2\Delta$, and the temperature is $T = 0.1\Delta$. To reach a high truncation tier, we adopt a slightly larger error tolerance for the reservoir memory decomposition: $E_c = 7.5\%$. From Eq. (6.2), we immediately have $P = 10$.

Table 1 compares the CPU time, physical memory, and indexing memory consumed by DEOM calculations carried out in the four different aforementioned modes. Also listed are the steady-state current, I, and the diagonal elements of the reduced system density matrix, ρ_s, obtained at different truncation tiers. The results are related to the steady-state solutions to the DEOM formalism; see Section 7.1 for details.

In terms of efficiency, the "sparse mode" indeed reduces the physical memory by more than one order of magnitude. The CPU time is also greatly shortened, with the zero elements of DDOs screened out of the hierarchy. As indicated by the calculated current I and ρ_s, the truncation of L-body dissipatons in the "derivative mode" amounts to the $(L+1)$-body truncation in the "standard mode". In other words, the "derivative mode" allows for accessing many-dissipatons dynamics that is one level higher, without increasing the cost of physical memory. This is because the $(L+1)$-body DDOs are treated on-the-fly by Eq. (4.50). The price to pay is the somewhat increased indexing memory. Nevertheless, the "derivative mode" proves to be very useful, since the saving of physical memory often exceeds the increase in indexing memory.

We proceed to examine how the four modes work for the time evolution of the same system of Table 1, but with the bias voltage being switched off at $t = 0$. The subsequent relaxation dynamics is governed by the DEOM (4.45) in the absence of bias. Figure 4 depicts the resulting time-dependent current through the right lead, $I_R(t)$, calculated with the "sparse" and "derivative+sparse" modes of DEOM truncated at different L-body levels. Apparently, the computed data converge quickly to the same exact curve as L increases, and the

Table 1 The upper table lists the CPU time (in seconds), physical memory, and indexing memory (in bytes) consumed by DEOM calculations in four different modes, and $L = 2, 3, 4, 5$ for the standard and sparse modes, whereas $L = 1, 2, 3, 4$ for the derivative-resum and derivative+sparse modes, respectively. "N/A" indicates that the results are unavailable because the computational cost exceeds the resources at our disposal. The lower table shows the calculated steady-state current I, and the diagonal elements of $\rho_s^{st} \equiv \rho^{(0);st}$. The system is a symmetric SIAM; see text for parameters. The particle-hole symmetry implies that $\langle\uparrow\downarrow|\rho_s^{st}|\uparrow\downarrow\rangle = \langle 0|\rho_s^{st}|0\rangle$, and the spin-degeneracy suggests that $\langle\uparrow|\rho_s^{st}|\uparrow\rangle = \langle\downarrow|\rho_s^{st}|\downarrow\rangle$. Both relations are clearly satisfied by the calculated results. It can be easily verified that the diagonal elements of ρ_s^{st} always correctly normalize to unity, i.e., $\text{tr}_s\rho_s = 1$. All data results are from Ref. [36] with permission, Copyright © 2015 AIP Publishing LLC.

Mode	CPU time (s)				Physical memory (byte)				Indexing memory (byte)			
Standard	1.6	38	0.9 k	N/A	5.0 M	0.2 G	3.2 G	70 G	0.8 M	24 M	0.6 G	6.4 G
Sparse	1.2	13	0.3 k	7.7 k	0.6 M	9.5 M	0.2 G	2.8 G	0.4 M	11 M	0.3 G	7.1 G
Derivative-resum	1.4	47	2.0 k	83 k	0.1 M	5.0 M	0.2 G	3.2 G	0.3 M	16 M	0.5 G	15 G
Derivative+sparse	1.4	33	1.1 k	42 k	0.1 M	0.6 M	9.5 M	0.2 G	0.3 M	15 M	0.5 G	14 G

Mode	Current I $(e\Delta/h \times 10^4)$				$\langle\uparrow\downarrow|\rho_s^{st}|\uparrow\downarrow\rangle$ or $\langle 0|\rho_s^{st}|0\rangle$				$\langle u|\rho_s^{st}|u\rangle$; $u = \uparrow$ or $\downarrow$			
Standard	4.956	8.980	7.725	N/A	0.040	0.050	0.047	N/A	0.460	0.450	0.453	N/A
Sparse	4.956	8.980	7.725	7.765	0.040	0.050	0.047	0.047	0.460	0.450	0.453	0.453
Derivative-resum	4.956	8.980	7.725	7.765	0.040	0.050	0.047	0.047	0.460	0.450	0.453	0.453
Derivative+sparse	4.956	8.980	7.725	7.765	0.040	0.050	0.047	0.047	0.460	0.450	0.453	0.453

110306-20

YiJing Yan, et al., Front. Phys. 11(4), 110306 (2016)
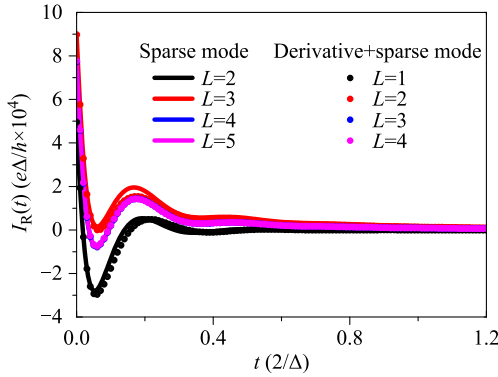
Fig. 4 Time-dependent current through the right lead, $I_R(t)$, for the SIAM studied in Table 1. The results of "sparse" and "derivative+sparse" modes are displayed. See the text for more details. Reprinted with permission from Ref. [36], Copyright 2015 AIP Publishing LLC.

L-body result of the "derivative+sparse mode" is close (but not exactly identical) to the $(L + 1)$-body "sparse mode" counterpart. For clarity, the results of "standard" and "derivative" modes are not presented. They are exactly the same as those of the corresponding sparse modes. Again, making use of the sparsity feature of DDOs leads to a saving of more than 95% of physical memory for the above time evolution calculations.

It is concluded from the above examples, as well as our extensive numerical tests, that among all the four modes the "sparse mode" has the best overall balance between efficiency and accuracy. If an on-the-fly indexing algorithm could be developed for fermionic systems, the cost of indexing memory would become trivial, and the "derivative+sparse mode" would be even more appealing. In terms of accuracy, all the four modes converge to the same results as L increases. This highlights the important fact that, while significantly enhancing the numerical efficiency, the newly developed techniques preserve the accuracy of the DEOM approach.

Note that the sparse-matrix feature also occurs in many optical spectroscopic problems, where individual DDOs are of the block matrix form [54, 55]. Difference blocks present distinct excitation manifolds that are coupled via external electromagnetic fields. Our bosonic DEOM platform for coherent two-dimensional spectroscopy also utilizes the sparsity feature [54, 55].

7   DEOM-space quantum mechanics

7.1   General remarks and stationary-state solutions

We would like to reemphasize that DEOM is a novel type of reduced dynamics theory. It projects the total system-and-bath composite ρ_T to a set of physically well-defined DDOs of Eqs. (3.20) or (4.36). Physically, the DEOM space describes both the system and the hybrid bath dynamics. Mathematically, it constitutes a linear space, giving rise to all standard quantum mechanics prescriptions, i.e., the Schrödinger, Heisenberg, and interaction pictures. Consequently, the DEOM-based evaluations cover not only the expectation values, but also various linear and nonlinear responses. These experimental measurables should be invariant in different DEOM prescriptions. This basic physical requirement will be exploited to scrutinize the "standard" and the novel derivative-resum truncation schemes. Only the latter preserves the invariance of the prescription; see the remarks towards the end of Section 7.4. Thus, we refer to the DEOM formalism in the Schrödinger prescription, with fermionic notations unless specified otherwise, for the EOMs (4.45) and (4.51) for $n < L$ and $n = L$, respectively, as well as the expression (4.50) for $n = L + 1$. The above concepts and pictures would be implied hereafter, unless specified otherwise.

The stationary solution of DEOM is of particular significance. In the absence of external fields, the stationary solution characterizes the thermodynamic equilibrium state of the local system in contact with a reservoir or bath environment; while under applied fields, it describes nonequilibrium steady states, in which the local system exchanges energy or particles with the environment at a constant rate. The collection of steady-states $\{\rho_j^{(n);st}\}$ is the DEOM-space projection of ρ_T^{st}. They are related to the initial DDOs for the DEOM evaluation of a variety of linear and nonlinear correlation functions, as to be elaborated later in the following two subsections.

In the framework of DEOM, there are two schemes to achieve stationary states: (i) start with an initial state close to the target stationary state in the physical phase space, and propagate the DEOM to $t \to \infty$; (ii) use the stationary condition $\dot{\rho}_j^{(n)} = 0$ explicitly, causing the DEOM to reduce to coupled linear equations for $\{\rho_j^{(n);st}\}$. To avoid the trivial zero solution, the normalization constraint $tr_s\rho^{(0)} = 1$ is included in the coupled equations. In practical calculations, an iterative quasi-minimal residual algorithm is employed for solving the large-sized coupled linear equations [56, 57]. In many cases, the above two schemes give the same stationary solution. However, for some systems, particularly those involved bound states (local system states that are uncoupled with the environment) [58], multiple steady states may exist. In such cases, the finally reached stationary state depends on the choice of initial state as well as the time-dependence of external fields.

YiJing Yan, et al., Front. Phys. 11(4), 110306 (2016)

110306-21

7.2 Onsets of DEOM-based dynamical evaluations

The application aspects of DEOM will be illustrated with electronic systems in the quantum transport setup described in Section 4. For clarity of presentation, we repeat Eq. (4.36) below:

$$\rho_{\boldsymbol{j}}^{(n)}(t) \equiv \mathrm{tr}_{\mathrm{B}}\big[(\hat{f}_{j_n}\cdots\hat{f}_{j_1})^{\circ}\rho_{\mathrm{T}}(t)\big]. \tag{7.1}$$

The steady-state solutions, $\{\rho_{\boldsymbol{j}}^{(n);\mathrm{st}}\}$, either equilibrium or nonequilibrium, were just described.

Time evolution occurs in the presence of time-dependent fields or when the initial DDOs are not at steady states. The expectation values of arbitrary dynamical variables are ($\mathrm{Tr} \equiv \mathrm{tr}_{\mathrm{s}}\mathrm{tr}_{\mathrm{B}}$)

$$\langle\hat{A}(t)\rangle \equiv \mathrm{Tr}[\hat{A}\rho_{\mathrm{T}}(t)]. \tag{7.2}$$

Universal characterizations also involve, in general, various spectra that are related to correlation functions, such as

$$\langle\hat{A}(t)\hat{B}(0)\rangle = \mathrm{Tr}\big\{\hat{A}[\mathrm{e}^{-\mathrm{i}\mathcal{L}_{\mathrm{T}}t}(\hat{B}\rho_{\mathrm{T}}^{\mathrm{st}})]\big\}.$$

It can be recast in the expectation value form as

$$\langle\hat{A}(t)\hat{B}(0)\rangle = \mathrm{Tr}\big[\hat{A}\rho_{\mathrm{T}}(t;\hat{B})\big], \tag{7.3}$$

where $\rho_{\mathrm{T}}(t;\hat{B}) \equiv \mathrm{e}^{-\mathrm{i}\mathcal{L}_{\mathrm{T}}t}(\hat{B}\rho_{\mathrm{T}}^{\mathrm{st}})$, with the initial value of $\rho_{\mathrm{T}}(t=0;\hat{B}) = \hat{B}\rho_{\mathrm{T}}^{\mathrm{st}}$.

The universal DEOM evaluation is to construct the following relation:

$$\mathrm{Tr}\big[\hat{A}\rho_{\mathrm{T}}(t)\big] = \sum_{n;\boldsymbol{j}} \mathrm{tr}_{\mathrm{s}}\big[\hat{A}_{\boldsymbol{j}}^{(n)}\rho_{\boldsymbol{j}}^{(n)}(t)\big]. \tag{7.4}$$

There are two issues on the above DEOM evaluation. One is related to the DEOM-space $\{\hat{A}_{\boldsymbol{j}}^{(n)}\}$ that corresponds to a given $\hat{A}$. The former, by definition, are exclusively the system-subspace operators, whereas the latter may involve the composite system-and-bath space.

Another issue is concerned with the initial DDOs. For the correlation function of Eq. (7.3), where $\rho_{\mathrm{T}}(0;\hat{B}) = \hat{B}\rho_{\mathrm{T}}^{\mathrm{st}}$, the required initial DDOs, defined via Eq. (7.1), are

$$\rho_{\boldsymbol{j}}^{(n)}(t=0;\hat{B}) \equiv \mathrm{tr}_{\mathrm{B}}\big[(\hat{f}_{j_n}\cdots\hat{f}_{j_1})^{\circ}(\hat{B}\rho_{\mathrm{T}}^{\mathrm{st}})\big]. \tag{7.5}$$

It should be expressed, within the DEOM framework, in terms of steady-state DDOs, in order to initiate the DEOM propagations of $\rho_{\boldsymbol{j}}^{(n)}(t)$ in Eq. (7.4). This issue could be nontrivial; see details in Section 7.3.

For purely local system operators, $\hat{A}_{\mathrm{S}}$ and $\hat{B}_{\mathrm{S}}$, the above two issues are trivial. Actually, the first issue of $\{\hat{A}_{\boldsymbol{j}}^{(n)}\}$ is simply to validate Eq. (7.4). The identity, $\mathrm{Tr}\big[\hat{A}_{\mathrm{S}}\rho_{\mathrm{T}}(t)\big] = \mathrm{tr}_{\mathrm{s}}\big[\hat{A}_{\mathrm{S}}\rho_{\mathrm{S}}(t)\big]$, leads to

$$\hat{A}_{\mathrm{S}} \Longrightarrow \big\{\hat{A}^{(0)} = \hat{A}_{\mathrm{S}}; \ \text{ else } \hat{A}_{\boldsymbol{j}}^{(n)} = 0\big\}. \tag{7.6}$$

Moreover, Eq. (7.5) immediately gives rise to

$$\rho_{\mathrm{T}}(0;\hat{B}_{\mathrm{S}}) = \hat{B}_{\mathrm{S}}\rho_{\mathrm{T}}^{\mathrm{st}} \Longrightarrow \big\{\rho_{\boldsymbol{j}}^{(n)}(0;\hat{B}_{\mathrm{S}}) = \hat{B}_{\mathrm{S}}\rho_{\boldsymbol{j}}^{(n);\mathrm{st}}\big\}. \tag{7.7}$$

The DEOM approach to $\langle\hat{A}_{\mathrm{S}}(t)\hat{B}_{\mathrm{S}}(0)\rangle$, Eqs. (7.3) via (7.4), is now evident: (i) Evaluate $\{\rho_{\boldsymbol{j}}^{(n);\mathrm{st}}\}$ via the steady-state solutions to the fermionic DEOM; (ii) Determine the initial DDOs, $\{\rho_{\boldsymbol{j}}^{(n)}(0;\hat{B}_{\mathrm{S}})\}$, according to Eqs. (7.7); (iii) Perform the DEOM propagation to obtain $\{\rho_{\boldsymbol{j}}^{(n)}(t;\hat{B}_{\mathrm{S}})\}$, and $\langle\hat{A}_{\mathrm{S}}(t)\hat{B}_{\mathrm{S}}(0)\rangle = \mathrm{tr}_{\mathrm{s}}[\hat{A}_{\mathrm{S}}\rho^{(0)}(t;\hat{B}_{\mathrm{S}})]$, along the propagation.

We may refer to the above local protocol, because it involves only local system operators [49, 54, 55, 59]. The evaluation of $\langle[\hat{A}_{\mathrm{S}}(t),\hat{B}_{\mathrm{S}}(0)]_{\pm}\rangle$ goes along with the initial $\rho_{\boldsymbol{j}}^{(n)}(0;\hat{B}_{\mathrm{S}}) = [\hat{B}_{\mathrm{S}},\rho_{\boldsymbol{j}}^{(n);\mathrm{st}}]_{\pm}$. The nonlinear correlation functions of local system operators are the same [54, 55]. The identification of Eq. (7.6) is mainly for the purpose of an efficient evaluation of nonlinear correlation functions based on the mixed Schrödinger-Heisenberg prescription [54, 55]; see Section 7.4.

In fact, the local protocol had been extensively utilized within the HEOM framework [49, 54, 55]. It arises from the response theory, as if the system Liouvillian would behave like $\mathcal{L}_{\mathrm{S}} + \hat{B}_{\mathrm{S}}\epsilon(t)$ [59]. Moreover, in the original fermionic HEOM paper [18], we had related the first-tier quantities, i.e., the one-body DDOs $\{\rho_j^{(1)}\}$, to transport current. Higher-order $\{\rho_{\boldsymbol{j}}^{(n>1)}\}$ were simply auxiliary quantities within the HEOM construction (cf. Section 5), but also irrelevant to the local protocol. HEOM-based benchmark results for Anderson impurity models showing significant Kondo resonance features had been extensively reported. The calculated properties include the Kondo hysteretic feature [47], thermopower with Kondo correlations [48], Aharonov–Bohm interferometer dynamics [36], and impurity spectral density [46, 49, 60].

7.3 Quantum transport current fluctuations

The transport current operator, $\hat{I}_{\alpha}$ of Eq. (4.5), is nonlocal, involved both local system $\{\hat{a}_u^{\sigma}\}$ and hybridizing bath reservoir operators $\{\hat{F}_{\alpha u}^{\sigma}\}$ of itinerary electrons. Following the decomposition of dissipatons, Eq. (4.26), it reads

$$\hat{I}_{\alpha} = \mathrm{i}\sum_{\sigma\kappa u}(\sigma\hat{a}_u^{\bar{\sigma}})\hat{f}_{\alpha\kappa u}^{\sigma} \equiv \mathrm{i}\sum_{j_{\alpha}\in j}\tilde{a}_{\bar{j}}\hat{f}_j. \tag{7.8}$$

Here, $j_{\alpha} \equiv \{\sigma\kappa u\} \in j \equiv \{\sigma\alpha\kappa u\}$ [cf. Eq. (4.35)]. Note that the above $\tilde{a}_{\bar{j}} = \tilde{a}_u^{\bar{\sigma}} \equiv \sigma\hat{a}_u^{\bar{\sigma}}$, is defined in parallel with Eq. (4.25), but it differs from that in Ref. [23] [Eq. (23) therein] by a sign. The mean current expression, in terms of DDOs, is then

$$I_\alpha(t) = \text{Tr}\big[\hat{I}_\alpha \rho_{\text{T}}(t)\big] = i \sum_{j_\alpha \in j} \text{tr}_{\text{S}}\big[\tilde{a}_{\bar{j}} \rho_j^{(1)}(t)\big]. \qquad (7.9)$$

This expression addresses the first issue underlying Eq. (7.4), with the following correspondence,

$$\hat{I}_\alpha \Longrightarrow \big\{\hat{A}_{\alpha j_\alpha}^{(1)} = i\tilde{a}_u^{\bar{\sigma}}; \ \text{else} \ \hat{A}_j^{(n)} = 0\big\}. \qquad (7.10)$$

Among all $\{\hat{A}_j^{(n)}\}$, only those $\hat{A}_j^{(1)}$ of specified α are nonzero.

Actually, Eq. (7.9) is sufficient to pin down the protocol of the DEOM approach to current-current correlation function [23]. In this sense, the identification Eq. (7.10) seems somewhat redundant. However, as we mentioned earlier, it will be essential for the mixed Schrödinger-Heisenberg prescription, which facilitates the evaluations of the nonlinear response functions; see Section 7.5.

Consider the lead-specific current-current correlation function [cf. Eqs. (7.3) and (7.9)]:

$$\langle \hat{I}_\alpha(t)\hat{I}_{\alpha'}(0)\rangle = i \sum_{j_\alpha \in j} \text{tr}_{\text{s}}\big[\tilde{a}_{\bar{j}} \rho_j^{(1)}(t; \hat{I}_{\alpha'})\big]. \qquad (7.11)$$

The required initial DDOs are [cf. Eqs. (7.5) and (7.8)]

$$\rho_{\boldsymbol{j}}^{(n)}(0; \hat{I}_{\alpha'}) = i \sum_{j'_{\alpha'} \in j'} \text{tr}_{\text{B}} \Big[\big(\hat{f}_{j_n} \cdots \hat{f}_{j_1}\big)^\circ \big(\tilde{a}_{\bar{j}'} \hat{f}_{j'} \rho_{\text{T}}^{\text{st}}\big)\Big]. \qquad (7.12)$$

Its evaluation involves the generalized Wick's theorem, Eq. (4.41) and Eq. (4.43), followed by some simple algebra. We obtain [cf. Eq. (4.44)]

$$\rho_{\boldsymbol{j}}^{(n)}(0; \hat{I}_{\alpha'}) = i \sum_{r=1}^n (-)^{n-r} \delta_{\alpha' \alpha_r} \Big(\sum_v \eta_{j_r v} \tilde{a}_v^{\sigma_r}\Big) \rho_{\boldsymbol{j}_r^-}^{(n-1);\text{st}}$$
$$+ i \sum_{j'_{\alpha'} \in j'} \tilde{a}_{\bar{j}'} \rho_{\boldsymbol{j}j'}^{(n+1);\text{st}}. \qquad (7.13)$$

Here, $\eta_{jv} \equiv \eta_{\alpha\kappa uv}^\sigma$. The nonlocal nature of the current operator, $\hat{I}_{\alpha'}$, is manifested via the dependence of $\rho_{\boldsymbol{j}}^{(n)}(0; \hat{I}_{\alpha'})$ on $\{\rho_{\boldsymbol{j}\pm}^{(n\pm1);\text{st}}\}$. The latter are the steady-state solutions to DEOM, under a time-independent bias voltage. The resulting initial $\{\rho_{\boldsymbol{j}}^{(n)}(0; \alpha')\}$ of Eq. (7.13) are then propagated, with the same DEOM, to obtain $\{\rho_{\boldsymbol{j}}^{(n)}(t; \alpha')\}$. Finally, the electrode-specific current correlation function, $\langle \hat{I}_\alpha(t)\hat{I}_{\alpha'}(0)\rangle$, is evaluated via Eq. (7.11).

The current noise spectrum is just the Fourier transform of $\langle \delta\hat{I}_\alpha(t)\delta\hat{I}_{\alpha'}(0)\rangle$, where $\delta\hat{I}_\alpha \equiv \hat{I}_\alpha - I_\alpha^{\text{st}}$. Based on accurate DEOM evaluations, we have recently investigated current noise spectra, for single-impurity Anderson model systems, in several typical transport regimes [23]. Besides the characteristic Kondo feature, we have also identified the signatures of anti-Stokes and destructive interference [23].

7.4 DEOM in Heisenberg prescription

The dissipatons-space for open quantum systems refers to the linearity of the DEOM formalism, which can be either bosonic [Eq. (3.24)] or fermionic [Eq. (4.45)]. Both are of linear form,

$$\dot{\boldsymbol{\rho}}(t) = -i\boldsymbol{\mathcal{L}}(t)\boldsymbol{\rho}(t). \qquad (7.14)$$

Here, $\boldsymbol{\mathcal{L}}(t)$ is specified by the closed set of DEOM, for either bosonic or fermionic DDOs. We adopt the generic form of $\boldsymbol{\rho} \equiv \{\rho_{\boldsymbol{n}}^{(n)}\}$, as highlighted in Eq. (2.3), where $\{\rho_{\boldsymbol{n}}^{(n \leq L)}(t)\}$ are governed by Eq. (7.14), but $\rho_{\boldsymbol{n}}^{(L+1)}(t)$ are expressed separately via Eq. (3.45) or (4.50). In other words, the complete DEOM theory is truly for $\{\rho_{\boldsymbol{n}}^{(n \leq L+1)}(t)\}$. This will become transparent with the Heisenberg prescription of DEOM [cf. Eq. (7.19)], which explicitly includes the EOM for the Heisenberg counterpart to $\rho_{\boldsymbol{n}}^{(L+1)}(t)$.

The Heisenberg picture goes with a time-independent $\boldsymbol{\mathcal{L}}$. It reads

$$\dot{\hat{\boldsymbol{A}}}(t) = -i\hat{\boldsymbol{A}}(t)\boldsymbol{\mathcal{L}}, \qquad (7.15)$$

with the initial conditions $\hat{\boldsymbol{A}}(0) \equiv \{\hat{A}_{\boldsymbol{n}}^{(n)}\}$ and the DEOM-space dynamical variables, such as those of Eqs. (7.6) and (7.10). As to be detailed below, Eq. (7.15) is actually a closed set equations for $\{\hat{A}_{\boldsymbol{n}}^{(n \leq L+1)}(t)\}$.

In the following derivation, we adopt the convention, in which DEOM-space states and dynamical variables are denoted with $|\boldsymbol{\rho}\rangle\rangle$ and $\langle\langle\hat{\boldsymbol{A}}|$, respectively. The DEOM-space inner product then follows

$$\langle\langle\hat{\boldsymbol{A}}|\boldsymbol{\rho}\rangle\rangle \equiv \sum_{\boldsymbol{n}} \langle\langle\hat{A}_{\boldsymbol{n}}^{(n)}|\rho_{\boldsymbol{n}}^{(n)}\rangle\rangle \equiv \sum_{\boldsymbol{n}} \text{tr}_{\text{s}}\big[\hat{A}_{\boldsymbol{n}}^{(n)}\rho_{\boldsymbol{n}}^{(n)}\big]. \quad (7.16)$$

It demands that the Heisenberg picture and Schrödinger picture be equivalent:

$$\langle\langle\dot{\hat{\boldsymbol{A}}}|\boldsymbol{\rho}\rangle\rangle = \langle\langle\hat{\boldsymbol{A}}|\dot{\boldsymbol{\rho}}\rangle\rangle. \qquad (7.17)$$

For fermionic DEOM (4.45), it demands

$$\langle\langle\dot{\hat{\boldsymbol{A}}}|\boldsymbol{\rho}\rangle\rangle \equiv \sum_{\{n;\boldsymbol{j}\}} \langle\langle\dot{\hat{A}}_{\boldsymbol{j}}^{(n)}|\rho_{\boldsymbol{j}}^{(n)}\rangle\rangle$$
$$= \sum_{\{n;\boldsymbol{j}\}} \Big\{ -\langle\langle\hat{A}_{\boldsymbol{j}}^{(n)}|\big(i\mathcal{L} + \gamma_{\boldsymbol{j}}^{(n)}\big)|\rho_{\boldsymbol{j}}^{(n)}\rangle\rangle$$
$$- i\sum_{r=1}^n (-)^{n-r} \langle\langle\hat{A}_{\boldsymbol{j}}^{(n)}|\mathcal{C}_{j_r}|\rho_{\boldsymbol{j}_r^-}^{(n-1)}\rangle\rangle$$
$$- i\sum_j \langle\langle\hat{A}_{\boldsymbol{j}}^{(n)}|\mathcal{A}_{\bar{j}}|\rho_{\boldsymbol{j}j}^{(n+1)}\rangle\rangle \Big\}. \qquad (7.18)$$

Together with the identity, $\rho_{\boldsymbol{j}}^{(n)} = (-)^{n-r}\rho_{\boldsymbol{j}_r^- j_r}^{(n)}$, and the derivative-resum scheme, Eq. (4.49) in the Schrödinger

YiJing Yan, et al., Front. Phys. 11(4), 110306 (2016)

110306-23

picture truncation, we finally obtain

$$\dot{\hat{A}}_{\boldsymbol{j}}^{(n \leqslant L)} = -\hat{A}_{\boldsymbol{j}}^{(n)} \left(\mathrm{i}\mathcal{L} + \gamma_{\boldsymbol{j}}^{(n)} \right) - \mathrm{i} \sum_j \hat{A}_{\boldsymbol{j}j}^{(n+1)} \mathcal{C}_j$$

$$-\mathrm{i} \sum_{r=1}^{n} (-)^{n-r} \hat{A}_{\boldsymbol{j}_r^-}^{(n-1)} \mathcal{A}_{\bar{j}_r}, \qquad (7.19a)$$

and

$$\dot{\hat{A}}_{\boldsymbol{j}j}^{(L+1)} = -\mathrm{i} \sum_j \hat{A}_{\boldsymbol{j}}^{(L)} \mathcal{A}_{\bar{j}}. \qquad (7.19b)$$

The Grassmannian superoperators, $\mathcal{A}_j$ and $\mathcal{C}_j$, preserve

$$\langle\!\langle (\hat{A}_{\boldsymbol{j}}^{(n)}\mathcal{O}) | \rho_{\boldsymbol{j}}^{(n)} \rangle\!\rangle = \langle\!\langle \hat{A}_{\boldsymbol{j}}^{(n)} | (\mathcal{O}\rho_{\boldsymbol{j}}^{(n)}) \rangle\!\rangle. \qquad (7.20)$$

It results in $\hat{A}_{\boldsymbol{j}}^{(n)}\mathcal{A}_j = [\hat{A}_{\boldsymbol{j}}^{(n)}, \hat{a}_j]_{\pm}$, with the even $(+)$ or odd $(-)$ fermionic parity that is exclusively dictated by its $\rho_{\boldsymbol{j}}^{(n)}$ counterpart; see Eq. (4.46). Apparently, Eq. (7.20) also includes the trivial case that $\hat{A}\mathcal{L} = [\hat{A}, H_\mathrm{s}]$, where $\mathcal{L}\rho = [H_\mathrm{s}, \rho]$.

Now, we return to the invariance issue of the prescriptions, in relation to the truncation schemes. Evidently, the derivative-resum scheme of Eq. (4.49) and its equivalent in Eq. (4.50) lead to the terminal DEOM (7.19b) and (4.51), in the Heisenberg and Schrödinger prescriptions, respectively. In other words, the derivative-resum scheme preserves the invariance of the prescriptions. All other existing schemes explicitly set all or some $\{\rho_{\boldsymbol{j}}^{(n>L)}\}$ to be zeroes. Those $\{\rho_{\boldsymbol{j}}^{(L+1)} = 0\}$ would just affect the $\hat{A}_{\boldsymbol{j}j}^{(L-1)}$-term in Eq. (7.19a), rather than the $\hat{A}_{\boldsymbol{j}j}^{(L+1)}$-term. None of the $\{\rho_{\boldsymbol{j}}^{(n>L)} = 0\}$-based schemes are formally transferable indifferent prescriptions. The derivative-resum scheme is the only one that maintains the invariance. The setup of Eqs. (4.49) and (4.50), which are the simplest derivative pair from Eq. (4.47), is also found to be the best [32].

7.5 Efficient evaluation of nonlinear correlation functions

The main usage of the Heisenberg DEOM prescription is concerned with an efficient evaluation of nonlinear correlation functions, such as

$$R(t_2, t_1) \equiv \langle \hat{B}(0)\hat{A}(t_1 + t_2)\hat{B}(t_1) \rangle$$
$$= \langle\!\langle \hat{A} | \mathrm{e}^{-\mathrm{i}\mathcal{L}_\mathrm{T}t_2} \hat{B}^{>} \mathrm{e}^{-\mathrm{i}\mathcal{L}_\mathrm{T}t_1} \hat{B}^{<} | \rho_\mathrm{T}^\mathrm{st} \rangle\!\rangle$$
$$= \langle\!\langle \hat{A} | \mathrm{e}^{-\mathrm{i}\mathcal{L}_\mathrm{T}t_2} \hat{B}^{>} \mathrm{e}^{-\mathrm{i}\mathcal{L}_\mathrm{T}t_1} | (\rho_\mathrm{T}^\mathrm{st}\hat{B}) \rangle\!\rangle$$
$$= \langle\!\langle \hat{A} | \mathrm{e}^{-\mathrm{i}\mathcal{L}_\mathrm{T}t_2} | [\hat{B}\rho_\mathrm{T}(t_1; \hat{B})] \rangle\!\rangle. \qquad (7.21)$$

Here, $\langle\!\langle \hat{A} | \rho_\mathrm{T} \rangle\!\rangle \equiv \mathrm{Tr}(\hat{A}\rho_\mathrm{T})$. The second expression follows immediately, as $\hat{A}(t) = \mathrm{e}^{\mathrm{i}H_\mathrm{T}t}\hat{A}\mathrm{e}^{-\mathrm{i}H_\mathrm{T}t} = \hat{A}\mathrm{e}^{-\mathrm{i}\mathcal{L}_\mathrm{T}t}$ and $\langle \hat{A} \rangle \equiv \mathrm{Tr}(\hat{A}\rho_\mathrm{T}^\mathrm{st})$. The third expression in Eq. (7.21)

prepares the initial $\rho_\mathrm{T}(t_1 = 0; \hat{B}) = (\rho_\mathrm{T}^\mathrm{st}\hat{B})$ such that $\rho_\mathrm{T}(t_1; \hat{B}) = \mathrm{e}^{-\mathrm{i}\mathcal{L}_\mathrm{T}t_1}\rho_\mathrm{T}(t_1 = 0; \hat{B})$. The last one prepares $\rho_\mathrm{T}(t_2 = 0 | t_1; \hat{B}) = \hat{B}\rho_\mathrm{T}(t_1; \hat{B})$. One could continue $\mathrm{e}^{-\mathrm{i}\mathcal{L}_\mathrm{T}t_2}[\hat{B}\rho_\mathrm{T}(t_1; \hat{B})] = \tilde{\rho}_\mathrm{T}(t_2; t_1; \hat{B})$, and evaluate Eq. (7.21) via $R(t_2, t_1) = \langle\!\langle \hat{A} | \tilde{\rho}_\mathrm{T}(t_2; t_1; \hat{B}) \rangle\!\rangle$. The implementation here is expensive, as it involves the correlated two-time propagations, both of which are in Schrödinger prescriptions. The implementation of the mixed Heisenberg-Schrödinger dynamics,

$$R(t_2, t_1) = \langle\!\langle \hat{A}(t_2) | \tilde{\rho}_\mathrm{T}(t_1; \hat{B}) \rangle\!\rangle, \qquad (7.22)$$

is surely preferred, where the t_2-propagation is treated separately, in terms of $\hat{A}(t_2)$ the time evolution of the dynamical variable.

The DEOM-space evaluation of Eq. (7.22) can be expressed, with the fermionic case for illustration, as

$$R(t_2, t_1) = \langle\!\langle \hat{\boldsymbol{A}}(t_2) | \tilde{\boldsymbol{\rho}}(t_1; \hat{B}) \rangle\!\rangle$$
$$= \sum_{n=1}^{L+1} \sum_{\boldsymbol{j}} \langle\!\langle \hat{A}_{\boldsymbol{j}}^{(n)}(t_2) | \tilde{\rho}_{\boldsymbol{j}}^{(n)}(t_1; \hat{B}) \rangle\!\rangle. \qquad (7.23)$$

Here, $\hat{\boldsymbol{A}}(t) = \{\hat{A}_{\boldsymbol{j}}^{(n)}(t)\}$ are governed by Eq. (7.19), starting from the initial $\hat{\boldsymbol{A}}(0) \equiv \hat{\boldsymbol{A}}$, as illustrated in Eqs. (7.6) and (7.10).

For $\tilde{\boldsymbol{\rho}}(t_1; \hat{B})$, the underlying DEOM is the collection of Eq. (4.45) for $n < L$, Eq. (4.51) for $n = L$, and Eq. (4.50) for $n = L + 1$. The evaluation of $\tilde{\boldsymbol{\rho}}(t_1; \hat{B})$, as inferred from Eqs. (7.21) and (7.22), can be summarized with the following correspondences,

$$\rho_\mathrm{T}^\mathrm{st} \Longrightarrow \boldsymbol{\rho}^\mathrm{st},$$
$$\rho_\mathrm{T}^\mathrm{st}\hat{B} \Longrightarrow \boldsymbol{\rho}(0; \hat{B}),$$
$$\mathrm{e}^{-\mathrm{i}\mathcal{L}_\mathrm{T}t_1}(\rho_\mathrm{T}^\mathrm{st}\hat{B}) \Longrightarrow \boldsymbol{\rho}(t_1; \hat{B}),$$
$$\hat{B}\rho_\mathrm{T}(t_1; \hat{B}) \Longrightarrow \tilde{\boldsymbol{\rho}}(t_1; \hat{B}). \qquad (7.24)$$

The four associated evaluations are as follows: (i) Calculate $\boldsymbol{\rho}^\mathrm{st} = \{\rho_{\boldsymbol{j}}^{(n);\mathrm{st}}\}$ via the steady-state solutions to the DEOM; (ii) Express $\boldsymbol{\rho}(t_1 = 0; \hat{B})$ in terms of $\boldsymbol{\rho}^\mathrm{st}$, as exemplified by Eqs. (7.7) and (7.13); (iii) Propagate $\boldsymbol{\rho}(t_1; \hat{B})$ with the DEOM; (iv) Same as (ii) above, but for $\tilde{\boldsymbol{\rho}}(t_1; \hat{B})$ to be expressed in terms of $\boldsymbol{\rho}(t_1; \hat{B})$.

Note that (ii) and (iv) above are to set the DEOM-space correspondences to $\hat{B}^{<}\rho_\mathrm{T}^\mathrm{st} = \rho_\mathrm{T}(t_1 = 0; \hat{B})$ and $\hat{B}^{>}\rho_\mathrm{T}(t_1; \hat{B}) = \rho_\mathrm{T}(t_2 = 0 | t_1; \hat{B})$, respectively. For the local system operator, $\hat{B}_\mathrm{s}$, both correspondences above are straightforward, according to Eqs. (7.7) except now $\boldsymbol{\rho}(t_1 = 0; \hat{B}_\mathrm{s}) = \boldsymbol{\rho}^\mathrm{st}\hat{B}_\mathrm{s}$, as the action of $\hat{B}_\mathrm{s}^{<}$ is involved. For the nonlocal operators, such as the transport current operator $\hat{I}_\alpha$ demonstrated in Section 7.2, the evaluations of (ii) and (iv) utilize the generalized Wick's theorem of Eq. (4.42) and Eq. (4.41), respectively.

8   Concluding remarks

We have thoroughly reviewed the DEOM theory, covering the unified law governing both systems and hybrid bath environment dynamics, and the underlying theorems and dissipaton algebra. Evidently, the dynamical variables, the DDOs of Eq. (3.20) or Eq. (4.36), represent many-dissipaton configurations. All these are essential ingredients of the DEOM framework.

We also have an optimal DEOM formalism. Besides minimum basis-set dissipatons (cf. Section 6.2), it also uses an optimal truncation scheme, the derivative-resum scheme, for high-order many-dissipaton effects (cf. Section 3.5 and Section 4.5). To our knowledge, this resum scheme is by far the only one that preserves the invariance principle of quantum mechanics prescriptions; see comments towards the end of Section 7.4. Dissipaton-configuration-adapted level truncation would also be possible. Work along this direction is in progress.

From the numerical perspective, DEOM inherits all virtues of the previously developed HEOM methods. Some recent advancements have been presented in Section 6. As a highly accurate method for characterizing strongly-correlated many-body open systems, DEOM/HEOM is a powerful complement to Kyldish non-equilibrium Green's function (NEGF) formalism [61–65] and the numerical renormalization group (NRG) method [66. 67]. In particular, for finite or high temperature cases, the NRG method becomes rather expensive [50], and neither NEGF or NRG is a real-time dynamics theory. The DEOM/HEOM method is definitely more than just a quantum impurity solver – it provides a universal and versatile framework for investigations of thermodynamic and dynamical properties of open systems at equilibrium or far from equilibrium. There is much more to explore and harvest with the DEOM, and we look forward to reporting further progress and achievements in the near future.

References

1. A. G. Redfield, The theory of relaxation processes, *Adv. Magn. Reson.* 1, 1 (1965)

2. G. Lindblad, On the generators of quantum dynamical semigroups, *Commun. Math. Phys.* 48(2), 119 (1976)

3. V. Gorini, A. Kossakowski, and E. C. G. Sudarshan, Completely positive dynamical semigroups of N-level systems, *J. Math. Phys.* 17(5), 821 (1976)

4. Y. J. Yan, Quantum Fokker-Planck theory in a non-Gaussian–Markovian medium, *Phys. Rev. A* 58(4), 2721 (1998)

5. R. X. Xu and Y. J. Yan, Theory of open quantum systems, *J. Chem. Phys.* 116(21), 9196 (2002)

6. Y. J. Yan and R. X. Xu, Quantum mechanics of dissipative systems, *Annu. Rev. Phys. Chem.* 56(1), 187 (2005)

7. R. P. Feynman and F. L. Jr Vernon, The theory of a general quantum system interacting with a linear dissipative system, *Ann. Phys.* 24, 118 (1963)

8. H. Kleinert, Path Integrals in Quantum Mechanics, Statistics, Polymer Physics, and Financial Markets, 5th Ed., Singapore: World Scientific, 2009

9. U. Weiss, Quantum Dissipative Systems, 3rd Ed., Series in Modern Condensed Matter Physics, Vol. 13, Singapore: World Scientific, 2008

10. J. S. Shao, Decoupling quantum dissipation interaction via stochastic fields, *J. Chem. Phys.* 120(11), 5053 (2004)

11. Y. A. Yan, F. Yang, Y. Liu, and J. S. Shao, Hierarchical approach based on stochastic decoupling to dissipative systems, *Chem. Phys. Lett.* 395(4–6), 216 (2004)

12. Y. Tanimura, Nonperturbative expansion method for a quantum system coupled to a harmonic-oscillator bath, *Phys. Rev. A* 41(12), 6676 (1990)

13. Y. Tanimura, Stochastic Liouville, Langevin, Fokker–Planck, and master equation approaches to quantum dissipative systems, *J. Phys. Soc. Jpn.* 75(8), 082001 (2006)

14. R. X. Xu, P. Cui, X. Q. Li, Y. Mo, and Y. J. Yan, Exact quantum master equation via the calculus on path integrals, *J. Chem. Phys.* 122(4), 041103 (2005)

15. R. X. Xu and Y. J. Yan, Dynamics of quantum dissipation systems interacting with bosonic canonical bath: Hierarchical equations of motion approach, *Phys. Rev. E* 75(3), 031107 (2007)

16. J. J. Ding, J. Xu, J. Hu, R. X. Xu, and Y. J. Yan, Optimized hierarchical equations of motion theory for Drude dissipation and efficient implementation to nonlinear spectroscopies, *J. Chem. Phys.* 135(16), 164107 (2011)

17. J. J. Ding, R. X. Xu, and Y. J. Yan, Optimizing hierarchical equations of motion for quantum dissipation and quantifying quantum bath effects on quantum transfer mechanisms, *J. Chem. Phys.* 136(22), 224103 (2012)

18. J. S. Jin, X. Zheng, and Y. J. Yan, Exact dynamics of dissipative electronic systems and quantum transport: Hierarchical equations of motion approach, *J. Chem. Phys.* 128(23), 234703 (2008)

19. Q. Shi, L. P. Chen, G. J. Nan, R. X. Xu, and Y. J. Yan, Electron transfer dynamics: Zusman equation versus exact theory, *J. Chem. Phys.* 130(16), 164518 (2009)

YiJing Yan, et al., Front. Phys. 11(4), 110306 (2016)

110306-25

20. K. B. Zhu, R. X. Xu, H. Y. Zhang, J. Hu, and Y. J. Yan, Hierarchical dynamics of correlated system-environment coherence and optical spectroscopy, *J. Phys. Chem. B* 115(18), 5678 (2011)

21. Y. J. Yan, Theory of open quantum systems with bath of electrons and phonons and spins: Many-dissipaton density matrixes approach, *J. Chem. Phys.* 140(5), 054105 (2014)

22. H. D. Zhang, R. X. Xu, X. Zheng, and Y. J. Yan, Nonperturbative spin-boson and spin-spin dynamics and nonlinear Fano interferences: A unified dissipaton theory based study, *J. Chem. Phys.* 142(2), 024112 (2015)

23. J. S. Jin, S. K. Wang, X. Zheng, and Y. J. Yan, Current noise spectra and mechanisms with dissipaton equation of motion theory, *J. Chem. Phys.* 142(23), 234108 (2015)

24. S. Mukamel, The Principles of Nonlinear Optical Spectroscopy, New York: Oxford University Press, 1995

25. Y. J. Yan and S. Mukamel, Electronic dephasing, vibrational relaxation, and solvent friction in molecular nonlinear optical lineshapes, *J. Chem. Phys.* 89(8), 5160 (1988)

26. A. O. Caldeira and A. J. Leggett, Quantum tunnelling in a dissipative system, *Ann. Phys.* 1983, 149: 374 [Erratum: 153, 445 (1984)]

27. A. O. Caldeira and A. J. Leggett, Path integral approach to quantum Brownian motion, *Physica A* 121(3), 587 (1983)

28. J. Hu, R. X. Xu, and Y. J. Yan, Padé spectrum decomposition of Fermi function and Bose function, *J. Chem. Phys.* 133(10), 101106 (2010)

29. J. Hu, M. Luo, F. Jiang, R. X. Xu, and Y. J. Yan, Padé spectrum decompositions of quantum distribution functions and optimal hierarchial equations of motion construction for quantum open systems, *J. Chem. Phys.* 134(24), 244106 (2011)

30. R. X. Xu, B. L. Tian, J. Xu, Q. Shi, and Y. J. Yan, Hierarchical quantum master equation with semiclassical Drude dissipation, *J. Chem. Phys.* 131(21), 214111 (2009)

31. B. L. Tian, J. J. Ding, R. X. Xu, and Y. J. Yan, Biexponential theory of Drude dissipation via hierarchical quantum master equation, *J. Chem. Phys.* 133(11), 114112 (2010)

32. H. D. Zhang and Y. J. Yan, Onsets of hierarchy truncation and self-consistent Born approximation with quantum mechanics prescriptions invariance, *J. Chem. Phys.* 143(21), 214112 (2015)

33. X. Zheng, R. X. Xu, J. Xu, J. S. Jin, J. Hu, and Y. J. Yan, Hierarchical equations of motion for quantum dissipation and quantum transport, *Prog. Chem.* 2012, 24(06): 1129, http://www.progchem.ac.cn/EN/abstract/abstract10858.shtml

34. P. Cui, X. Q. Li, J. S. Shao, and Y. J. Yan, Quantum transport from the perspective of quantum open systems, *Phys. Lett. A* 357(6), 449 (2006)

35. J. S. Jin, J. Li, Y. Liu, X. Q. Li, and Y. J. Yan, Improved master equation approach to quantum transport: From Born to self-consistent Born approximation, *J. Chem. Phys.* 140(24), 244111 (2014)

36. D. Hou, S. K. Wang, R. L. Wang, L. Z. Ye, R. X. Xu, X. Zheng, and Y. J. Yan, Improving the efficiency of hierarchical equations of motion approach and application to coherent dynamics in Aharonov–Bohm interferometers, *J. Chem. Phys.* 142(10), 104112 (2015)

37. Y. Tanimura and P. G. Wolynes, Quantum and classical Fokker–Planck equations for a Guassian–Markovian noise bath, *Phys. Rev. A* 43(8), 4131 (1991)

38. X. Q. Li and Y. J. Yan, Quantum master equation scheme of time-dependent density functional theory to time-dependent transport in nanoelectronic devices, *Phys. Rev. B* 75(7), 075114 (2007)

39. Y. Tanimura, Real-time and imaginary-time quantum hierarchal Fokker–Planck equations, *J. Chem. Phys.* 142(14), 144110 (2015)

40. L. H. Ryder, Quantum Field Theory, 2nd Ed., Cambridge: Cambridge University Press, 1996

41. H. D. Zhang, J. Xu, R. X. Xu, and Y. J. Yan, Modified Zusman qquation for quantum solvation dynamics and rate processes, in: Reaction Rate Constant Computations: Theories and Applications, edited by K.-L. Han and T.-S. Chu, pp. 319–336, Ch. 13, RSC Theoretical and Computational Chemistry Series No.6, 2014, http://dx.doi.org/10.1039/9781849737753-00319

42. X. Zheng, J. S. Jin, and Y. J. Yan, Dynamic electronic response of a quantum dot driven by time-dependent voltage, *J. Chem. Phys.* 129(18), 184112 (2008)

43. X. Zheng, J. S. Jin, and Y. J. Yan, Dynamic Coulomb blockade in single-lead quantum dots, *New J. Phys.* 10(9), 093016 (2008)

44. X. Zheng, J. Y. Luo, J. S. Jin, and Y. J. Yan, Complex non-Markovian effect on time-dependent quantum transport, *J. Chem. Phys.* 130(12), 124508 (2009)

45. F. Jiang, J. S. Jin, S. K. Wang, and Y. J. Yan, Inelastic electron transport through mesoscopic systems: Heating versus cooling and sequential tunneling versus cotunneling processes, *Phys. Rev. B* 85(24), 245427 (2012)

46. S. K. Wang, X. Zheng, J. S. Jin, and Y. J. Yan, Hierarchical Liouville-space approach to nonequilibrium dynamic properties of quantum impurity systems, *Phys. Rev. B* 88(3), 035129 (2013)

47. X. Zheng, Y. J. Yan, and M. Di Ventra, Kondo memory in driven strongly correlated quantum dots, *Phys. Rev. Lett.* 111(8), 086601 (2013)

48. L. Z. Ye, D. Hou, R. L. Wang, D. W. Cao, X. Zheng, and Y. J. Yan, Thermopower of few-electron quantum dots with Kondo correlations, *Phys. Rev. B* 90(16), 165116 (2014)

49. Z. H. Li, N. H. Tong, X. Zheng, D. Hou, J. H. Wei, J. Hu, and Y. J. Yan, Hierarchical Liouville-space approach for accurate and universal characterization of quantum impurity systems, *Phys. Rev. Lett.* 109(26), 266403 (2012)

50. D. Hou, R. Wang, X. Zheng, N. H. Tong, J. H. Wei, and Y. J. Yan, Hierarchical equations of motion for impurity solver

in dynamical mean-field theory, *Phys. Rev. B* 90(4), 045141 (2014)

51. T. Ozaki, Continued fraction representation of the Fermi-Dirac function for large-scale electronic structure calculations, *Phys. Rev. B* 75(3), 035123 (2007)

52. P. W. Anderson, Localized magnetic states in metals, *Phys. Rev.* 124(1), 41 (1961)

53. Y. Meir, N. S. Wingreen, and P. A. Lee, Low-temperature transport through a quantum dot: The Anderson model out of equilibrium, *Phys. Rev. Lett.* 70(17), 2601 (1993)

54. J. Xu, R. X. Xu, D. Abramavicius, H. D. Zhang, and Y. J. Yan, Advancing hierarchical equations of motion for efficient evaluation of coherent two-dimensional spectroscopy, *Chin. J. Chem. Phys.* 24(5), 497 (2011)

55. J. Xu, H. D. Zhang, R. X. Xu, and Y. J. Yan, Correlated driving and dissipation in two-dimensional spectroscopy, *J. Chem. Phys.* 138(2), 024106 (2013)

56. R. W. Freund and N. M. Nachtigal, QMR: A quasiminimal residual method for non-Hermitian linear systems, *Numer. Math.* 60(1), 315 (1991)

57. R. W. Freund, A transpose-free quasi-minimal residual algorithm for non-Hermitian linear systems, *SIAM J. Sci. Comput.* 14(2), 470 (1993)

58. G. Stefanucci, Bound states in ab initio approaches to quantum transport: A time-dependent formulation, *Phys. Rev. B* 75(19), 195115 (2007)

59. Y. Mo, R. X. Xu, P. Cui, and Y. J. Yan, Correlation and response functions with non-Markovian dissipation: A reduced Liouville-space theory, *J. Chem. Phys.* 122(8), 084115 (2005)

60. Y. X. Cheng, W. J. Hou, Y. D. Wang, Z. H. Li, J. H. Wei, and Y. J. Yan, Time-dependent transport through quantum-impurity systems with Kondo resonance, *New J. Phys.* 17(3), 033009 (2015)

61. J. Rammer and H. Smith, Quantum field-theoretical methods in transport theory of metals, *Rev. Mod. Phys.* 58(2), 323 (1986)

62. H. Haug and A. P. Jauho, Quantum Kinetics in Transport and Optics of Semiconductors, 2nd Ed., Berlin: Springer, 2007

63. A. Croy and U. Saalmann, Propagation scheme for nonequilibrium dynamics of electron transport in nanoscale devices, *Phys. Rev. B* 80(24), 245311 (2009)

64. J. S. Wang, B. K. Agarwalla, H. Li, and J. Thingna, Nonequilibrium Green's function method for quantum thermal transport, *Front. Phys.* 9(6), 673 (2014)

65. W. Ji, H. Q. Xu, and H. Guo, Quantum description of transport phenomena: Recent progress, *Front. Phys.* 9(6), 671 (2014)

66. K. G. Wilson, The renormalization group: Critical phenomena and Kondo problem, *Rev. Mod. Phys.* 47(4), 773 (1975)

67. R. Bulla, T. A. Costi, and T. Pruschke, Numerical renormalization group method for quantum impurity systems, *Rev. Mod. Phys.* 80(2), 395 (2008)

Frontiers of Physics

YiJing Yan, et al., Front. Phys. 11(4), 110306 (2016)

110306-27